

# POSITIVE FLOW-SPINES AND CONTACT 3-MANIFOLDS

IPPEI ISHII, MASAHARU ISHIKAWA, YUYA KODA, AND HIRONOBU NAOE

ABSTRACT. We say that a contact structure on a closed, connected, oriented, smooth 3-manifold is supported by a flow-spine if it has a contact form whose Reeb flow is a flow of the flow-spine. We then define a map from the set of positive flow-spines to the set of contact 3-manifolds up to contactomorphism by sending a positive flow-spine to the supported contact 3-manifold and show that this map is well-defined and surjective. We also determine the contact 3-manifolds supported by positive flow-spines with up to 3 vertices. As an application, we introduce the complexity for contact 3-manifolds and determine the contact 3-manifolds with complexity up to 3.

## CONTENTS

|  |    |
|--|----|
| 1. Introduction  | 1  |
| 2. Contact 3-manifolds   | 5  |
| 3. Flow-spines and DS-diagrams                                 | 7  |
| 4. Admissibility and positivity                                | 13 |
| 5. Reference 1-forms of positive flow-spines                   | 20 |
| 6. Existence   | 31 |
| 7. Uniqueness  | 36 |
| 8. Surjectivity  | 42 |
| 9. Determine contact structures of some positive flow-spines   | 51 |
| Appendix A. List of positive flow-spines with up to 3 vertices | 68 |
| References   | 71 |

## 1. INTRODUCTION

Triangulation is one of the basic tools to analyze topological manifolds and, in 3-dimensional manifold theory, it is often used to understand geometric and combinatorial structures like ideal triangulations in hyperbolic geometry, normal surfaces for decomposition of 3-manifolds and quantum invariants based on the  $6j$ -symbols. The dual of a triangulation is a polyhedron with simple vertices. It also has many applications such as branched surfaces for studying laminations and foliations and effective calculus of various invariants. A *spine* is a 2-dimensional polyhedron embedded in a closed 3-manifold obtained from the manifold by removing an open ball and collapsing it from the boundary. For instance, the 2-skeleton of the dual of a one-vertex triangulation is a spine. There are several useful aspects of spines. One is the tabulation of 3-manifolds using the complexity of almost-simple spines due to Matveev [39, 40]. Tabulation is a kind of

classification and plays an important role as a treasury of concrete examples that lead us to deep understanding of research object, like the knot table in knot theory. Various studies on the Matveev complexity are ongoing as studies of those of lens spaces and certain hyperbolic manifolds [1, 15, 29, 30, 31, 32, 45, 49, 50].

Another aspect of spines can be found in the study of non-singular flows in 3-manifolds. For a given non-singular flow, set a disk transverse to the flow and intersecting all orbits, and then float the boundary of the disk smoothly until it arrives in the disk itself. The object obtained in this way is a spine equipped with a special structure, called a *flow-spine*. A flow-spine was introduced by the first author in [26] and developed further in [27, 11]. This is very useful when one studies non-singular flow combinatorially since any non-singular flow has a flow-spine [26]. A spine is described by a decorated trivalent graph on  $S^2$  called the *DS-diagram*, that was introduced in a paper of Ikeda and Inoue [25]. The DS is an abbreviation of Dehn-Seifert. A flow-spine is described by a DS-diagram with a specified simple loop called an *E-cycle*. Flow-spines are also studied by Benedetti and Petronio in [2] in the context of branched standard spines.

A contact structure is a hyperplane distribution that is non-integrable everywhere. In this paper, all 3-manifolds are oriented, and contact structures are always assumed to be positive, that is, a contact form  $\alpha$  satisfies  $\alpha \wedge d\alpha > 0$  with respect to the orientation on the ambient 3-manifold. Flexibility of contact structures allows us to study them combinatorially, especially in the 3-dimensional case. Martinet and Lutz developed Dehn surgery technique for contact 3-manifolds [38, 37], and Thurston and Winkelnkemper related contact structures to open book decompositions of 3-manifolds [47]. Tightness and fillability were introduced and studied by Bennequin [4], Eliashberg [7, 8, 9], Gromov [21] and many other mathematicians. Great progress had been made by Giroux. There are two big directions in his works on 3-dimensional contact topology: one is convex surface theory [17] and the other is the so-called Giroux correspondence [19]. Convex surface theory allows us to use cut-and-paste methods for studying contact 3-manifolds more flexibly. This technique is mainly used when one studies classification of tight contact structures on 3-manifolds. The most famous application is the existence of a closed, orientable 3-manifold that does not admit a tight contact structure due to Etnyre and Honda [14]. The Giroux correspondence gives us an easy way to “see” contact structures via open book decompositions, and it is especially useful when one wants to show Stein fillability of contact structures given in terms of open books. Branched surfaces are sometimes used in the study of contact structures, see for instance [3, 6].

The aim of this paper is to relate triangulation of 3-manifolds to contact structures via flow-spines, by regarding Reeb flows as flows of flow-spines. This idea had appeared in the paper of Benedetti and Petronio [3]. They focused on the characteristic foliation on a branched standard spine embedded in a contact 3-manifold and studied the contact structure using techniques in convex surface theory of Giroux. The point is that they did not use Reeb vector fields so much since convex surface theory uses rather contact vector fields. In this paper, we focus on Reeb flows more and define the correspondence between flow-spines and contact structures as follows:

*Definition.* (1) A flow  $\mathcal{F}$  is said to be *carried by a flow-spine*  $P$  if  $\mathcal{F}$  is a flow of  $P$ .

- (2) A contact structure  $\xi$  on  $M$  is said to be *supported* by a flow-spine  $P$  if there exists a contact form  $\alpha$  on  $M$  such that  $\xi = \ker \alpha$  and its Reeb flow is carried by  $P$ .

To our aim, we need to introduce a notion of positivity for flow-spines. Each region of a flow-spine is canonically oriented since it is transverse to the flow. This structure is called a *branching*. A branched simple polyhedron has two kinds of vertices: the vertex on the left in Figure 1 is said to be of  *$\ell$ -type* and the one on the right is of  *$r$ -type*. We define a flow-spine to be *positive* if it has at least one vertex and all vertices are of  $\ell$ -type<sup>1</sup>. An essential reason for concerning this condition is that we cannot expect one of the existence and the uniqueness of a contact manifold for a given flow-spine without this condition, see Theorem 4.3. Another reason, which is more technical, is that a 1-form called a *reference 1-form*, which plays a key role in the proof of Theorem 1.1, cannot be defined unless we restrict flow-spines to positive ones.

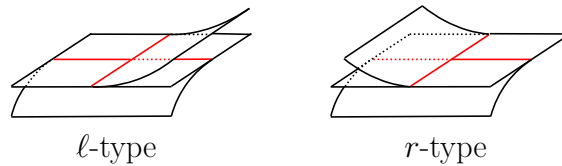


FIGURE 1. Vertices of  $\ell$ -type and  $r$ -type. Here, the ambient space is equipped with the right-handed orientation.

With these observations, we restrict our attention to positive flow-spines. Our main theorems are the following.

**Theorem 1.1.** *For any positive flow-spine  $P$  of a closed, oriented 3-manifold  $M$ , there exists a unique contact structure supported by  $P$  up to isotopy.*

Recall that two contact structures  $\xi_0$  and  $\xi_1$  are said to be *isotopic* if there exists a one-parameter family of contact forms connecting two contact forms  $\alpha_0$  and  $\alpha_1$  whose kernel are  $\xi_0$  and  $\xi_1$ , respectively. In particular,  $(M, \xi_0)$  and  $(M, \xi_1)$  are contactomorphic by Gray's stability [20].

**Theorem 1.2.** *For any closed, connected, oriented contact 3-manifold  $(M, \xi)$ , there exists a positive flow-spine  $P$  of  $M$  that supports  $\xi$ .*

These theorems show the existence of the surjection

$$\{\text{Positive flow-spines of } M\}/\text{isotopy} \rightarrow \{\text{Contact structures on } M\}/\text{isotopy}$$

for any closed, connected, oriented, smooth 3-manifold  $M$  and the surjection

$$(1.1) \quad \begin{aligned} &\{\text{Positive flow-spines}\}/\text{homeomorphism} \\ &\rightarrow \{\text{Contact 3-manifolds}\}/\text{contactomorphism}. \end{aligned}$$

<sup>1</sup> In Section 3.3, two flow-spines  $P_+(\mathcal{F}, \Sigma)$  and  $P_-(\mathcal{F}, \Sigma)$  are obtained from a normal pair  $(\mathcal{F}, \Sigma)$ . In [26],  $P_+(\mathcal{F}, \Sigma)$  is called a positive flow-spine and  $P_-(\mathcal{F}, \Sigma)$  is a negative one. The positivity for flow-spines introduced in this paper is different from the one for  $P_+(\mathcal{F}, \Sigma)$  introduced in [26].

To get the one-to-one correspondence, we need to find suitable moves of positive flow-spines. Moves of flow-spines are known in [27, 2, 11]. However moves of positive flow-spines have never been studied. Such moves are very rare since most known moves for flow-spines yield  $r$ -type vertices. Theorem 1.2 implies that any flow-spine can be deformed to a positive one by regular moves, see Corollary 8.3.

To prove Theorem 1.1, we first give a reference 1-form  $\eta$  on the 3-manifold  $M$  with respect to the flow-spine  $P$  explicitly and then consider a contact form on  $M$  of the form  $\hat{\beta} + R\eta$ , where  $\hat{\beta}$  is a 1-form defined by extending a 1-form  $\beta$  on  $P$  with  $d\beta > 0$  to the complement  $M \setminus P$  and  $R$  is a sufficiently large positive real number. This is analogous to the contact form  $(1-t)\beta + t\phi^*\beta + Rdt$  for open books used by Thurston and Winkelnkemper and then in the Giroux correspondence, where  $\phi$  is the monodromy diffeomorphism and  $t \in S^1$  is the parameter of pages of the open book. The discussion in the open book case is easier because  $dt$  is closed. In the case of flow-spine, although  $\eta$  is not closed, it satisfies  $\eta \wedge d\eta \geq 0$ , that is, it gives a confoliation [10]. We use the positivity of flow-spines to get this property. Then Theorem 1.1 follows by the same strategy as the Giroux correspondence though the argument is much more complicated. Theorem 1.2 is proved by giving a positive flow-spine explicitly. In the proof, we first use the existence of an open book for a given contact 3-manifold, due to Giroux, and then make a positive flow-spine from the open book. The proof is done by showing that the contact structure supported by this flow-spine is isotopic to the original one.

The second surjection (1.1) obtained from our main theorems allows us to define the complexity for contact 3-manifolds as the Matveev complexity for usual 3-manifolds. That is, we define the complexity  $c(M, \xi)$  of a contact 3-manifold  $(M, \xi)$  to be the minimum number of vertices of positive flow-spines supporting  $\xi$ , where  $M$  is a closed, connected, oriented 3-manifold and  $\xi$  is a contact structure on  $M$ . In the final part of this paper we determine the supported contact structures of several positive flow-spines. To determine them, we read off the Seifert fibrations from their DS-diagrams and use branched cover technique and specific Dehn surgeries called *coil surgeries*. For example, by considering branched covers, we may determine that the complexity of the quaternion space with canonical contact structure is 3 and that of the Poincaré homology 3-sphere with the canonical contact structure is 5. Here the canonical contact structure means the contact structure of the link of a complex hypersurface singularity given by its complex tangency, which is uniquely determined by [5]. In particular, we determine the supported contact structures for all positive flow-spines with up to 3 vertices and obtain the following tabulation.

**Theorem 1.3.** *The contact manifolds with complexity up to 3 are determined as follows:*

- (1)  $c(M, \xi) = 1$  if and only if  $(M, \xi) = (S^3, \xi_{\text{std}})$ ;
- (2)  $c(M, \xi) = 2$  if and only if  $(M, \xi) = (\mathbb{R}P^3, \xi_{\text{tight}})$  or  $(L(3, 2), \xi_{\text{tight}})$ ;
- (3)  $c(M, \xi) = 3$  if and only if  $(M, \xi) = (L(3, 1), \xi_{\text{tight}}), (L(4, 3), \xi_{\text{tight}}), (L(5, 2), \xi_{\text{tight}})$  or the quaternion space with the canonical contact structure.

Here  $\xi_{\text{std}}$  denote the standard contact structure on  $S^3$  and  $\xi_{\text{tight}}$  a tight contact structure.

All the contact manifolds with complexity up to 3 are tight. In some sense, this means that tight contact manifolds have smaller complexities than overtwisted ones.

This paper is organized as follows: In Section 2, we shortly recall known results in 3-dimensional contact topology that will be used in this paper. In Section 3, we introduce flow-spines and DS-diagrams. New observation starts from Section 4, where we introduce the admissibility condition and the notion of positivity for flow-spines. In Section 5, we introduce the reference 1-form  $\eta$  for a positive flow-spine that plays an important role in the proof of Theorem 1.1. The proof of the existence of the supported contact structure in Theorem 1.1 is given in Section 6 and the proof of its uniqueness is given in Section 7. Section 8 is devoted to the proof of Theorem 1.2. In Section 9, we introduce several techniques to determine the supported contact structures for given positive flow-spines and prove Theorem 1.3. The list of positive flow-spines with up to 3 vertices is given in the appendix.

The authors wish to express their gratitude to Riccardo Benedetti for many insightful comments. The second author would like to thank Shin Handa and Atsushi Ichikawa for useful discussions in the early stages of research. The second author is supported by JSPS KAKENHI Grant Numbers JP19K03499, JP17H06128 and Keio University Academic Development Funds for Individual Research. The third author is supported by JSPS KAKENHI Grant Numbers JP15H03620, JP17K05254, JP17H06463, and JST CREST Grant Number JPMJCR17J4. The fourth author is supported by JSPS KAKENHI Grant Number JP19K21019.

## 2. CONTACT 3-MANIFOLDS

Throughout this paper, for a polyhedral space  $X$ ,  $\text{Int } X$  represents the interior of  $X$ ,  $\partial X$  represents the boundary of  $X$ , and  $\text{Nbd}(Y; X)$  represents a closed regular neighborhood of a subspace  $Y$  of  $X$  in  $X$ , where  $X$  is equipped with the natural PL structure if  $X$  is a smooth manifold. The set  $\text{Int Nbd}(Y; X)$  is the interior of  $\text{Nbd}(Y; X)$  in  $X$ .

In this section, we briefly recall notions and known results in 3-dimensional contact topology that will be used in this paper. The reader may find general explanation, for instance, in [13, 16, 42].

Let  $M$  be a closed, oriented, smooth 3-manifold. A *contact structure* on  $M$  is the 2-plane field on  $M$  given by the kernel of a 1-form  $\alpha$  on  $M$  satisfying  $\alpha \wedge d\alpha \neq 0$  everywhere. The 1-form  $\alpha$  is called a *contact form*. If  $\alpha \wedge d\alpha > 0$  everywhere on  $M$  then the contact structure given by  $\ker \alpha$  is called a *positive contact structure* and the 1-form  $\alpha$  is called a *positive contact form*. The pair of a closed, oriented, smooth 3-manifold  $M$  and a contact structure  $\xi = \ker \alpha$  on  $M$  is called a *contact 3-manifold* and denoted by  $(M, \xi)$ . In this paper, by a contact structure we mean a positive one.

There are two ways of classification of contact 3-manifolds: up to isotopy and up to contactomorphism. Two contact structures  $\xi$  and  $\xi'$  on  $M$  are said to be *isotopic* if there exists a one-parameter family of contact forms  $\alpha_t$ ,  $t \in [0, 1]$ , such that  $\xi = \ker \alpha_0$  and  $\xi' = \ker \alpha_1$ . Two contact 3-manifolds  $(M, \xi)$  and  $(M', \xi')$  are said to be *contactomorphic* if there exists a diffeomorphism  $\phi : M \rightarrow M'$  such that  $\phi_*(\xi) = \xi'$ . The map  $\phi$  is called a *contactomorphism*. If  $M = M'$  then we also say that  $\xi$  and  $\xi'$  are contactomorphic. The Gray theorem states that if two contact structures are isotopic then they are contactomorphic [20].

The contact structure  $\xi_{\text{std}}$  on  $S^3$  given as the kernel of the 1-form  $\alpha_{\text{std}} = \sum_{j=1}^2 (x_j dy_j - y_j dx_j)|_{S^3}$  is called the *standard contact structure on  $S^3$* , where  $(x_1 + \sqrt{-1}y_1, x_2 + \sqrt{-1}y_2)$  are the standard coordinates of  $\mathbb{C}^2$  and  $S^3$  is the unit sphere in  $\mathbb{C}^2$ . We also say that  $\xi_{\text{std}}$  is the 2-plane field given by the complex tangency at each point of  $S^3$  in  $\mathbb{C}^2$ . This contact structure satisfies the following important property, called “tightness”, which was shown by Bennequin [4]. A contact structure  $\xi$  on  $M$  is said to be *tight* if there does not exist a disk  $D$  embedded in  $M$  such that  $\partial D$  is everywhere tangent to  $\xi$  and the framing of  $D$  along  $\partial D$  coincides with that of  $\xi$ . Otherwise  $\xi$  is said to be *overtwisted* and the disk  $D$  is called an *overtwisted disk*. Note that the tightness is an invariant of contact 3-manifolds up to contactomorphism. Due to Eliashberg, it is shown that the classification of overtwisted contact structures on  $M$  up to isotopy is equivalent to the classification of homotopy classes of 2-plane fields on  $M$  [7]. Therefore, in 3-dimensional contact topology, determining tightness of contact 3-manifolds and classifying tight contact 3-manifolds become crucial problems.

It is shown by Eliashberg [9] that  $S^3$ ,  $S^2 \times S^1$  and  $\mathbb{RP}^3$  admit the unique tight contact structure. The tight contact structures on the lens space  $L(p, q)$  are classified by Giroux [18] and Honda [22]. The number of isotopy classes of tight contact structures of  $L(p, q)$  is determined by  $p$  and  $q$ . For convenience, we write the numbers for first few lens spaces in Table 1 below. The involution of  $L(p, q)$  gives a contactomorphism between the contact structures corresponding to the euler classes  $e \in H_1(L(p, q); \mathbb{Z})$  and  $p - e \in H_1(L(p, q); \mathbb{Z})$ , see [12, 22]. The numbers of contactomorphism classes are also written in the table.

| 3-manifold | $S^3$ | $\mathbb{RP}^3$ | $L(3, 1)$ | $L(3, 2)$ | $L(4, 1)$ | $L(4, 3)$ | $L(5, 1)$ | $L(5, 2)$ | $L(5, 4)$ |
|------------|-------|-----------------|-----------|-----------|-----------|-----------|-----------|-----------|-----------|
| isotopy    | 1     | 1               | 2         | 1         | 3         | 1         | 4         | 2         | 1         |
| contactom. | 1     | 1               | 1         | 1         | 2         | 1         | 2         | 1         | 1         |

TABLE 1. The numbers of isotopy classes and contactomorphism classes of tight contact structures.

Next we introduce the Reeb vector field. Let  $\alpha$  be a contact form on  $M$ . A vector field  $X$  on  $M$  determined by the conditions  $d\alpha(X, \cdot) = 0$  and  $\alpha(X) = 1$  is called the *Reeb vector field* of  $\alpha$  on  $M$ . Such a vector field is uniquely determined by  $\alpha$  and we denote it by  $R_\alpha$ . The non-singular flow on a 3-manifold  $M$  generated by a Reeb vector field is called a *Reeb flow*.

The Reeb vector field plays important roles in many studies in contact geometry and topology. In 3-dimensional contact topology, it is used to give a correspondence between contact structures and open book decompositions of 3-manifolds. Let  $\Sigma$  be an oriented, compact surface with boundary and  $\phi : \Sigma \rightarrow \Sigma$  be a diffeomorphism such that  $\phi|_{\partial\Sigma}$  is the identity map on  $\partial\Sigma$ . If a closed, oriented 3-manifold  $M$  is orientation-preservingly homeomorphic to the quotient space obtained from  $\Sigma \times [0, 1]$  by the identification  $(x, 1) \sim (\phi(x), 0)$  for  $x \in \Sigma$  and  $(y, 0) \sim (y, t)$  for each  $y \in \partial\Sigma$  and any  $t \in [0, 1]$ , then we say that it is an open book decomposition of  $M$ . The image  $L$  of  $\partial\Sigma$  in  $M$  by the quotient map is called the *binding*, which equips the orientation as the boundary of  $\Sigma$ . The image of the surface  $\Sigma \times \{t\}$  in  $M$  is called a *page*. We denote the open book by  $(M, \Sigma, L, \phi)$ .

A contact structure  $\xi$  on  $M$  is said to be *supported* by an open book  $(M, \Sigma, L, \phi)$  if there exists a contact form  $\alpha$  on  $M$  such that  $\xi = \ker \alpha$  and the Reeb vector field  $R_\alpha$  of  $\alpha$  satisfies that

- $R_\alpha$  is tangent to  $L$  and the orientation on  $L$  induced from  $\Sigma$  coincides with the direction of  $R_\alpha$ , and
- $R_\alpha$  is positively transverse to  $\text{Int } \Sigma \times \{t\}$  for any  $t \in [0, 1]$ .

Any open book has a supported contact structure and this is used by Thurston and Winkelnkemper to prove that any closed, oriented, smooth 3-manifold admits a contact structure [47]. Note that the existence of a contact structure for any 3-manifold was first proved by Martinet [38]. Giroux then showed that the contact structure supported by a given open book is unique up to isotopy [19]. He also proved the following theorem, that will be used in the proof of Theorem 1.2.

**Theorem 2.1** (Giroux, cf. [13]). *For any contact 3-manifold  $(M, \xi)$ , there exists an open book decomposition of  $M$  that supports  $\xi$ .*

These results of Giroux give the surjection

$$\{\text{Open book decompositions of } M\}/\text{isotopy} \rightarrow \{\text{Contact structures on } M\}/\text{isotopy}$$

for any closed, oriented, smooth 3-manifold  $M$  and the surjection

$$\{\text{Open books}\}/\text{homeomorphism} \rightarrow \{\text{Contact 3-manifolds}\}/\text{contactomorphism}.$$

Taking the quotient of the set of open books of  $M$  by an operation for pages of open books, called *stabilizations*, we can think one-to-one correspondence between open books and contact 3-manifolds, that is called the *Giroux correspondence*.

### 3. FLOW-SPINES AND DS-DIAGRAMS

**3.1. Branched polyhedron.** A compact topological space  $P$  is called a *simple polyhedron*, or a *quasi-standard polyhedron*, if every point of  $P$  has a regular neighborhood homeomorphic to one of the three local models shown in Figure 2. A point whose regular neighborhood is shaped on the model (iii) is called a *true vertex* of  $P$  (or *vertex* for short), and we denote the set of true vertices of  $P$  by  $V(P)$ . The set of points whose regular neighborhoods are shaped on the models (ii) and (iii) is called the *singular set* of  $P$ , and we denote it by  $S(P)$ . Each connected component of  $P \setminus S(P)$  is called a *region* of  $P$  and each connected component of  $S(P) \setminus V(P)$  is called an *edge* of  $P$ . A simple polyhedron  $P$  is said to be *special*, or *standard*, if each region of  $P$  is an open disk and each edge of  $P$  is an open arc. Throughout this paper, we assume that all regions are orientable.

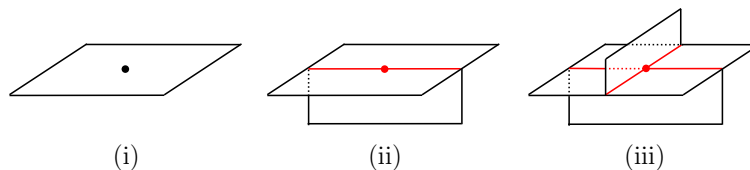


FIGURE 2. The local models of a simple polyhedron.

A *branching* of a simple polyhedron  $P$  is an assignment of orientations to regions of  $P$  such that the three orientations on each edge of  $P$  induced by the three adjacent regions do not agree. We note that even though each region of a simple polyhedron  $P$  is orientable,  $P$  does not necessarily admit a branching. See [26, 2, 33, 44] for general properties of branched polyhedra.

**3.2. Flow-spines and DS-diagrams.** A polyhedron  $P$  is called a *spine* of a closed, connected, oriented 3-manifold  $M$  if it is embedded in  $M$  and  $M$  with removing an open ball collapses onto  $P$ . If a spine is simple then it is called a *simple spine*.

If a spine  $P$  admits a branching, then it allows us to smoothen  $P$  in the ambient manifold  $M$  as in the local models shown in Figure 3. A point of  $P$  whose regular neighborhood is shaped on the model (iii) is called a *vertex of  $\ell$ -type* and that on the model (iv) is a *vertex of  $r$ -type*.

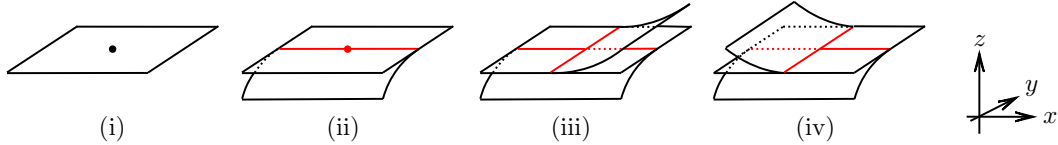


FIGURE 3. The local models of a branched simple polyhedron.

*Definition.* Let  $M$  be a closed, connected, oriented 3-manifold.

- (1) Let  $(M, \mathcal{F})$  be a pair of  $M$  and a non-singular flow  $\mathcal{F}$  on  $M$ . A simple spine  $P$  of  $M$  is called a *flow-spine* of  $(M, \mathcal{F})$  if, for each point  $p \in P$ , there exists a positive coordinate chart  $(U; x, y, z)$  of  $M$  around  $p$  such that  $(U, p)$  is one of the models in Figure 3, where  $\mathcal{F}|_U$  is generated by  $\frac{\partial}{\partial z}$ , and  $\mathcal{F}|_{M \setminus P}$  is a constant vertical flow shown in Figure 4.
- (2) A branched simple spine  $P$  of  $M$  is called a *flow-spine* of  $M$  if it is a flow-spine of  $(M, \mathcal{F})$  for some non-singular flow  $\mathcal{F}$  on  $M$ . The flow  $\mathcal{F}$  is said to be *carried by  $P$* .

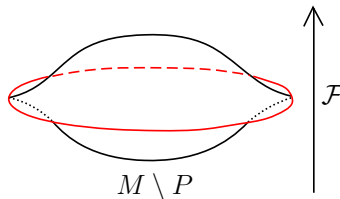


FIGURE 4. The flow in the complement  $M \setminus P$ .

Let  $B^3$  be the unit ball in  $\mathbb{R}^3$  equipped with the right-handed orientation. Consider a homeomorphism  $\iota$  from  $M \setminus P$  to the interior of  $B^3$  that takes the biggest horizontal open disk in Figure 4 to the horizontal open disk bounded by the equator  $E$  of  $B^3$ . Now we take the geometric completions of these open balls. Then the inverse map  $\iota^{-1}$  induces

a continuous map  $j$  from  $B^3$  to  $M$  that maps the boundary  $S^2$  of  $B^3$  to the flow-spine  $P$ . The preimage of the singular set  $S(P)$  of  $P$  by the map  $j$  constitutes a trivalent graph  $G$  on  $S^2$  containing the equator  $E$ . The map  $j$  restricted to  $S^2$ , denoted by  $j'$ , is called the *identification map*.

Let  $R_1, R_2, \dots, R_n$  be the regions of  $P$  that are oriented so that the flow  $\mathcal{F}$  is positively transverse to these regions. Let  $S^+$  and  $S^-$  denote the upper and lower hemispheres of  $S^2$ , respectively. The identification map  $j'$  satisfies the following properties:

- The preimage of each region  $R_i$  by  $j'$  consists of two connected regions  $R_i^+$  and  $R_i^-$  bounded by  $G$  each of which is homeomorphic to  $R_i$  and which are contained in  $S^+$  and  $S^-$ , respectively.
- The orientation of  $R_i^+$  (respectively,  $R_i^-$ ) induced from that of  $B^3$  coincides with (respectively, is opposite to) the orientation of  $R_i$  through the map  $j'$ .

The 3-manifold  $M$  is restored from  $B^3$  by identifying the pairs of regions  $R_i^+$  and  $R_i^-$  for  $i = 1, \dots, n$ .

*Definition.* The trivalent graph  $G$  on  $S^2$  equipped with the identification map  $j'$  obtained from a flow-spine  $P$  of  $M$  as above is called the *DS-diagram* of  $P$ . The equator  $E$  in  $G$  is called the *E-cycle* of  $G$ . The *E-cycle* is oriented as the boundary of  $S^+$  with the orientation induced from that of  $B^3$ .

**Remark 3.1.** (1) *To be precise, the DS-diagram defined above is a DS-diagram with an E-cycle. If a simple spine is given then we may obtain its DS-diagram without E-cycles in the same manner. There is a formal definition of E-cycles for DS-diagrams, see [27]. Note that a DS-diagram of a simple spine may have several possible positions of E-cycles. In this paper, by a DS-diagram we mean a DS-diagram with a fixed E-cycle.*

- (2) *Conversely, if a DS-diagram  $G$  with an E-cycle is given, we may obtain a closed 3-manifold  $M$  from the diagram by using the identification map  $j'$ . The image  $j'(S^2)$  in  $j(B^3) = M$  is a flow-spine of  $M$ .*

For convenience, taking the stereographic projection  $\pi$  of  $S^2$  from the south pole, we describe the DS-diagram  $G$  on the real plane  $\mathbb{R}^2$  so that  $\pi(E)$  is the unit circle,  $\pi(S^+)$  is the inside of  $\pi(E)$  and  $\pi(S^-)$  is the outside. The real plane  $\mathbb{R}^2$  is oriented such that it coincides with that of  $S^2$  as the boundary of  $B^3$ . The image  $\pi(R_i^+)$  lies on  $\pi(S^+)$  (respectively,  $\pi(R_i^-)$  lies on  $\pi(S^-)$ ) and its orientation induced from that of  $R_i$  coincides with (respectively, is opposite to) the orientation of  $\mathbb{R}^2$ . For simplicity, we denote  $\pi(E)$ ,  $\pi(R_i^+)$  and  $\pi(R_i^-)$  by  $E$ ,  $R_i^+$  and  $R_i^-$ , respectively.

*Example 1.* Consider the diagram described on the left in Figure 5. The 3-manifold  $M$  is obtained from  $B^3$  by identifying  $R_i^+$  and  $R_i^-$  for  $i = 1, 2$  so that the labeled edges along their boundary coincide. Let  $P$  be the simple spine obtained as the image of  $S^2$  by the identification map  $j'$ . The edges with label  $e_i$  are the preimage of the edge  $e_i$  of  $P$  by  $j'$  and the vertices with label  $v$  are the preimage of the vertex  $v$  of  $P$ . The right-top is the union of  $\text{Nbd}(S(P); P)$  and the region  $R_2$ , which is obtained from the union of  $R_2^+$ ,  $R_2^-$  and neighborhoods of the edges and the vertices by identifying them by  $j'$ . The polyhedron  $P$  is obtained from this branched polyhedron by attaching the

region  $R_1$  along the boundary. Remark that the branched polyhedron on the right-top in Figure 5 is abstract, not an object embedded in  $\mathbb{R}^3$ . The polyhedron  $P$  embedded in  $\mathbb{R}^3 \subset S^3$  is described on the right-bottom. This polyhedron can be obtained from the 3-ball by collapsing from the boundary. Hence it is a spine of  $S^3$ . Furthermore, setting a flow in  $\text{Nbd}(P; S^3)$  positively transverse to  $P$  and extending it to  $S^3 \setminus P$  canonically as in Figure 4, we may see that  $P$  is a flow-spine of  $S^3$ . It will be shown in Lemma 9.1 that the flow tangent to the Seifert fibration whose regular orbit is a  $(2, 3)$ -torus knot is carried by  $P$ . Thus, it supports the standard contact structure on  $S^3$ , which will be stated in Corollary 9.2. This flow-spine is called the *positive abalone*. The flow-spine obtained from the mirror of the DS-diagram on the left in Figure 5 is called the *negative abalone*. The abalone in Figure 5 is named “positive” since it supports the standard contact structure on  $S^3$ . The underlying abstract simple polyhedra of the positive and negative abalones are the same. This polyhedron first appeared in [23]. See also [24].

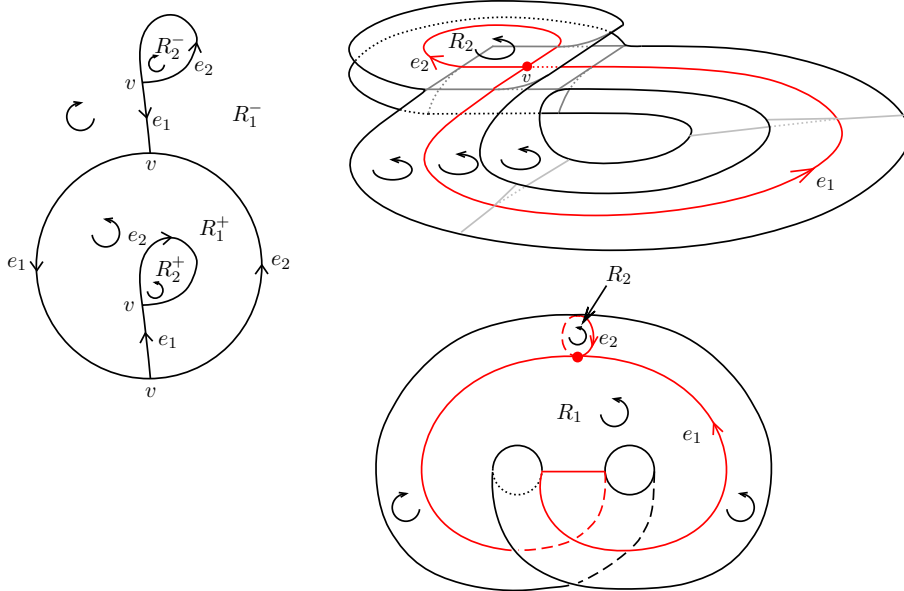


FIGURE 5. The positive abalone. The left diagram is its DS-diagram, the right-top is the union of  $\text{Nbd}(S(P); P)$  and the region  $R_2$  with branching structure, and the right-bottom is the positive abalone embedded in  $S^3$ .

**3.3. Normal pairs.** In this subsection, we introduce the flow-spine from a normal pair. This is the original definition of a flow-spine given in [26]. Let  $\mathcal{F}$  be a non-singular flow on  $M$ . A compact surface  $\Sigma$  embedded in  $M$  with boundary  $\partial\Sigma$  is called a *compact local section* of  $\mathcal{F}$  if it is included in an open surface that is transverse to  $\mathcal{F}$  everywhere. We define two functions  $T_+$  and  $T_-$  on  $M$  as

$$T_+(x) = \inf\{t > 0 \mid \mathcal{F}(x; t) \in \Sigma\} \text{ and}$$

$$T_-(x) = \sup\{t < 0 \mid \mathcal{F}(x; t) \in \Sigma\},$$

where  $\mathcal{F}(x; t)$  means that the flow  $\mathcal{F}$  brings the point  $x$  to the point  $\mathcal{F}(x; t)$  after the time  $t \in \mathbb{R}$ . We set  $T_+(x) = \infty$  (respectively,  $T_-(x) = -\infty$ ) if  $\mathcal{F}(x; t) \notin \Sigma$  for any  $t > 0$  (respectively,  $t < 0$ ). If  $T_+(x) < \infty$  (respectively,  $T_-(x) > -\infty$ ) then we define  $\hat{T}_+(x)$  (respectively,  $\hat{T}_-(x)$ ) by  $\mathcal{F}(x; T_+(x))$  (respectively,  $\mathcal{F}(x; T_-(x))$ ).

*Definition.* The pair  $(\mathcal{F}, \Sigma)$  of a non-singular flow  $\mathcal{F}$  on  $M$  and its compact local section  $\Sigma$  is called a *normal pair* on  $M$  if

- (i)  $\Sigma$  is a 2-disk,
- (ii) any orbit of  $\mathcal{F}$  intersects  $\text{Int } \Sigma$ ,
- (iii) if  $x \in \partial\Sigma$  and  $\hat{T}_+(x) \in \partial\Sigma$  then  $\partial\Sigma$  and  $\mathcal{F}(\partial\Sigma; T_+(x))$  intersect at  $\hat{T}_+(x)$  transversely, and
- (iv) if  $x \in \partial\Sigma$  and  $\hat{T}_+(x) \in \partial\Sigma$  then  $\hat{T}_+(\hat{T}_+(x)) \in \text{Int } \Sigma$ .

The conditions (iii) and (iv) are satisfied by setting  $\Sigma$  in general position.

For a normal pair  $(\mathcal{F}, \Sigma)$ , let  $P_+(\mathcal{F}, \Sigma)$  and  $P_-(\mathcal{F}, \Sigma)$  be the subsets of  $M$  defined as

$$P_+(\mathcal{F}, \Sigma) = \Sigma \cup \{\mathcal{F}(x; t) \mid x \in \partial\Sigma, 0 \leq t \leq T_+(x)\} \text{ and}$$

$$P_-(\mathcal{F}, \Sigma) = \Sigma \cup \{\mathcal{F}(x; t) \mid x \in \partial\Sigma, T_-(x) \leq t \leq 0\}.$$

Roughly speaking, the subsets  $P_+(\mathcal{F}, \Sigma)$  and  $P_-(\mathcal{F}, \Sigma)$  are obtained from  $\Sigma$  by floating  $\partial\Sigma$  by the flow  $\mathcal{F}$  and  $-\mathcal{F}$ , respectively. Therefore, they are simple polyhedra. Floating  $\text{Nbd}(\partial\Sigma; \Sigma)$ , instead of  $\partial\Sigma$ , smoothly, we can easily see that these polyhedra are flow-spines.

An important fact is that any non-singular flow has a normal pair and hence the following theorem holds.

**Theorem 3.2** ([26]). *Any pair  $(M, \mathcal{F})$  of a closed, connected, oriented, smooth 3-manifold  $M$  and a non-singular flow  $\mathcal{F}$  on  $M$  admits a flow-spine.*

The existence of a normal pair of a given flow after a slight deformation is mentioned in [26, Remark (1) in page 509]. We may easily remove the necessity of a slight deformation of the flow as follows. For each point  $x$  in  $M$ , we choose a pair of a flow-box of  $\mathcal{F}$  and a disk intersecting all orbits of  $\mathcal{F}$  in the flow-box transversely. Since  $M$  is compact, we may choose a finite set of these flow-boxes so that the union of the disks in these flow-boxes intersects all orbits of  $\mathcal{F}$ . We then isotope the positions of these disks with keeping the same property so that they are disjoint. Then the disk  $\Sigma$  of a normal pair can be obtained by connecting these disks by bands transverse to  $\mathcal{F}$  as done in the proof of [26, Theorem 1.1]. The flow-spine in Theorem 3.2 is obtained from the normal pair  $(\mathcal{F}, \Sigma)$  by [26, Theorem 1.2].

The disk of a normal pair is restored from a flow-spine by cleaving it along the singular set as shown in Figure 6. The flow-spine in the figure is  $P_+(\mathcal{F}, \Sigma)$  for this normal pair  $(\mathcal{F}, \Sigma)$ . Assign the orientation to  $\partial\Sigma$  induced from that of  $\Sigma$ , which is the orientation indicated in the figure, and observe the function  $T_+$  from  $\partial\Sigma$  to  $\mathbb{R}$ . This function is left-continuous at the point  $x$  in the figure if the vertex is of  $\ell$ -type and it is right-continuous if the vertex is of  $r$ -type.

**3.4. Regular moves.** In this subsection, we introduce two kinds of moves of branched simple polyhedra.

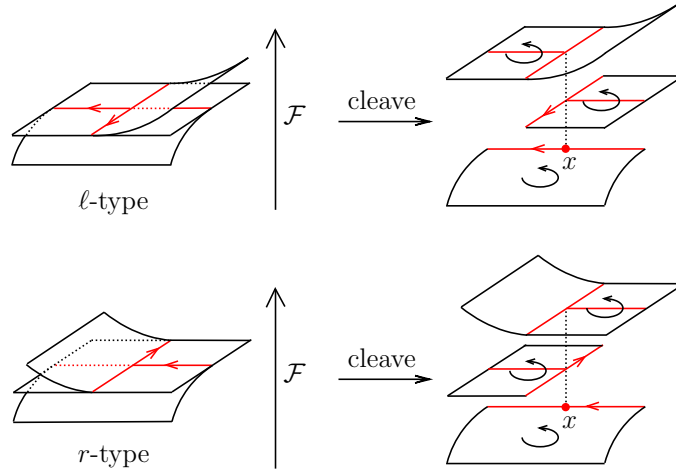


FIGURE 6. Cleave the flow-spine and obtain the disk of a normal pair.

- Definition.* (1) The moves shown in Figure 7 and their mirrors are called *first regular moves* [27] or *Matveev-Piergallini moves* [2].
- (2) The moves shown in Figure 8 and their mirrors are called *second regular moves* [27] or *lune moves* [40].

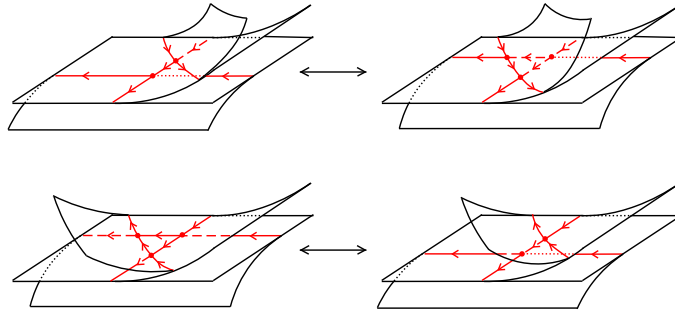


FIGURE 7. First regular moves.

These moves are enough to trace deformation of non-singular flows in 3-manifolds. Two non-singular flows  $\mathcal{F}_1$  and  $\mathcal{F}_2$  in a closed, orientable 3-manifold are said to be *homotopic* if there exists a smooth deformation from  $\mathcal{F}_1$  to  $\mathcal{F}_2$  in the set of non-singular flows.

**Theorem 3.3** ([27]). *Let  $P_1$  and  $P_2$  be flow-spines of a closed, orientable 3-manifold  $M$ . Let  $\mathcal{F}_1$  and  $\mathcal{F}_2$  be flows on  $M$  carried by  $P_1$  and  $P_2$ , respectively. Suppose that  $\mathcal{F}_1$  and  $\mathcal{F}_2$  are homotopic. Then  $P_1$  is obtained from  $P_2$  by applying first and second regular moves successively.*

**Remark 3.4.** *We may apply the moves from the left to the right in Figures 7 and 8 with fixing the flow carried by the flow-spine. On the other hand, we may need to homotope*

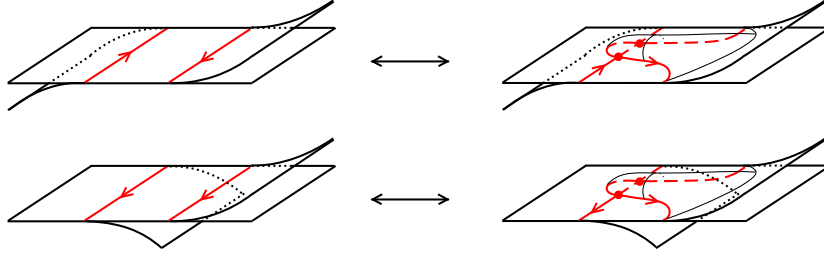


FIGURE 8. Second regular moves.

the flow when we apply the moves from the right to the left. Sometimes, such homotopy move cannot be obtained in the set of Reeb flows, see the proof of Theorem 4.3 below.

#### 4. ADMISSIBILITY AND POSITIVITY

**4.1. Admissibility condition.** Let  $M$  be a closed, connected, oriented 3-manifold. Let  $P$  be a branched simple spine of  $M$  and  $R_1, \dots, R_n$  be the regions of  $P$ . Assign orientations to these regions so that they satisfy the branching condition. Let  $\bar{R}_i$  be the metric completion of  $R_i$  with the path metric inherited from a Riemannian metric on  $R_i$ . Let  $\kappa_i : \bar{R}_i \rightarrow M$  be the natural extension of the inclusion  $R_i \rightarrow M$ . Assign an orientation to each edge of  $P$  in an arbitrary way.

*Definition.* A branched simple spine  $P$  is said to be *admissible* if there exists an assignment of real numbers  $x_1, \dots, x_m$  to the edges  $e_1, \dots, e_m$ , respectively, of  $P$  such that for any  $i \in \{1, \dots, n\}$

$$(4.1) \quad \sum_{\tilde{e}_j \subset \partial \bar{R}_i} \varepsilon_{ij} x_j > 0,$$

where  $\tilde{e}_j$  is an open interval or a circle on  $\partial \bar{R}_i$  such that  $\kappa_i|_{\tilde{e}_j} : \tilde{e}_j \rightarrow e_j$  is a homeomorphism, and  $\varepsilon_{ij} = 1$  if the orientation of  $e_j$  coincides with that of  $\kappa_i(\tilde{e}_j)$  induced from the orientation of  $R_i$  and  $\varepsilon_{ij} = -1$  otherwise.

*Example 2.* Let  $P$  be the positive abalone in Figure 5 embedded in  $S^3$ . Suppose that there exists a contact structure supported by  $P$ , that is, there exists a contact form  $\alpha$  on  $S^3$  whose Reeb flow is carried by  $P$ . The abalone  $P$  is obtained from the branched polyhedron described on the right-top in the figure by attaching the disk corresponding to the region  $R_1$ . Since the Reeb flow is transverse to the regions  $R_1$  and  $R_2$ , the integrated values  $\int_{\partial R_1} \alpha$  and  $\int_{\partial R_2} \alpha$  should be positive, where the orientation of  $\partial R_i$  is induced from that of  $R_i$  for each  $i = 1, 2$ . From the figure, we see that  $\partial R_1 = e_1 + 2e_2$  and  $\partial R_2 = -e_2$ . Setting  $x_1 = \int_{e_1} \alpha$  and  $x_2 = \int_{e_2} \alpha$ , we have the inequalities  $x_1 + 2x_2 > 0$  and  $x_2 < 0$ . Therefore, the existence of an assignment of real numbers  $x_1, x_2$  satisfying these inequalities to the edges  $e_1, e_2$  is a necessary condition for  $\text{Nbd}(P; S^3)$  to have a contact form whose Reeb flow is positively transverse to  $P$ . This is the admissibility condition. Since  $(x_1, x_2) = (3, -1)$  satisfies the two inequalities, the positive abalone  $P$  is admissible.

There are many flow-spines that satisfy the admissibility condition. Below, we show that any branched special spine of a rational homology 3-sphere satisfies the condition.

Let  $m'$  be the rank of  $H_1(S(P); \mathbb{Z})$ . Take a maximal tree  $T$  of  $S(P)$  and assign 0 to the edges on  $T$ . Let  $e_{j_1}, \dots, e_{j_{m'}}$  be the edges on  $S(P)$  not contained in  $T$  and set

$$a_{ij} = \sum_{\tilde{e}_j \subset \partial \tilde{R}_i} \varepsilon_{ij}$$

for  $i = 1, \dots, n$  and  $j = j_1, \dots, j_{m'}$ . In this setting,  $P$  is admissible if and only if the set

$$C(P) = \{(x_1, \dots, x_{m'}) \in \mathbb{R}^{m'} \mid a_{ij_1}x_1 + \dots + a_{ij_{m'}}x_{m'} > 0, \ i = 1, \dots, n\}$$

is non-empty.

Let  $A$  be the  $n \times m'$  matrix with the entries  $a_{ij}$ . If the spine is special then  $A$  is a regular matrix.

**Lemma 4.1.** *Let  $P$  be a branched special spine of  $M$ . Then  $\det(A) \neq 0$  if and only if  $M$  is a rational homology 3-sphere.*

*Proof.* The manifold  $M$  has a cell decomposition whose 0-cells are the vertices of  $S(P)$ , 1-cells correspond to the edges of  $S(P)$ , 2-cells correspond to the open disks  $P \setminus S(P)$  and 3-cell corresponds to the open 3-ball  $M \setminus P$ . Consider the chain complex of this decomposition:

$$0 \rightarrow C_3 \xrightarrow{\partial_3} C_2 \xrightarrow{\partial_2} C_1 \xrightarrow{\partial_1} C_0 \rightarrow 0,$$

where  $C_i$  is the chain of  $i$ -dimensional cells. The map  $\partial_3$  is the zero map because each 2-cell appears twice on the boundary of the 3-cell with opposite orientations. The map  $\partial_2$  is given by the matrix  $A$ . Since  $H_2(M; \mathbb{Z})$  has no torsion,  $\det(A) \neq 0$  if and only if  $H_2(M; \mathbb{Z}) = 0$ . By Poincaré duality and the universal coefficient theorem,  $H_2(M; \mathbb{Z}) = 0$  if and only if  $H_i(M; \mathbb{Q}) = H_i(S^3; \mathbb{Q})$  for  $i \in \mathbb{Z}$ . Thus the assertion follows.  $\square$

**Proposition 4.2.** *A branched special spine of a rational homology 3-sphere is admissible.*

*Proof.* The set  $C(P)$  is the union of the  $m'$  open half spaces in  $\mathbb{R}^{m'}$  given by  $a_{ij_1}x_1 + \dots + a_{ij_{m'}}x_{m'} > 0$  for  $i = 1, \dots, m'$ . Since we are considering a rational homology 3-sphere, we have  $\det(A) \neq 0$  by Lemma 4.1. Therefore the vectors  ${}^t(a_{ij_1}, \dots, a_{ij_{m'}})$ ,  $i = 1, \dots, m'$ , are linearly independent and hence  $C(P)$  is non-empty.  $\square$

*Example 3.* Let  $S$  be an oriented 2-sphere with two disjoint oriented disks  $D_1$  and  $D_2$  in  $S$  and let  $P$  be the branched polyhedron obtained from  $S$  by identifying  $D_1$  and  $D_2$  by an orientation-preserving diffeomorphism. Then  $P$  is a flow-spine of  $S^2 \times S^1$  without vertices (cf. [11, Remark 1.2]). The flow described in Figure 9 is a flow carried by  $P$ . This flow-spine satisfies  $C(P) = \emptyset$  and hence it is not admissible. In particular, there does not exist a contact form on  $S^2 \times S^1$  whose Reeb flow is positively transverse to  $P$ .

*Example 4.* Let  $P$  be the flow-spine given by the DS-diagram in Figure 10. This polyhedron is special and has 4 vertices. From the cell decomposition of  $P$ , we may easily see that the closed 3-manifold  $M_P$  of  $P$  satisfies  $H_1(M_P; \mathbb{Z}) \cong \mathbb{Z}$ . Since there is no closed, orientable, irreducible 3-manifold  $M$  with  $H_1(M; \mathbb{Z}) \cong \mathbb{Z}$  and with complexity up to 4 in the table of 3-manifolds [40], the 3-manifold  $M_P$  is  $S^2 \times S^1$ . Since  $S^2 \times S^1$  is not

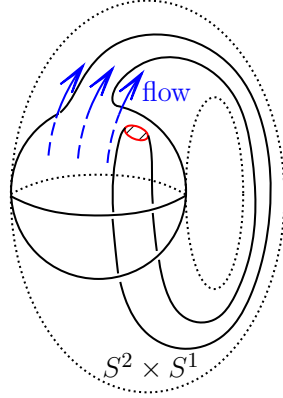


FIGURE 9. A flow-spine of  $S^2 \times S^1$  with  $C(P) = \emptyset$ .

a rational homology 3-sphere, it satisfies  $\det(A) = 0$  by Lemma 4.1. However we have  $C(P) \neq \emptyset$ , and hence it is admissible.

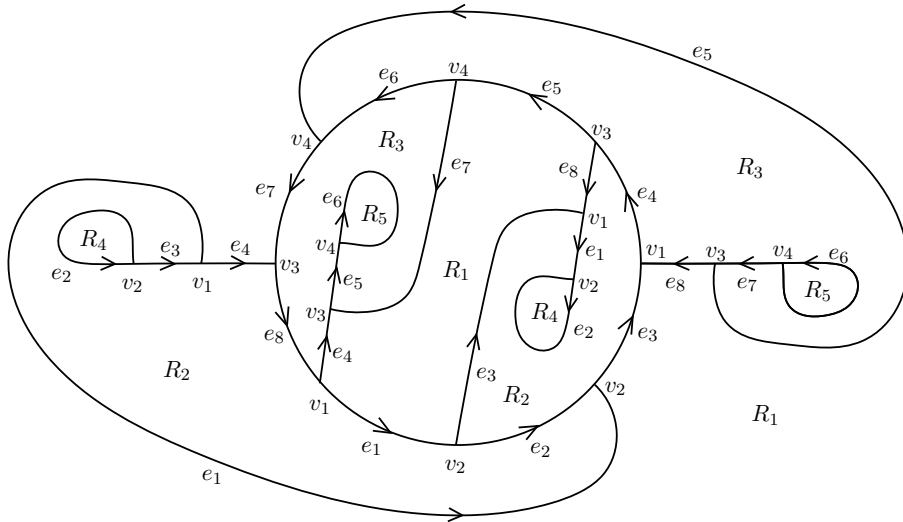


FIGURE 10. A DS-diagram of a flow-spine of  $S^2 \times S^1$  with  $C(P) \neq \emptyset$ .

**4.2. Necessity of positivity.** As mentioned in the introduction, we define the positivity of a flow-spine as follows.

*Definition.* A flow-spine is said to be *positive* if it has at least one vertex and all vertices are of  $\ell$ -type.

Although there is a flow-spine that is not positive but carries a Reeb flow, we need to restrict our discussion to positive flow-spines. The reason is that either the existence

or the uniqueness of a contact manifold for a given flow-spine does not hold at least in some case as we will prove in the following theorem. Recall that a contact structure  $\xi$  on  $M$  is said to be *supported* by a flow-spine  $P$  if there exists a contact form  $\alpha$  such that  $\xi = \ker \alpha$  and its Reeb flow is carried by  $P$ .

**Theorem 4.3.** *Suppose that  $M$  admits a tight contact structure. Then one of the following holds:*

- (1) *There exists a flow-spine of  $M$  that does not support any contact structure.*
- (2) *There exists a flow-spine of  $M$  supporting two contact structures that are not contactomorphic.*

*Proof.* Let  $\xi_0$  and  $\xi_1$  be contact structures on  $M$  that belong to the same homotopy class of 2-plane fields. Let  $\mathcal{F}_0$  and  $\mathcal{F}_1$  be Reeb flows generated by Reeb vector fields of  $\xi_0$  and  $\xi_1$ , respectively. These flows are homotopic. Let  $P_0$  and  $P_1$  be flow-spines that carry  $\mathcal{F}_0$  and  $\mathcal{F}_1$ , respectively.

Suppose that  $\xi_0$  is tight, and let  $\xi_1$  be an overtwisted contact structure on  $M$  obtained from  $\xi_0$  by applying a Lutz full-twist [37]. Note that a Lutz full-twist does not change the homotopy class of  $\xi_0$ . By Theorem 3.3, there exists a sequence  $P_0 = Q_1, Q_2, \dots, Q_m = P_1$  of flow-spines such that  $Q_{i+1}$  is obtained from  $Q_i$  by some regular move for  $i = 1, \dots, m-1$ . Now assume that both of the statements (1) and (2) in the assertion do not hold. Then each  $Q_i$  supports a unique contact structure up to contactomorphism. Since the regular moves from the left to the right in Figures 7 and 8 can be applied with fixing the flows, the contact structures supported by  $Q_i$  and  $Q_{i+1}$  are contactomorphic. Hence  $\xi_0$  and  $\xi_1$  are contactomorphic and this is a contradiction.  $\square$

**Remark 4.4.** *The positive abalone in Figure 5 is a positive flow-spine. The flow-spine in Example 3 carries a flow transverse to  $S^2 \times \{t\}$  for any  $t \in S^1$ . Such a flow cannot be a Reeb flow. This flow-spine is not positive by definition. The flow-spine in Example 4 is positive. The flow carried by this flow-spine is not homotopic to the flow carried by the flow-spine in Example 3. This can be verified by using the Reidemeister-Turaev torsion, see [34, 35].*

**4.3. Admissibility of positive flow-spines.** In this subsection, we prove the following proposition.

**Proposition 4.5.** *Any positive flow-spine satisfies the admissibility condition.*

Let  $P$  be a positive flow-spine. In the DS-diagram of  $P$ , the preimage of each edge  $e_j$  of  $P$  by the identification map  $j'$  consists of three copies of  $e_j$ , one lies on the  $E$ -cycle, another one lies in the inside of the  $E$ -cycle and the last one lies outside. The diagram in a neighborhood of an edge on the  $E$ -cycle is one of the four cases described on the top in Figure 11, the corresponding part of the spine is described in the middle, and the diagram in a neighborhood of the corresponding edge in the inside of the  $E$ -cycle is as shown on the bottom. The  $E$ -cycles in the top and bottom figures are described by dashed lines.

We put the labels  $A^-$  and  $A^+$  to the two sides of each edge of type  $a$  as shown on the bottom in Figure 11 and we put the labels  $B^-, B^+, C^-, C^+, D^-, D^+$  in the same manner.

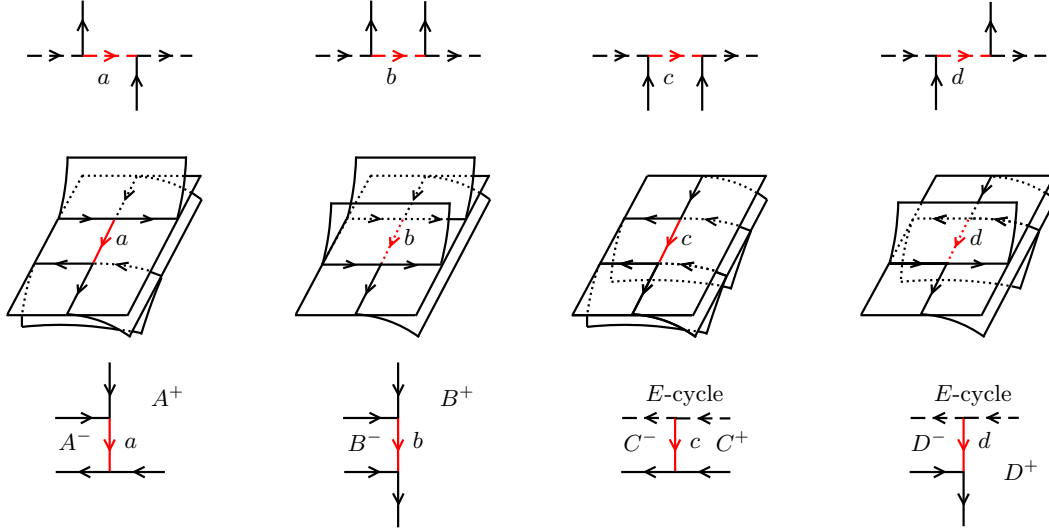


FIGURE 11. Neighborhoods of edges on a DS-diagram.

**Lemma 4.6.** *A region in the inside of the  $E$ -cycle in a DS-diagram and not adjacent to the  $E$ -cycle has only label  $A^-$ .*

*Proof.* Let  $R^+$  be a region in the assertion. From the bottom figures in Figure 11, we see that  $\partial R^+$  does not contain edges of type  $c$  and  $d$ . Hence  $R^+$  has only labels  $A^-$ ,  $A^+$ ,  $B^-$  and  $B^+$ . We observe how the orientations on the edges change when we travel along  $\partial R^+$ . We say that the orientation of an edge is “consistent” if it coincides with that of  $\partial R^+$  and “opposite” otherwise. From the bottom figures in Figure 11, we see that the orientation changes from “consistent” to “opposite” after passing through the sides  $A^+$  and  $B^-$  and there is no case where the orientation changes from “opposite” to “consistent”. Hence  $R^+$  cannot have labels  $A^+$  and  $B^-$ . Moreover, since the orientations of the edges near the sides  $A^-$  and  $B^+$  are “opposite” and “consistent”, respectively,  $R^+$  can have either only label  $A^-$  or only label  $B^+$ . Suppose that it has only label  $B^+$ . Then, from the middle figure in Figure 11, we see that  $j'(\partial R^+)$  corresponds to the  $E$ -cycle. However, in the same figure, we see that there is an edge of  $P$  that is not contained in  $j'(\partial R^+)$ . Since  $S(P)$  is the image of the  $E$ -cycle by  $j'$ , we have a contradiction.  $\square$

Now we prove the proposition.

*Proof of Proposition 4.5.* We set the assignment  $x$  of a real number  $x(e_j)$  to each edge  $e_j$  of the singular set  $S(P)$  of a positive flow-spine  $P$  as

$$\begin{cases} x(e_j) = -\frac{1}{2} & \text{if } e_j \text{ is of type } a \\ x(e_j) = 2 & \text{if } e_j \text{ is of type } b \\ x(e_j) = 3 & \text{if } e_j \text{ is of type } c \\ x(e_j) = 4 & \text{if } e_j \text{ is of type } d. \end{cases}$$

By Lemma 4.6, if a region  $R^+$  lies inside the  $E$ -cycle and is not adjacent to the  $E$ -cycle then  $\sum_{\tilde{e}_j \subset \partial \bar{R}} \varepsilon_{ij} x(e_j) > 0$ .

Let  $R^+$  be a region of the DS-diagram of  $P$  lying inside the  $E$ -cycle and adjacent to the  $E$ -cycle. The boundary  $\partial R^+$  of  $R^+$  consists of an alternative sequence  $p_1, q_1, p_2, q_2, \dots, p_m, q_m$  of paths  $p_1, \dots, p_m$  on the  $E$ -cycle and paths  $q_1, \dots, q_m$  lying inside the  $E$ -cycle, see Figure 12. The orientation of each edge on the path  $p_i$  is consistent with the orientation of  $\partial R^+$ . The starting edge of the path  $q_i$  is of type  $c$  if the label on the region  $R^+$  is  $C^+$  and of type  $d$  if it is  $D^+$ . Their orientations are consistent with that of  $\partial R^+$ . We follow  $q_i$  from the starting edge and check if the orientations of the edges are consistent with or opposite to that of  $\partial R^+$ . From the four figures on the bottom in Figure 11, we see that the orientation changes from “consistent” to “opposite” when  $\partial R^+$  passes through an edge with label  $A^+, B^-, C^+$  or  $D^-$ , and there is no edge where the orientation changes from “opposite” to “consistent”. This means that the path  $q_i$  divides into two paths  $q'_i$  and  $q''_i$  so that the orientations of all edges on  $q'_i$  are consistent with that of  $\partial R^+$  and those of all edges of  $q''_i$  are opposite.

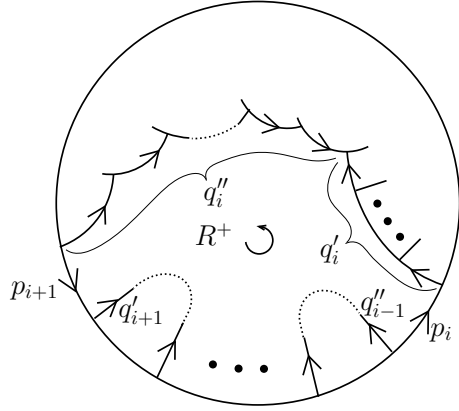


FIGURE 12. The paths  $p_i$  and  $q_i$ , where  $q_i$  is the concatenation of  $q'_i$  and  $q''_i$ .

We are going to observe which types of edges can appear on each of paths  $p_i$  and  $q_i$ . By the four figures on the top in Figure 11, the sequence of types of the edges of  $p_i$  is either  $b$  or  $ac^{n_1}d$ , where  $n_1 \geq 0$ . The sum  $x(p_i)$  of the assignment  $x$  to the edges on  $p_i$  is

$$x(p_i) = \begin{cases} 2 & \text{if the type is } b \\ -\frac{1}{2} + 3n_1 + 4 = 3n_1 + \frac{7}{2} & \text{if the type is } ac^{n_1}d. \end{cases}$$

By the four figures on the bottom in Figure 11, the sequence of types of the edges of  $q'_i$  is either  $c$  or  $db^{n_2}a$ , where  $n_2 \geq 0$ , and the sum  $x(q'_i)$  of the assignment  $x$  to the edges on  $q'_i$  is

$$x(q'_i) = \begin{cases} 3 & \text{if the type is } c \\ 4 + 2n_2 - \frac{1}{2} = 2n_2 + \frac{7}{2} & \text{if the type is } db^{n_2}a. \end{cases}$$

By the same figures, the sequence of types of the edges of  $q_i''$  is either  $d^{-1}$  or  $b^{-1}a^{-n_3}c^{-1}$ , where  $n_3 \geq 0$ , and the sum  $x(q_i'')$  of the assignment  $x$  to the edges on  $q_i''$  is

$$x(q_i'') = \begin{cases} -4 & \text{if the type is } d^{-1} \\ -2 + \frac{1}{2}n_3 - 3 = \frac{1}{2}n_3 - 5 & \text{if the type is } b^{-1}a^{-n_3}c^{-1}. \end{cases}$$

The minimum values of  $x(p_i)$ ,  $x(q_i')$  and  $x(q_i'')$  are 2, 3 and  $-5$ , respectively. Hence the sum of real numbers on the edges on  $\partial R^+$  is positive unless the types of  $p_i$ ,  $q_i'$  and  $q_i''$  are  $b$ ,  $c$  and  $b^{-1}c^{-1}$ , respectively, for all  $i = 1, \dots, m$ .

Suppose that the boundary  $\partial R^+$  of  $R^+$  consists of a sequence of edges

$$(4.2) \quad b_1 c_1 b_2^{-1} c_2^{-1} b_3 c_3 b_4^{-1} c_4^{-1} \cdots b_{2\ell-1} c_{2\ell-1} b_{2\ell}^{-1} c_{2\ell}^{-1},$$

where  $b_j$  is an edge of type  $b$  and  $c_j$  is an edge of type  $c$ . For each  $j = 1, \dots, \ell$ , we set a relation  $\succ$  between two edges  $b_{2j-1}$  and  $b_{2j}$  as  $b_{2j-1} \succ b_{2j}$ . For each region inside the  $E$ -cycle whose boundary is given in the above form, we give the relation  $\succ$  to the edges of type  $b$  in the same manner.

Now assume that there exists a sequence of edges  $e_1, e_2, \dots, e_k$  of  $P$  of type  $b$  that gives a cyclic order as  $e_1 \succ e_2 \succ \cdots \succ e_k \succ e_{k+1} = e_1$ . For each  $s = 1, \dots, k$ , the relation  $e_s \succ e_{s+1}$  implies that there exists a region whose boundary contains the sequence  $e_s f_s e_{s+1}^{-1} f_{s+1}^{-1}$ , where  $f_s$  and  $f_{s+1}$  are edges of type  $c$ . However, this is impossible since the edges  $f_1, \dots, f_{k-1}$  appear on the  $E$ -cycle as shown in Figure 13 and we cannot set  $f_k$  for  $e_k \succ e_1$ . This means that  $\succ$  is a partial order for the edges of  $P$  of type  $b$ .

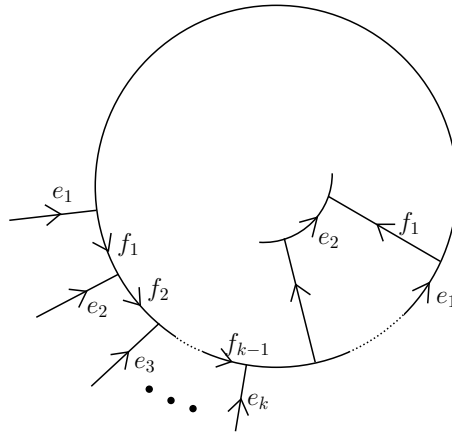


FIGURE 13. Positions of  $e_s$  for  $s = 1, \dots, k$  and  $f_s$  for  $s = 1, \dots, k - 1$ .

Let  $\{e_1, \dots, e_{n_b}\}$  be the set of edges of  $P$  of type  $b$ , equipped with the partial order  $\succ$ . We modify the assignment  $x$  to these edges as  $x(e_j) = 2 + \delta_j$ , where  $\delta_j$ 's are sufficiently small positive real numbers such that  $\delta_{j_1} > \delta_{j_2}$  if  $e_{j_1} \succ e_{j_2}$ . Then the sum of the real numbers assigned to the edges in (4.2) becomes positive. This shows that the modified assignment satisfies the admissibility condition.  $\square$

## 5. REFERENCE 1-FORMS OF POSITIVE FLOW-SPINES

Let  $M$  be a closed, connected, oriented, smooth 3-manifold and  $P$  be a positive flow-spine of  $M$ . In this section, we define a 1-form  $\eta$  on  $M$  associated with  $P$  such that  $\eta \wedge d\eta \geq 0$  using the decomposition (5.1).

**5.1. Decomposition and gluing maps.** For a positive flow-spine  $P$  of  $M$ , set  $Q = \text{Nbd}(S(P); P)$  and let  $\mathcal{R}_i$  be the connected component of  $P \setminus \text{Int } Q$  contained in the region  $R_i$  of  $P$ . Let  $\text{Nbd}(S(P); M)$  be a neighborhood of  $S(P)$  in  $M$ , choose a neighborhood  $N_P = \text{Nbd}(P; M)$  of  $P$  in  $M$  sufficiently thin with respect to  $\text{Nbd}(S(P); M)$  and set  $N_Q = \text{Nbd}(P; M) \cap \text{Nbd}(S(P); M)$ . Then  $M$  decomposes as

$$(5.1) \quad M = N_P \cup N_D = \left( N_Q \cup \bigcup_{i=1}^n N_{\mathcal{R}_i} \right) \cup N_D,$$

where  $N_{\mathcal{R}_i}$  is the connected component of the closure of  $N_P \setminus N_Q$  containing  $\mathcal{R}_i$ , which is diffeomorphic to  $\mathcal{R}_i \times [0, 1]$ , and  $N_D$  is the closure of  $M \setminus N_P$ , which is a 3-ball. By identifying the 3-ball  $B^3$  in Section 3.2 with  $N_D$ , we draw the  $E$ -cycle on  $\partial N_D$  and regard  $N_D$  as  $D^2 \times [0, 1]$ , where  $D^2$  is the unit 2-disk, so that a tubular neighborhood of the  $E$ -cycle on  $\partial N_D$  corresponds to  $\partial D^2 \times [0, 1]$ .

To define the gluing maps of these pieces, we re-choose  $N_{\mathcal{R}_i}$  and  $N_D$  slightly larger. For  $i = 1, \dots, n$ , we denote the gluing map of  $N_{\mathcal{R}_i}$  to  $N_Q$  by  $g_{\mathcal{R}_i}$ , which is a diffeomorphism  $g_{\mathcal{R}_i} : N_{\mathcal{R}'_i} \rightarrow N_Q$  to the image, where  $\mathcal{R}'_i = \text{Nbd}(\partial \mathcal{R}_i; \mathcal{R}_i)$  and  $N_{\mathcal{R}'_i} = \mathcal{R}'_i \times [0, 1] \subset N_{\mathcal{R}_i}$ . Also, we denote the gluing map of  $N_D$  to  $N_P$  by  $g_D$ , which is a diffeomorphism  $g_D : \text{Nbd}(\partial N_D; N_D) \rightarrow N_P$  to the image.

We may assume that a flow carried by  $P$  is positively transverse to  $D^2 \times \{t_0\}$  on  $N_D$  and  $\mathcal{R}_i \times \{t_0\}$  on  $N_{\mathcal{R}_i}$  for any  $t_0 \in [0, 1]$ .

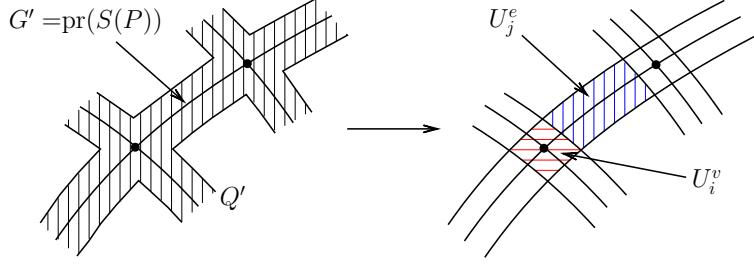
**5.2. Construction on  $N_Q$ .** First we define a 1-form on  $N_Q$ . Let  $Q'$  be an oriented compact surface with an embedded graph  $G'$  such that

- (1)  $Q'$  collapses onto  $G'$  and
- (2) there exists a continuous map  $\text{pr}_Q : Q \rightarrow Q'$  such that  $\text{pr}_Q|_{S(P)}$  is an embedding of the graph  $S(P)$  into  $Q'$  with  $G' = \text{pr}_Q(S(P))$  and  $\text{pr}_Q|_{Q \setminus S(P)}$  is an orientation-preserving local diffeomorphism.

We then fix a projection  $\text{pr} : N_Q \rightarrow Q'$  such that  $\text{pr}|_Q = \text{pr}_Q$ .

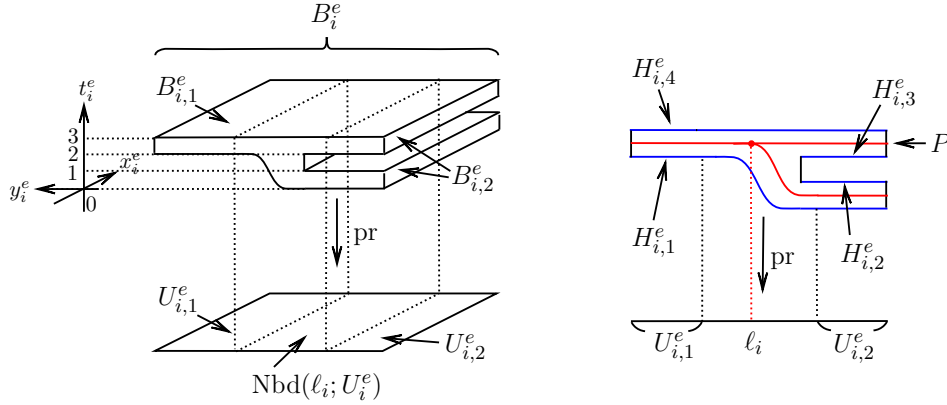
Next we decompose  $Q'$  into rectangles  $U_1^e, \dots, U_{n_e}^e$  corresponding to the images of neighborhoods of the edges  $e_1, \dots, e_{n_e}$  of  $P$  and rectangles  $U_1^v, \dots, U_{n_v}^v$  corresponding to those of vertices  $v_1, \dots, v_{n_v}$  of  $P$  as shown in Figure 14.

For each  $U_i^e$ , the preimage  $B_i^e = \text{pr}^{-1}(U_i^e)$  has a shape as shown on the left in Figure 15. According to the order determined by the flow, we denote the horizontal faces of  $B_i^e$  by  $H_{i,1}^e, H_{i,2}^e, H_{i,3}^e$  and  $H_{i,4}^e$ . These faces are indicated on the right in the figure, where  $H_{i,2}^e$  and  $H_{i,4}^e$  are top faces of  $B_i^e$  and  $H_{i,1}^e$  and  $H_{i,3}^e$  are bottom faces of  $B_i^e$ . Set  $\ell_i = \text{pr}(S(P) \cap B_i^e)$ . The complement  $U_i^e \setminus \text{Int } \text{Nbd}(\ell_i; U_i^e)$  of an open neighborhood of  $\ell_i$  in  $U_i^e$  consists of two connected components. We denote by  $U_{i,1}^e$  the component whose preimage by  $\text{pr}$  is connected, and by  $U_{i,2}^e$  the component whose preimage has two connected components. Set  $B_{i,j}^e = \text{pr}^{-1}(U_{i,j}^e)$  for  $j = 1, 2$ . We fix coordinates  $(x_i^e, y_i^e, t_i^e)$  on  $B_i^e$  such that


 FIGURE 14. Rectangular decomposition of  $Q'$ .

- $B_{i,2}^e \subset \{0 \leq y_i^e \leq 1\}$ ,  $B_{i,1}^e \subset \{2 \leq y_i^e \leq 3\}$ ,
- $H_{i,2}^e \subset \{t_i^e = 1\}$ ,  $H_{i,3}^e \subset \{t_i^e = 2\}$ ,  $H_{i,4}^e \subset \{t_i^e = 3\}$ ,
- $H_{i,1}^e \subset \{t_i^e = h(y_i^e)\}$ , where  $h : [0, 3] \rightarrow [0, 2]$  is a monotone increasing smooth function such that  $h(y_i^e) = 0$  for  $0 \leq y_i^e \leq 1$  and  $h(y_i^e) = 2$  for  $2 \leq y_i^e \leq 3$ .

We can think that  $B_i^e$  is embedded in the cube  $[0, L] \times [0, 3] \times [0, 3]$  with the coordinates  $(x_i^e, y_i^e, t_i^e)$ , where  $L$  is a positive real number. Note that  $L$  should be large enough so that  $N_P$  can be constructed from the pieces  $N_Q$  and  $N_{\mathcal{R}_i}$  for  $i = 1, \dots, n$ .


 FIGURE 15. The neighborhood  $B_i^e$  of a triple line  $e_i$  of  $P$ .

Since  $P$  is a positive flow-spine, each vertex is of  $\ell$ -type. For each  $U_i^v$ , the preimage  $B_i^v = \text{pr}^{-1}(U_i^v)$  has a shape as shown on the left in Figure 16. According to the order determined by the flow, we denote the horizontal faces of  $B_i^v$  by  $H_{i,1}^v, H_{i,2}^v, H_{i,3}^v, H_{i,2'}^v, H_{i,3'}^v, H_{i,4}^v$ . These faces are indicated on the left in the figure, where  $H_{i,2}^v, H_{i,2'}^v$  and  $H_{i,4}^v$  are top faces of  $B_i^v$  drawn in red, and  $H_{i,1}^v, H_{i,3}^v$  and  $H_{i,3'}^v$  are bottom faces of  $B_i^v$  drawn in blue. The image of  $S(P) \cap B_i^v$  by  $\text{pr}$  consists of two lines  $\ell_i$  and  $\ell_i'$  intersecting transversely at the image  $\text{pr}(v_i)$  of the vertex  $v_i$  in  $B_i^v$ . We set  $\ell_i$  to be the line that does not intersect  $\text{pr}(H_{i,2}^v)$  and  $\ell_i'$  to be the other line, which does not intersect  $\text{pr}(H_{i,2'}^v)$ . We denote by  $U_{i,1}^v$  the connected component of the complement  $U_i^v \setminus \text{Int Nbd}(\ell_i; U_i^v)$  of an open neighborhood of  $\ell_i$  whose preimage by  $\text{pr}$  is connected and by  $U_{i,2}^v$  the component of the

complement whose preimage by  $\text{pr}$  is not connected. Similarly, we denote by  $U_{i,1}^v$ , the connected component of the complement  $U_i^v \setminus \text{Int Nbd}(\ell'_i; U_i^v)$  of an open neighborhood of  $\ell'_i$  whose preimage by  $\text{pr}$  is connected and by  $U_{i,2'}^v$  the component of the complement whose preimage by  $\text{pr}$  is not connected. We set  $B_{i,j}^v = \text{pr}^{-1}(U_{i,j}^v)$  for  $j = 1, 2, 1', 2'$ .

Set coordinates  $(x_i^v, y_i^v, t_i^v)$  on  $B_i^v$  such that

- $B_{i,2}^v \subset \{0 \leq y_i^v \leq 1\}$ ,  $B_{i,1}^v \subset \{2 \leq y_i^v \leq 3\}$ ,
- $B_{i,2'}^v \subset \{0 \leq x_i^v \leq 1\}$ ,  $B_{i,1'}^v \subset \{2 \leq x_i^v \leq 3\}$ ,
- $H_{i,2}^v \subset \{t_i^v = 3\}$ ,  $H_{i,3}^v \subset \{t_i^v = 4\}$ ,  $H_{i,4}^v \subset \{t_i^v = 5\}$ ,
- $H_{i,3'}^v \subset \{t_i^v = h(y_i^v) + 2\}$ ,  $H_{i,2'}^v \subset \{t_i^v = h(y_i^v) + 1\}$ ,
- $H_{i,1}^v \subset \{t_i^v = \hat{h}(x_i^v, y_i^v)\}$ , where  $\hat{h} : [0, 3] \times [0, 3] \rightarrow [0, 4]$  is a smooth function such that  $\partial h / \partial x_i^v \geq 0$ ,  $\partial h / \partial y_i^v \geq 0$ ,  $\hat{h}(x_i^v, y_i^v) = h(y_i^v)$  for  $(x_i^v, y_i^v) \in U_{i,2'}^v$ ,  $\hat{h}(x_i^v, y_i^v) = h(y_i^v) + 2$  for  $(x_i^v, y_i^v) \in U_{i,1'}^v$ ,  $\hat{h}(x_i^v, y_i^v) = h(x_i^v)$  for  $(x_i^v, y_i^v) \in U_{i,2}^v$  and  $\hat{h}(x_i^v, y_i^v) = h(x_i^v) + 2$  for  $(x_i^v, y_i^v) \in U_{i,1}^v$ .

We can think that  $B_i^v$  is embedded in the cube  $[0, 3] \times [0, 3] \times [0, 5]$  with the coordinates  $(x_i^v, y_i^v, t_i^v)$ .

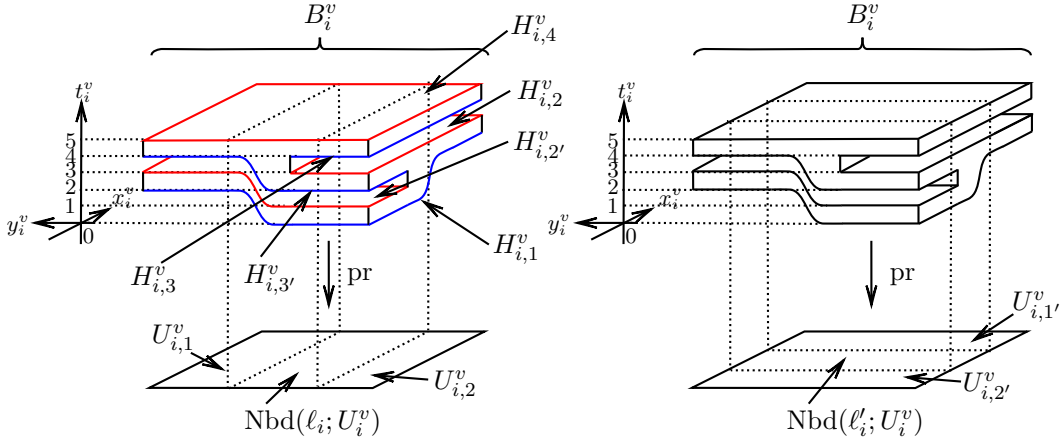


FIGURE 16. The neighborhood  $B_i^v$  of a vertex  $v_i$  of  $P$  of  $\ell$ -type.

On each  $B_i^k$ , where  $k = e$  or  $v$ , we define a 1-form  $\eta_i^k$  on  $B_i^k$  by  $\eta_i^k = dt_i^k$ . We can glue the 1-forms  $\eta_i^e$  for  $i = 1, \dots, n_e$  and  $\eta_j^v$  for  $j = 1, \dots, n_v$  canonically. We denote the 1-form on  $N_Q$  obtained in this way by  $\eta_Q$ .

**5.3. Construction on  $N_P$ .** Recall that the 3-manifold  $M$  is obtained from  $N_Q$  by attaching  $N_{\mathcal{R}_i}$ ,  $i = 1, \dots, n$ , where  $P \cap \mathcal{R}_i$  is regarded as  $\mathcal{R}_i \times \{1/2\} \subset N_{\mathcal{R}_i}$ , and then filling the boundary of  $N_P$  by  $N_D$ .

Set  $N_{\mathcal{R}_i} = \mathcal{R}_i \times [0, 1]$  and let  $t_i$  be the coordinate of  $[0, 1]$ . We choose the gluing map  $g_{\mathcal{R}_i}$  of  $N_{\mathcal{R}_i}$  to  $N_Q$  so that

(e-gl) the gluing part of  $B_j^e$  with  $\bigcup_{i=1}^n N_{\mathcal{R}_i}$  is exactly  $B_{j,1}^e \cup B_{j,2}^e$ ,

(e-01)  $t_j^e \circ g_{\mathcal{R}_i} = t_i$  on  $g_{\mathcal{R}_i}^{-1}(B_{j,2}^e \cap \{0 \leq t_j^e \leq 1\})$ ,

- (e-23)  $t_j^e \circ g_{\mathcal{R}_i} = t_i + 2$  on  $g_{\mathcal{R}_i}^{-1}((B_{j,1}^e \cup B_{j,2}^e) \cap \{2 \leq t_j^e \leq 3\})$ ,  
 (v-gl) the gluing part of  $B_j^v$  with  $\bigcup_{i=1}^n N_{\mathcal{R}_i}$  is exactly the union of  $B_{j,p}^v \cap B_{j,q}^v$ , where  $p$  and  $q$  run over  $\{1, 2, 1', 2'\}$  with  $p \neq q$ ,  $B_{j,2}^v \cap \{4 \leq t_j^v \leq 5\}$  and  $W_j^v$  with rounding the corners along  $B_j^v \cap \text{pr}^{-1}(\partial \text{Nbd}(\ell_j; U_j^v) \cap \partial \text{Nbd}(\ell'_j; U_j^v))$  smoothly, where

$$W_j^v = B_{j,2'}^v \cap \text{pr}^{-1}(\text{Nbd}(\ell_j; U_j^v)) \cap \{h(y_j^v) \leq t_j^v \leq h(y_j^v) + 1\},$$

see the right in Figure 17.

- (v-01)  $t_j^v \circ g_{\mathcal{R}_i} = t_i$  on  $g_{\mathcal{R}_i}^{-1}((B_{j,2}^v \cap B_{j,2'}^v) \cap \{0 \leq t_j^v \leq 1\})$ ,  
 (v-23)  $t_j^v \circ g_{\mathcal{R}_i} = t_i + 2$  on  $g_{\mathcal{R}_i}^{-1}(((B_{j,1}^v \cap B_{j,2'}^v) \cup (B_{j,2}^v \cap B_{j,1'}^v) \cup (B_{j,2}^v \cap B_{j,2'}^v)) \cap \{2 \leq t_j^v \leq 3\})$ ,  
 (v-45)  $t_j^v \circ g_{\mathcal{R}_i} = t_i + 4$  on  $g_{\mathcal{R}_i}^{-1}(((B_{j,1}^v \cap B_{j,1'}^v) \cup (B_{j,1}^v \cap B_{j,2'}^v) \cup B_{j,2}^v) \cap \{4 \leq t_j^v \leq 5\})$ ,  
 (v-W)  $t_j^v \circ g_{\mathcal{R}_i} = t_i + h(y_j^v)$  on  $W_{i,j} = g_{\mathcal{R}_i}^{-1}(W_j^v)$ .

In the above notation,  $t_j^k$ ,  $k = e$  or  $v$ , is regarded as the coordinate function whose image is the  $t_j^k$ -coordinate.

Let  $\mathcal{R}'_i$  be a collar neighborhood of  $\mathcal{R}_i$  such that  $\mathcal{R}'_i \times [0, 1] = g_{\mathcal{R}_i}^{-1}(N_Q)$ , and set  $N_{\mathcal{R}'_i} = \mathcal{R}'_i \times [0, 1] \subset \mathcal{R}_i \times [0, 1] = N_{\mathcal{R}_i}$ . Choose coordinates  $(r_i, \theta_i)$  on  $\mathcal{R}'_i$  so that  $\{r_i = 0\} = \partial \mathcal{R}'_i \setminus \partial \mathcal{R}_i$ ,  $\{r_i = 1\} = \partial \mathcal{R}_i$  and the orientation of  $(r_i, \theta_i)$  coincides with that of  $\mathcal{R}_i$ , see the left in Figure 17.

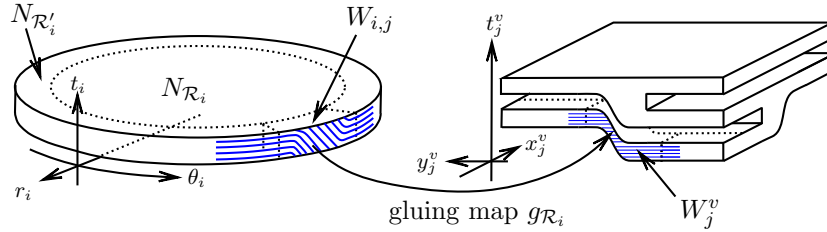


FIGURE 17. Characteristic foliation of  $\ker \eta_Q$  on  $\partial \mathcal{R}_i \times [0, 1]$ .

**Remark 5.1.** As described on the left in Figure 17, the characteristic foliation of  $\ker \eta_Q$  has negative slope as the standard contact structure on  $\mathbb{R}^3$ . Intuitively, this is the reason why we have the inequality  $\eta \wedge d\eta \geq 0$  in Lemma 5.9. Remark that the figure on the right in Figure 17 is a neighborhood of an  $\ell$ -type vertex and we cannot expect the same inequality for an  $r$ -type vertex.

For each  $W_{i,j}$ , the gluing map  $g_{\mathcal{R}_i}|_{W_{i,j}} : W_{i,j} \rightarrow B_j^v$  is given as

$$(5.2) \quad (r_i, \theta_i, t_i) \mapsto (r_i, c_i(\theta_i - c_{i,j}), t_i + h_{i,j}(\theta_i)),$$

where  $c_i$  and  $c_{i,j}$  are real numbers chosen so that  $c_i(\theta_i - c_{i,j})$  coincides with the  $y_j^v$ -coordinate on  $B_j^v$ , and  $h_{i,j}$  is the smooth function given by  $h_{i,j}(\theta_i) = h(c_i(\theta_i - c_{i,j}))$ . Note that the function  $h_{i,j}$  is monotone increasing.

The gluing map  $g_{\mathcal{R}_i}$  induces a 1-form  $\eta_{\mathcal{R}'_i}$  on  $N_{\mathcal{R}'_i}$  as  $\eta_{\mathcal{R}'_i} = g_{\mathcal{R}_i}^* \eta_Q$ . Due to the choice of  $g_{\mathcal{R}_i}$ , we have  $\eta_{\mathcal{R}'_i} = dt_i$  on  $N_{\mathcal{R}'_i} \setminus \bigcup_j W_{i,j}$ , where  $j$  runs over the indices of  $B_j^v$  adjacent to  $\mathcal{R}_i$ .

We define a 1-form  $\eta_{\mathcal{R}_i}$  on  $N_{\mathcal{R}_i}$  as

$$(5.3) \quad \eta_{\mathcal{R}_i} = (1 - \sigma(r_i))dt_i + \sigma(r_i)\eta_{\mathcal{R}'_i},$$

where  $\sigma(r_i)$  is a monotone increasing smooth function such that  $\sigma(\varepsilon) = 0$  and  $\sigma(1-\varepsilon) = 1$  for any sufficiently small  $\varepsilon \geq 0$ .

**Lemma 5.2.**

$$\eta_{\mathcal{R}_i} = \begin{cases} dt_i & \text{on } N_{\mathcal{R}_i} \setminus \bigcup_j W_{i,j} \\ dt_i + \sigma(r_i)\frac{dh_{i,j}}{d\theta_i}(\theta_i)d\theta_i & \text{on } W_{i,j}. \end{cases}$$

*Proof.* On each  $W_{i,j}$ , by (5.2), we have  $t_j^v = t_i + h_{i,j}(\theta_i)$ . Hence  $\eta_{\mathcal{R}'_i} = g_{\mathcal{R}_i}^* dt_j^v = dt_i + \frac{dh_{i,j}}{d\theta_i}(\theta_i)d\theta_i$ . By (5.3), we have  $\eta_{\mathcal{R}'_i} = dt_i + \sigma(r_i)\frac{dh_{i,j}}{d\theta_i}(\theta_i)d\theta_i$ . On  $N_{\mathcal{R}_i} \setminus \bigcup_j W_{i,j}$ , since  $\eta_{\mathcal{R}'_i} = g_{\mathcal{R}_i}^* dt_j^k = dt_i$  for  $k = e$  and  $v$ , we have  $\eta_{\mathcal{R}_i} = dt_i$  by (5.3).  $\square$

Gluing  $N_Q$  with 1-form  $\eta_Q$  and  $N_{\mathcal{R}_i}$  with the 1-form  $\eta_{\mathcal{R}_i}$  for  $i = 1, \dots, n$ , we obtain a 1-form  $\eta_P$  on the whole  $N_P$ .

**Lemma 5.3.**

$$d\eta_P = \begin{cases} 0 & \text{on } N_P \setminus \bigcup_{i,j} W_{i,j} \\ \frac{d\sigma}{dr_i}(r_i)\frac{dh_{i,j}}{d\theta_i}(\theta_i)dr_i \wedge d\theta_i & \text{on } W_{i,j}. \end{cases}$$

*Proof.* Since  $\eta_P = dt_j^e$  on  $\text{pr}^{-1}(\text{Nbd}(\ell_j; U_j^e))$ ,  $\eta_P = dt_j^v$  on  $\text{pr}^{-1}(\text{Nbd}(\ell_j; U_j^v) \cup \text{Nbd}(\ell'_j; U_j^v)) \setminus W_j^v$  and  $\eta_P = dt_i$  on  $N_{\mathcal{R}_i} \setminus \bigcup_j W_{i,j}$  by Lemma 5.2, we have  $d\eta_P = 0$  on  $N_P \setminus \bigcup_{i,j} W_{i,j}$ . On each  $W_{i,j}$ , the 2-form in the assertion follows from Lemma 5.2.  $\square$

**Lemma 5.4.** (1)  $\eta_P \wedge d\eta_P = 0$  on  $N_P \setminus \bigcup_{i,j} W_{i,j}$ .  
(2)  $\eta_P \wedge d\eta_P \geq 0$  on  $W_{i,j}$ .

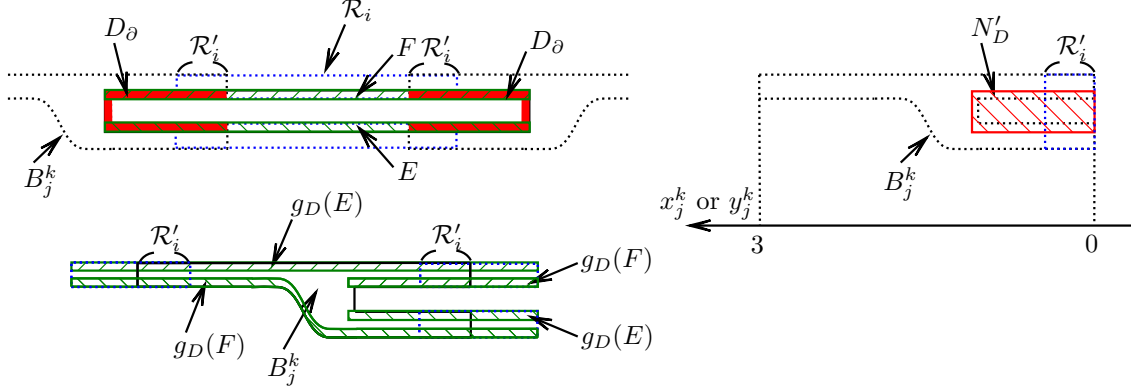
*Proof.* The assertion (1) follows from Lemma 5.3. We prove the assertion (2). The function  $h_{i,j}$  is monotone increasing. We also have  $\frac{d\sigma}{dr_i}(r_i) \geq 0$ . Hence, by Lemmas 5.2 and 5.3,

$$\begin{aligned} \eta_{\mathcal{R}_i} \wedge d\eta_{\mathcal{R}_i} &= \left( dt_i + \sigma(r_i)\frac{dh_{i,j}}{d\theta_i}(\theta_i)d\theta_i \right) \wedge \left( \frac{d\sigma}{dr_i}(r_i)\frac{dh_{i,j}}{d\theta_i}(\theta_i)dr_i \wedge d\theta_i \right) \\ &= \frac{d\sigma}{dr_i}(r_i)\frac{dh_{i,j}}{d\theta_i}(\theta_i)dr_i \wedge d\theta_i \wedge dt_i \geq 0. \end{aligned}$$

$\square$

**5.4. Construction on the whole  $M$ .** Finally we extend the 1-form  $\eta_P$  on  $N_P$  to the whole  $M$ . For convenience, we set  $N_D = D^2 \times [-\varepsilon, 1 + \varepsilon]$  for a sufficiently small  $\varepsilon > 0$ , instead of  $D^2 \times [0, 1]$ . Set  $E = D^2 \times [-\varepsilon, 0]$  and  $F = D^2 \times [1, 1 + \varepsilon]$ , and denote the restrictions of  $g_D$  to  $E$  and  $F$  by  $g_E$  and  $g_F$ , respectively. Set  $D_\partial$  to be the union of the connected components of  $B_j^k \cap g_D(N_D)$  that intersect the vertical faces of  $\partial B_j^k$  corresponding to the  $E$ -cycle, where  $B_j^k$  runs over the indices  $j = 1, \dots, n_e$  for  $k = e$  and  $j = 1, \dots, n_v$  for  $k = v$ . See the left in Figure 18.

We choose the coordinates  $(u, v, w)$  of  $N_D = D^2 \times [-\varepsilon, 1 + \varepsilon]$  so that they satisfy the following:


 FIGURE 18. Positions of  $E$ ,  $F$ ,  $D_\partial$  and  $N'_D$ .

(B-D') Set  $N'_D = \{(u, v, w) \in N_D \mid (u, v, 0) \in g_D^{-1}(D_\partial)\}$ . We think of  $N'_D$  as being embedded in the union of the cubes  $[0, L] \times [0, 3] \times [0, 3]$  containing  $B_j^e$  and the cubes  $[0, 3]^2 \times [0, 5]$  containing  $B_j^v$  so that

$$t_j^k \circ g_D(u, v, w) = \begin{cases} w + 1 & k = e \text{ and } g_D(u, v, 0) \in B_j^e \\ w + 3 & k = v \text{ and } g_D(u, v, 0) \in H_{j,2}^v \subset B_j^v \\ w + t_j^v \circ g_D(u, v, 0) & k = v \text{ and } g_D(u, v, 0) \in H_{j,2'}^v \subset B_j^v \end{cases}$$

and the first two coordinates of  $B_j^k$  do not depend on the coordinate  $w$ . See the right in Figure 18. Note that  $t_j^v \circ g_D(u, v, 0) = h_{i,j}(\theta_i) + 1$  on the connected component of  $N'_D \cap g_D^{-1}(B_j^v)$  containing  $g_D^{-1}(H_{j,2'}^v)$ , where  $i$  is the index  $i$  of  $W_{i,j}$  and  $(r_i, \theta_i, t_i)$  are the coordinates of  $g_D^{-1}(B_j^v) \cap N_{\mathcal{R}'_i}$ .

(R-E) The coordinates  $(u, v, w)$  on  $E \cap g_D^{-1}(N_{\mathcal{R}'_i})$  are chosen so that

$$t_i \circ g_D(u, v, w) = w + 1$$

and the first two coordinates of  $N_{\mathcal{R}'_i} = \mathcal{R}'_i \times [0, 1]$  do not depend on  $w$ .

(R-F) The coordinates  $(u, v, w)$  on  $F \cap g_D^{-1}(N_{\mathcal{R}'_i})$  are chosen so that

$$t_i \circ g_D(u, v, w) = w - 1$$

and the first two coordinates of  $N_{\mathcal{R}'_i} = \mathcal{R}'_i \times [0, 1]$  do not depend on  $w$ .

(B-E) The coordinates  $(u, v, w)$  on the connected component of  $E \cap g_D^{-1}(B_j^k)$  containing  $g_D^{-1}(H_{j,4}^k)$  are chosen so that

$$t_j^k \circ g_D(u, v, w) = w + c,$$

where  $c = 3$  if  $k = e$  and  $c = 5$  if  $k = v$ , and the first two coordinates of  $B_j^k$  do not depend on  $w$ .

(B-F) The coordinates  $(u, v, w)$  on the connected component of  $F \cap g_D^{-1}(B_j^k)$  containing  $g_D^{-1}(H_{j,1}^k)$  are chosen so that

$$t_j^k \circ g_D(u, v, w) = w + t_j^k \circ g_D(u, v, 0)$$

and the first two coordinates of  $B_j^k$  do not depend on  $w$ .

Due to the choice of these coordinates, we see that each of the 1-forms  $g_E^*\eta_P$  on  $E$  and  $g_F^*\eta_P$  on  $F$  is invariant under translation to the  $w$ -coordinate, which allows us to extend these forms to the whole  $N_D$  canonically. Let  $\eta_E$  and  $\eta_F$  denote the 1-forms on  $N_D$  obtained by extending  $g_E^*\eta_P$  on  $E$  and  $g_F^*\eta_P$  on  $F$  to  $N_D$ , respectively. We then define the 1-form  $\eta_D$  on  $N_D$  as

$$(5.4) \quad \eta_D = (1 - \tau(w))\eta_E + \tau(w)\eta_F,$$

where  $\tau : [-\varepsilon, 1+\varepsilon] \rightarrow [0, 1]$  is a monotone increasing smooth function such that  $\tau(w) = 0$  for  $-\varepsilon \leq w \leq 0$  and  $\tau(w) = 1$  for  $1 \leq w \leq 1 + \varepsilon$ .

By the construction, we have  $g_D^*\eta_P = \eta_D$  on  $E \cup F$ . Thus, for gluing the 1-forms  $\eta_D$  on  $N_D$  and  $\eta_P$  on  $N_P$ , it is enough to show their coincidence on  $N_D'' = \{(u, v, w) \in N_D \mid g_D(u, v, 1/2) \in N_Q\}$ , see Figure 19.

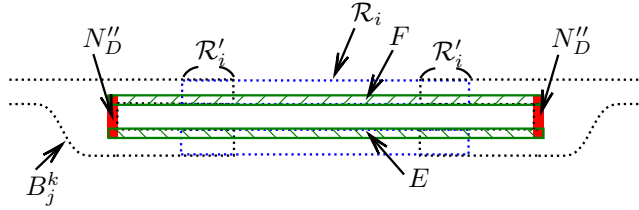


FIGURE 19. The set  $N_D''$ .

**Lemma 5.5.**  $g_D^*\eta_P = \eta_D$  on  $N_D''$ .

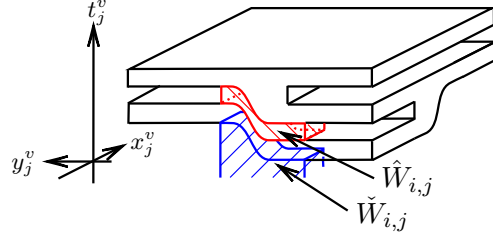
*Proof.* Since  $\eta_E = g_E^*\eta_P$  on  $E \cap N_D''$  and  $\eta_F = g_F^*\eta_P$  on  $F \cap N_D''$  are given as the pull-backs of the same form  $\eta_P = dt_j^k$  and  $(u, v, w)$  satisfies the condition (B-D'), we have  $\eta_E = \eta_F$  on  $N_D''$ . Since  $g_E^*\eta_P = \eta_D$  on  $E \cap N_D''$ ,  $g_F^*\eta_P = \eta_D$  on  $F \cap N_D''$  and both of  $g_D^*\eta_P$  and  $\eta_D$  are defined on  $N_D''$  by the linear sum of those on  $E \cap N_D''$  and  $F \cap N_D''$  as in (5.4), we have  $g_D^*\eta_P = \eta_D$  on  $N_D''$ .  $\square$

Thus the 1-forms  $\eta_D$  on  $N_D$  and  $\eta_P$  on  $N_P$  are glued along  $g_D^{-1}(N_P)$ , which we denote by  $\eta$ .

Topologically, the decomposition of  $M$  into  $B_j^e$  ( $j = 1, \dots, n_e$ ),  $B_j^v$  ( $j = 1, \dots, n_v$ ),  $N_{\mathcal{R}_i}$  ( $i = 1, \dots, n$ ) and  $N_D$  depends only on the positive flow-spine  $P$ . We then choose coordinates  $(x_j^e, y_j^e, t_j^e)$ ,  $(x_j^v, y_j^v, t_j^v)$ ,  $(r_i, \theta_i, t_i)$ ,  $(u, v, w)$  on these pieces and define the 1-form  $\eta$  by using these coordinates.

*Definition.* Let  $\mathcal{C}$  be coordinates on the pieces of the decomposition of  $M$  with respect to  $P$ . We call  $\mathcal{C}$  a *coordinate system of  $M$  with respect to  $P$*  and the 1-form  $\eta$  obtained from  $\mathcal{C}$  as above the *reference 1-form of  $(P, \mathcal{C})$* .

In the rest of this section, we discuss some properties of  $\eta$  and  $dw$  on  $N_D$  and prove the inequality  $\eta \wedge d\eta \geq 0$ . Set  $\hat{W}_{i,j} = \{(u, v, w) \in N_D \mid g_D(u, v, 0) \in W_{i,j}\}$  and  $\check{W}_{i,j} = \{(u, v, w) \in N_D \mid g_D(u, v, 1) \in W_{i,j}\}$ , see Figure 20, and then set  $\hat{W} = \bigcup_{i,j} \hat{W}_{i,j}$  and  $\check{W} = \bigcup_{i,j} \check{W}_{i,j}$ .


 FIGURE 20. The sets  $\hat{W}_{i,j}$  and  $\check{W}_{i,j}$ .

We first introduce the sets  $S_E$  and  $S_F$  on  $D^2 \times \{-\varepsilon\}$  and  $D^2 \times \{1 + \varepsilon\}$ , respectively. Roughly speaking,  $S_E$  and  $S_F$  are graphs of the DS-diagram of  $P$  on the lower and upper hemispheres, respectively, when we regard  $N_D$  as the 3-ball for the DS-diagram. For each  $i = 1, \dots, n_e$ , we set  $T_{i,E}^e = B_i^e \cap \{y_i^e = \frac{3}{2}\} \cap g_D(D^2 \times \{-\varepsilon\})$  and  $T_{i,F}^e = B_i^e \cap \{y_i^e = \frac{3}{2}\} \cap g_D(D^2 \times \{1 + \varepsilon\})$ . For each  $j = 1, \dots, n_v$ , we set

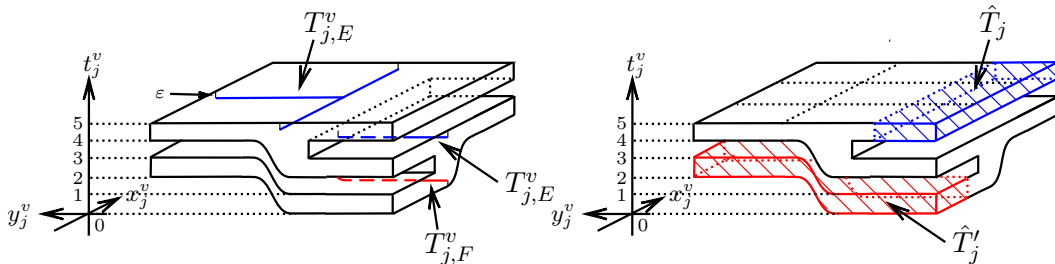
$$T_{j,E}^v = B_j^v \cap g_D(D^2 \times \{-\varepsilon\}) \cap \left( \left\{ y_j^v = \frac{3}{2}, t_j^v > 4 \right\} \cup \left\{ x_j^v = \frac{3}{2}, \frac{3}{2} \leq y_j^v \leq 3 \right\} \cup \left\{ x_j^v = \frac{3}{2}, t_j^v < 3 \right\} \right)$$

and

$$T_{j,F}^v = B_j^v \cap g_D(D^2 \times \{1 + \varepsilon\}) \cap \left( \left\{ x_j^v = \frac{3}{2}, t_j^v < 4 \right\} \cup \left\{ y_j^v = \frac{3}{2}, \frac{3}{2} \leq x_j^v \leq 3, \right\} \cup \left\{ y_j^v = \frac{3}{2}, t_j^v > 2 \right\} \right).$$

See the left in Figure 21, where most parts of  $T_{j,F}^v$  are hidden behind. Then  $S_E$  and  $S_F$  are set as

$$S_E = g_D^{-1} \left( \left( \bigcup_{i=1}^{n_e} T_{i,E}^e \right) \cup \left( \bigcup_{j=1}^{n_v} T_{j,E}^v \right) \right) \quad \text{and} \quad S_F = g_D^{-1} \left( \left( \bigcup_{i=1}^{n_e} T_{i,F}^e \right) \cup \left( \bigcup_{j=1}^{n_v} T_{j,F}^v \right) \right).$$


 FIGURE 21. The sets  $T_{j,E}^v$ , (a piece of)  $T_{j,F}^v$ ,  $\hat{T}_j$  and  $\hat{T}'_j$ .

To explain the properties of  $\eta$  and  $dw$ , we decompose  $N_D$  into several pieces and observe them on each of these pieces. Recall that the coordinates  $(x_j^e, y_j^e, t_j^e)$  on  $B_j^e$  and

$(x_j^v, y_j^v, t_j^v)$  on  $B_j^v$  are chosen, in Section 5.2, such that

$$\begin{aligned} \text{pr}^{-1}(\text{Nbd}(\ell_j; U_j^e)) &= \{(x_j^e, y_j^e, t_j^e) \in B_j^e \mid 1 \leq y_j^e \leq 2\}, \\ \text{pr}^{-1}(\text{Nbd}(\ell_j; U_j^v)) &= \{(x_j^v, y_j^v, t_j^v) \in B_j^v \mid 1 \leq y_j^v \leq 2\}, \text{ and} \\ \text{pr}^{-1}(\text{Nbd}(\ell'_j; U_j^v)) &= \{(x_j^v, y_j^v, t_j^v) \in B_j^v \mid 1 \leq x_j^v \leq 2\}. \end{aligned}$$

Let  $N'_Q \subset N_Q$  be the closure of the union of  $\text{pr}^{-1}(\text{Nbd}(\ell_i; U_i^e))$  for  $i = 1, \dots, n_e$  and  $\text{pr}^{-1}(\text{Nbd}(\ell_j; U_j^v) \cup \text{Nbd}(\ell'_j; U_j^v)) \setminus (\hat{T}_j \cup \hat{T}'_j)$  for  $j = 1, \dots, n_v$  in  $N_Q$ , where

$$\hat{T}_j = B_{j,2}^v \cap \{(x_j^v, y_j^v, t_j^v) \in B_j^v \mid 4 \leq t_j^v \leq 5\}$$

and

$$\hat{T}'_j = B_{j,2'}^v \cap \{(x_j^v, y_j^v, t_j^v) \in B_j^v \mid h(y_j^v) \leq t_j^v \leq h(y_j^v) + 1\},$$

see the right in Figure 21. Then we set  $A_F = g_F^{-1}(N'_Q) \cap (D^2 \times \{1 + \varepsilon\})$  and  $N_A = (A_F \times [-\varepsilon, 1 + \varepsilon]) \cup \check{W}$ . See Figure 22, where  $\text{pr}_{D^2}$  is the first projection  $N_D = D^2 \times [-\varepsilon, 1 + \varepsilon] \rightarrow D^2$ ,

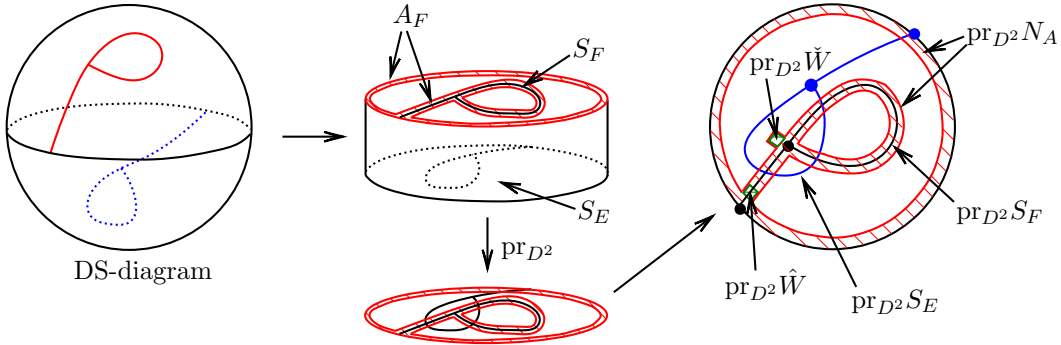


FIGURE 22. The positions of  $S_E$ ,  $S_F$ ,  $A_F$ ,  $N_A$ ,  $\hat{W}_{i,j}$  and  $\check{W}_{i,j}$ .

The next lemma is about  $\eta$  outside  $\hat{W} \cup \check{W}$ .

- Lemma 5.6.** (1)  $\eta_D = dw$  on  $N_D \setminus N_A$ .  
(2)  $d\eta_E = d\eta_F = 0$  on  $N_A \setminus (\hat{W} \cup \check{W})$ .  
(3)  $\eta_E = dw$  on  $N_A \setminus N'_D$ .  
(4)  $\eta_E = \eta_F = dw$  on  $N'_D \setminus \hat{W}$ .

*Proof.* On  $E \setminus N_A$ ,  $\eta_E$  is given by either  $g_D^* dt_i$  by Lemma 5.2 or  $g_D^* dt_j^k$ ,  $k = e$  or  $v$ , by the construction of  $\eta_E$ . Hence  $\eta_E = dw$  outside  $N_A$  by the conditions (B-D'), (R-E) and (B-E). Note that  $\hat{W} \cup \check{W} \subset N_A$ . Next we observe  $\eta_F$  on  $F \setminus N_A$ . This piece is the disjoint union of  $g_F^{-1}(N_{\mathcal{R}_i}) \setminus \check{W}$  for  $i = 1, \dots, n$ , and we have  $\eta_F = g_D^* dt_i$  on each  $g_F^{-1}(N_{\mathcal{R}_i}) \setminus \check{W}$ . Since  $dw = g_D^* dt_i$  by the condition (R-F), we have  $\eta_F = dw$ . Thus, by (5.4), we have the assertion (1).

Since  $\eta_P$  is defined as  $dt_j^k$  on  $(g_E(E \cap N_A) \cap B_j^k) \setminus W_j^v$  and  $dt_i$  on  $(g_E(E \cap N_A) \cap N_{\mathcal{R}_i}) \setminus \bigcup_j W_{i,j}$ , we have  $d\eta_E = 0$  on  $N_A \setminus \hat{W}$ . We also have  $d\eta_F = 0$  on  $N_A \setminus \check{W}$  by the same

reason. This proves the assertion (2). On  $N_A \setminus N'_D$ ,  $\eta_E$  is given by either  $g_D^* dt_i$  by Lemma 5.2 or  $g_D^* dt_j^k$  by the construction of  $\eta_E$ . Hence  $\eta_E = dw$  by the conditions (R-E) and (B-E). This proves the assertion (3). The assertion (4) follows from the condition (B-D').  $\square$

In the next two lemmas, we discuss  $dw$  and  $\eta$  on  $\hat{W}$  and  $\check{W}$ . The 1-form  $g_E^* dt_i$  on  $E \cap \hat{W}_{i,j}$  is invariant under translation to the  $w$ -coordinate. We extend it to the whole  $\hat{W}_{i,j}$  by this invariance and denote it again by  $g_E^* dt_i$ . This is used in (1) below. The extensions in (3) below are also given by the same idea.

**Lemma 5.7.** (1)  $dw = g_E^* dt_i$  on  $\hat{W}_{i,j}$ .  
 (2)  $\eta_E = g_E^* \left( dt_i + \sigma(r_i) \frac{dh_{i,j}}{d\theta_i}(\theta_i) d\theta_i \right)$  on  $E \cap \hat{W}_{i,j}$ .  
 (3)  $\eta_F = g_F^* dt_j^k = dw + g_E^* \left( \frac{dh_{i,j}}{d\theta_i}(\theta_i) d\theta_i \right) = g_E^* \left( dt_i + \frac{dh_{i,j}}{d\theta_i}(\theta_i) d\theta_i \right)$  on  $F \cap \hat{W}_{i,j}$ ,  
 where  $g_E^* \left( \frac{dh_{i,j}}{d\theta_i}(\theta_i) d\theta_i \right)$  and  $g_E^* \left( dt_i + \frac{dh_{i,j}}{d\theta_i}(\theta_i) d\theta_i \right)$  are the extensions of those on  $E \cap \hat{W}_{i,j}$  to the whole  $\hat{W}_{i,j}$ .

*Proof.* Since  $dt_j^k = dw + \frac{dh_{i,j}}{d\theta_i}(\theta_i) d\theta_i$  by the condition (B-D') and  $dt_j^k = dt_i + \frac{dh_{i,j}}{d\theta_i}(\theta_i) d\theta_i$  by the definition of  $g_{\mathcal{R}_i}$  on  $W_{i,j}$ , we have  $dw = g_E^* dt_i$  on  $E \cap \hat{W}_{i,j}$ . Since both of  $dw$  and  $g_E^* dt_i$  are invariant under translation to the  $w$ -coordinate, the assertion (1) holds. On  $E \cap \hat{W}_{i,j}$ , we have the assertion (2) by Lemma 5.2. On  $F \cap \hat{W}_{i,j}$ ,  $g_F^* dt_j^k = dw + g_F^* \left( \frac{dh_{i,j}}{d\theta_i}(\theta_i) d\theta_i \right) = dw + g_E^* \left( \frac{dh_{i,j}}{d\theta_i}(\theta_i) d\theta_i \right)$  by the condition (B-D') and  $g_F^* dt_j^k = g_E^* dt_j^k = g_E^* \left( dt_i + \frac{dh_{i,j}}{d\theta_i}(\theta_i) d\theta_i \right)$  by the condition (B-D') and the gluing map (5.2). Thus the assertion (3) holds.  $\square$

The 1-form  $g_F^* dt_i$  on  $F \cap \check{W}_{i,j}$  is invariant under translation to the  $w$ -coordinate. We extend it to the whole  $\check{W}_{i,j}$  by this invariance and denote it by again by  $g_F^* dt_i$ .

**Lemma 5.8.** (1)  $dw = g_F^* dt_i$  on  $\check{W}_{i,j}$ .  
 (2)  $\eta_E = dw$  on  $E \cap \check{W}_{i,j}$ .  
 (3)  $\eta_F = g_F^* \left( dt_i + \sigma(r_i) \frac{dh_{i,j}}{d\theta_i}(\theta_i) d\theta_i \right)$  on  $F \cap \check{W}_{i,j}$ .

*Proof.* Since  $dt_j^k = dw + \frac{dh_{i,j}}{d\theta_i}(\theta_i) d\theta_i$  by the condition (B-F) and  $dt_j^k = dt_i + \frac{dh_{i,j}}{d\theta_i}(\theta_i) d\theta_i$  by the gluing map (5.2), we have  $dw = g_F^* dt_i$  on  $F \cap \check{W}_{i,j}$ . Since both of  $dw$  and  $g_F^* dt_i$  are invariant under translation to the  $w$ -coordinate, the assertion (1) holds. The assertion (2) follows from the property that  $\hat{W} \cap \check{W} = \emptyset$ . The assertion (3) follows from Lemma 5.2.  $\square$

The next inequality is important for making contact forms in the proof of Theorem 1.1.

**Lemma 5.9.**  $\eta \wedge d\eta \geq 0$  on  $M$ .

*Proof.* The inequality holds on  $M \setminus N_D$  by Lemma 5.4. On  $N_D \setminus N_A$ ,  $\eta \wedge d\eta = 0$  by Lemma 5.6 (1). From (5.4), we have

$$\begin{aligned}
\eta_D \wedge d\eta_D &= ((1 - \tau(w))\eta_E + \tau(w)\eta_F) \wedge \left( -\frac{d\tau}{dw}(w)dw \wedge \eta_E \right. \\
&\quad \left. + (1 - \tau(w))d\eta_E + \frac{d\tau}{dw}(w)dw \wedge \eta_F + \tau(w)d\eta_F \right) \\
&= (1 - \tau(w))^2\eta_E \wedge d\eta_E + (1 - \tau(w))\frac{d\tau}{dw}(w)\eta_E \wedge dw \wedge \eta_F \\
&\quad + (1 - \tau(w))\tau(w)\eta_E \wedge d\eta_F - \tau(w)\frac{d\tau}{dw}(w)\eta_F \wedge dw \wedge \eta_E \\
&\quad + (1 - \tau(w))\tau(w)\eta_F \wedge d\eta_E + \tau(w)^2\eta_F \wedge d\eta_F \\
&= (1 - \tau(w))^2\eta_E \wedge d\eta_E + \frac{d\tau}{dw}(w)\eta_E \wedge dw \wedge \eta_F \\
&\quad + (1 - \tau(w))\tau(w)(\eta_E \wedge d\eta_F + \eta_F \wedge d\eta_E) + \tau(w)^2\eta_F \wedge d\eta_F.
\end{aligned}$$

This form vanishes on  $N_A \setminus (\hat{W} \cup \check{W})$  by Lemma 5.6. Thus it is enough to show the inequality on  $\hat{W} \cup \check{W}$ .

Let  $(g_E^*dt)_{\hat{W}_{i,j}}$  denote the extension of  $g_E^*dt_i$  on  $E \cap \hat{W}_{i,j}$  to  $\hat{W}_{i,j}$ . By Lemma 5.7 (2) and (3), we have  $\eta_E \wedge (g_E^*dt)_{\hat{W}_{i,j}} \wedge \eta_F = 0$  on  $\hat{W}_{i,j}$ . By Lemma 5.7 (1),  $dw = (g_E^*dt)_{\hat{W}_{i,j}}$ . Hence the term  $\frac{d\tau}{dw}(w)\eta_E \wedge dw \wedge \eta_F$  vanishes on  $\hat{W}_{i,j}$ . The terms with  $d\eta_F$  vanish since  $d\eta_F = 0$  by Lemma 5.7 (3). The 3-form  $\eta_E \wedge d\eta_E$  is calculated, by Lemma 5.7 (2), as

$$\begin{aligned}
\eta_E \wedge d\eta_E &= g_E^* \left( dt_i + \sigma(r_i) \frac{dh_{i,j}}{d\theta_i}(\theta_i) d\theta_i \right) \wedge g_E^* \left( \frac{d\sigma}{dr_i}(r_i) \frac{dh_{i,j}}{d\theta_i}(\theta_i) dr_i \wedge d\theta_i \right) \\
&= g_E^* \left( \frac{d\sigma}{dr_i}(r_i) \frac{dh_{i,j}}{d\theta_i}(\theta_i) dr_i \wedge d\theta_i \wedge dt_i \right),
\end{aligned}$$

where the pull-backs of forms by  $g_E$  are regarded as their extensions to  $N_D$ . Also, by Lemma 5.7 (2) and (3), we have

$$\begin{aligned}
\eta_F \wedge d\eta_E &= g_E^* \left( dt_i + \frac{dh_{i,j}}{d\theta_i}(\theta_i) d\theta_i \right) \wedge g_E^* \left( \frac{d\sigma}{dr_i}(r_i) \frac{dh_{i,j}}{d\theta_i}(\theta_i) dr_i \wedge d\theta_i \right) \\
&= g_E^* \left( \frac{d\sigma}{dr_i}(r_i) \frac{dh_{i,j}}{d\theta_i}(\theta_i) dr_i \wedge d\theta_i \wedge dt_i \right),
\end{aligned}$$

where the pull-backs of forms by  $g_E$  are regarded as their extensions to  $N_D$ . Since  $\sigma$  and  $h_{i,j}$  are monotone increasing, these two terms are non-negative. Thus  $\eta_D \wedge d\eta_D \geq 0$  on  $\hat{W}$ .

On  $\check{W}_{i,j}$ , by Lemma 5.8 (2),

$$d\eta_D = d((1 - \tau(w))\eta_E + \tau(w)\eta_F) = \frac{d\tau}{dw}dw \wedge \eta_F + \tau(w)d\eta_F$$

and hence, by Lemma 5.8, we have

$$\begin{aligned} \eta_D \wedge d\eta_D &= (1 - \tau(w))\tau(w)dw \wedge d\eta_F + \tau(w)^2\eta_F \wedge d\eta_F \\ &= \tau(w)g_F^* \left( \frac{d\sigma}{dr_i}(r_i) \frac{dh_{i,j}}{d\theta_i}(\theta_i) dr_i \wedge d\theta_i \wedge dt_i \right) \geq 0, \end{aligned}$$

where the pull-back of a form by  $g_F$  is regarded as its extension to  $N_D$ . This completes the proof.  $\square$

## 6. EXISTENCE

We use the same notations as in the previous section. In this section, we prove the following theorem.

**Theorem 6.1.** *Let  $P$  be a positive flow-spine of a closed, connected, oriented, smooth 3-manifold  $M$ . Then there exists a contact form on  $M$  whose Reeb flow is carried by  $P$ .*

**6.1. The 1-form  $\beta$  on  $P$ .** In this subsection, we construct a 1-form  $\beta$  on a positive flow-spine  $P$  of  $M$  that will be used to give a contact form on  $M$ .

Let  $P$  be a positive flow-spine of  $M$ . We assume that  $P$  is embedded in  $M$  so that, for each edge  $e$  of  $P$ , the closure of the union of any pair of adjacent regions that induce opposite orientations to  $e$  is smooth along  $e$ . Hereafter, a 1-form on  $P$  means that it is obtained by gluing the pullback of a 1-form on  $Q'$  by the projection  $\text{pr}_Q : Q \rightarrow Q'$  and 1-forms on the smooth surfaces  $R_1, \dots, R_n$ .

Set  $G_E = \text{pr}_{D^2}(S_E)$  and  $G_F = \text{pr}_{D^2}(S_F)$ . Each region  $R_i$  of  $P$  corresponds to a region  $S_i$  on  $D^2$  bounded by  $G_E \cup \partial D^2$  as  $S_i = \text{pr}_{D^2} \circ g_D^{-1}(R_i \times \{1\})$ . Each region  $S_i$  divides into several regions by  $G_F$ . For example, the 1-gon bounded by  $G_E$  in Figure 23 divides into three regions by  $G_F$ . We denote the graph  $(\text{pr}_{R_i} \circ g_E \circ \text{pr}_{D^2}^{-1})(G_F \cap S_i)$  on  $R_i$  by  $G_{R_i}$ , the neighborhood  $\text{pr}_{R_i} \circ g_D(N_A)$  of  $G_{R_i} \cup \partial R_i$  in  $R_i$  by  $A_{R_i}$  and the connected components of  $R_i \setminus G_{R_i}$  by  $R_{i1}, \dots, R_{in_i}$ , see Figure 23.

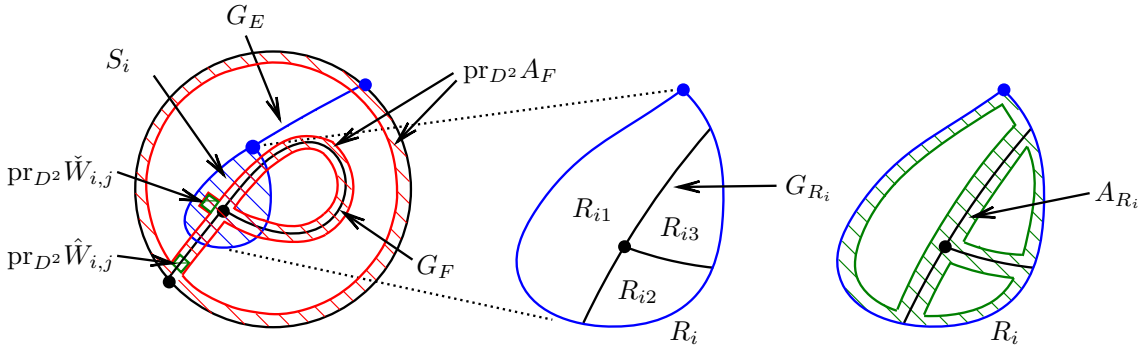


FIGURE 23. The graph  $G_{R_i}$ , the divided regions  $R_{i1}, \dots, R_{in_i}$  and the neighborhood  $A_{R_i}$ .

We may choose a coordinate system  $\mathcal{C}$  of  $M$  with respect to  $P$  so as to satisfy the conditions (B-D'), (R-E), (R-F), (B-E) and (B-F) in the previous section and the following additional condition:

(A) There exists a deformation retraction from  $A_{R_i}$  to  $G_{R_i} \cup \partial R_i$  in each  $R_i$ .

*Definition.* A coordinate system  $\mathcal{C}$  is said to be *non-degenerate* if it satisfies the conditions (B-D'), (R-E), (R-F), (B-E), (B-F) and (A).

For a 1-form  $\beta$  on  $P$ , let  $\hat{\beta}$  be the 1-form on  $N_P$  defined by  $\text{pr}^*\beta$  on  $N_Q$  and

$$(6.1) \quad (1 - \sigma(r_i))(\text{pr}_Q \circ g_{\mathcal{R}_i})^*\beta + \sigma(r_i)\text{pr}_{\mathcal{R}_i}^*\beta$$

on  $N_{\mathcal{R}_i}$ . The 1-forms  $g_E^*\hat{\beta}$  on  $E$  and  $g_F^*\hat{\beta}$  on  $F$  can extend to the whole  $N_D$  since they are invariant under translation to the  $w$ -coordinate. Let  $\hat{\beta}_E$  and  $\hat{\beta}_F$  denote the 1-forms on  $N_D$  obtained by extending  $g_E^*\hat{\beta}$  on  $E$  and  $g_F^*\hat{\beta}$  on  $F$  to  $N_D$ , respectively.

**Lemma 6.2.** *The 1-form  $\hat{\beta}$  does not depend on the variable  $t_j^k$  on  $B_j^k$  for  $k = e, v$  and the variable  $t_i$  on  $N_{\mathcal{R}_i}$ .*

*Proof.* On  $N_P \setminus \bigcup_{i,j} W_{i,j}$ , the assertion is obvious from the construction of  $\hat{\beta}$ . On  $W_{i,j}$ , both of  $(\text{pr}_Q \circ g_{\mathcal{R}_i})^*\beta$  and  $\text{pr}_{\mathcal{R}_i}^*\beta$  depend only on the coordinates  $(r_i, \theta_i)$  by (6.1). Thus the assertion follows.  $\square$

Let  $\eta$  be the reference 1-form of  $(P, \mathcal{C})$ , where  $\mathcal{C}$  is a non-degenerate coordinate system. Let  $\eta_E$  and  $\eta_F$  be the 1-forms on  $N_D$  used when we define  $\eta$  in the previous section.

**Lemma 6.3.** *There exists a 1-form  $\beta$  on  $P$  such that*

- (a)  $d\beta > 0$  on  $P$ , and
- (b)  $\max\{|B_E|, |B_F|\} < \frac{1}{2} \min\{d\hat{\beta}_E \wedge \eta, d\hat{\beta}_F \wedge \eta\}$  on  $N_A$ ,

where

$$B_E = \hat{\beta}_E \wedge \left( -\frac{d\tau}{dw}(w)\eta \wedge dw + (1 - \tau(w))d\eta \right) \quad \text{and}$$

$$B_F = \hat{\beta}_F \wedge \left( \frac{d\tau}{dw}(w)\eta \wedge dw + \tau(w)d\eta \right).$$

*Proof.* Since  $P$  is a positive flow-spine, it satisfies the admissibility condition by Proposition 4.5. Hence we can choose real numbers  $x_1, \dots, x_m$  that satisfy inequality (4.1). Each region  $R_i$  divides into several regions  $R_{ij}$  by  $G_{R_i}$ . If an edge  $e$  of  $S(P)$  with a real number  $x(e)$  divides into  $k_e$  edges, then we assign  $x(e)/k_e$  to each of the  $k_e$  edges, where the orientations of the  $k_e$  edges are chosen so that they are consistent with that of  $e$ . We then assign orientations to the edges of  $G_{R_i}$  and assign real numbers to them so that, for each region  $R_{ij}$ , the sum of all assigned real numbers along  $\partial R_{ij}$  is strictly positive. The existence of such an assignment will be proved in Lemma 6.4 below.

Now we take the real 2-plane  $\mathbb{R}^2$  with the coordinates  $(x, y)$  and set the 1-form  $x^s dy$  on it, where  $s$  is a positive real number. Set  $U = \{(x, y) \in \mathbb{R}^2 \mid 0 < x < 1\}$ . For each vertex  $v$  of  $\text{pr}(S(P))$ , we choose an open disk  $Q_v$  in  $U$  with the 1-form  $x^s dy$ . For each edge  $e$  of  $\text{pr}(S(P))$  connecting vertices  $v_1$  and  $v_2$ , we choose an embedded arc  $\gamma_e$  in  $U$  with an open neighborhood  $Q_e$  in  $U$  satisfying that

- (1) the 1-form on  $Q_e$  near the endpoints coincides with those on  $Q_{v_1}$  and  $Q_{v_2}$ , and
- (2)  $\int_{\gamma_e} x^s dy = x(e)$ , where  $x(e)$  is the real number assigned to the edge  $e$ .

We call the neighborhood  $Q_e$  an *open band*. We can find such an open band since the 1-form  $x^s dy$  does not depend on the  $y$ -coordinate while the integrated value depends on the  $y$ -coordinate. By gluing such 1-forms for all open disks  $\{Q_v\}$  and open bands  $\{Q_e\}$  and identifying the union of these pieces with  $Q'$  so that the arc in each open band is sent to the corresponding edge of  $S(P)$  in  $Q'$ , we obtain a 1-form  $\beta_{Q'}$  on  $Q'$ .

We then define a 1-form  $\beta_Q$  on  $Q$  by  $\text{pr}_Q^* \beta_{Q'}$ , where  $\text{pr}_Q : Q \rightarrow Q'$  is the projection introduced in Section 5.2.

On each  $R_i$ , we set the 1-form on  $g_{R_i}^{-1}(Q)$  by  $g_{R_i}^* \beta_Q$ , where  $g_{R_i} : \mathcal{R}'_i \times \{\frac{1}{2}\} \rightarrow Q$  is the restriction of  $g_{R_i}$  to  $\mathcal{R}'_i \times \{\frac{1}{2}\}$ . Note that  $g_{R_i}^* \beta_Q$  is induced from the form  $x^s dy$  on  $U$  for each of neighborhoods of vertices and edges of  $S(P)$  in  $\partial R_i$ . We then extend it to a 1-form  $\beta_{A_{R_i}}$  on  $A_{R_i}$  using  $x^s dy$  by the same manner. Next, we extend the 1-form  $\beta_{A_{R_i}}$  to the whole  $R_i$  by using the argument of Thurston and Winkelnkemper [47]. For each region  $R_{ij}$ , choose a volume form  $\Omega_{ij}$  on  $R_{ij}$  that satisfies  $\int_{R_{ij}} \Omega_{ij} = \int_{\partial R_{ij}} \beta_{A_{R_i}}$  and  $\Omega_{ij} = d(\beta_{A_{R_i}})$  on  $A_{R_i} \cap R_{ij}$ . Let  $\beta'_{R_{ij}}$  be any 1-form on  $R_{ij}$  that equals  $\beta_{A_{R_i}}$  on  $A_{R_i} \cap R_{ij}$ . By Stokes' theorem, we have

$$\int_{R_{ij}} (\Omega_{ij} - d\beta'_{R_{ij}}) = \int_{R_{ij}} \Omega_{ij} - \int_{\partial R_{ij}} \beta'_{R_{ij}} = \int_{R_{ij}} \Omega_{ij} - \int_{\partial R_{ij}} \beta_{A_{R_i}} = 0.$$

The closed 2-form  $\Omega_{ij} - d\beta'_{R_{ij}}$  represents the trivial class in cohomology vanishing on  $A_{R_i} \cap R_{ij}$ . By de Rham's theorem, there is a 1-form  $\zeta_{i,j}$  on  $R_{ij}$  vanishing on  $A_{R_i} \cap R_{ij}$  and satisfying  $d\zeta_{i,j} = \Omega_{ij} - d\beta'_{R_{ij}}$ . Define  $\beta_{R_{ij}} = \beta'_{R_{ij}} + \zeta_{i,j}$ . Then  $d\beta_{R_{ij}} = \Omega_{ij}$  is a volume form on  $R_{ij}$  and  $\beta_{R_{ij}}$  coincides with  $\beta_{A_{R_i}}$  on  $A_{R_i} \cap R_{ij}$ .

Gluing  $\beta_{A_{R_i}}$  on  $A_{R_i}$  and  $\beta_{R_{ij}}$  on  $R_{ij}$ 's for each  $R_i$  and then gluing them with the 1-forms  $\beta_Q$  on  $Q$ , we obtain a 1-form  $\beta$  on  $P$  that satisfies  $d\beta > 0$  on  $P$ .

Next we check the condition (b). By the construction,  $\hat{\beta}_E$  and  $\hat{\beta}_F$  on  $N_A$  are defined by gluing 1-forms of type  $x^s dy$ . The convergence of  $x^s dy$  as  $s$  goes to the infinity is faster than that of  $d(x^s dy) = sx^{s-1} dx \wedge dy$  since  $0 < x < 1$ . Hence the inequality on  $N_A$  in the condition (b) is satisfied for a sufficiently large  $s$  if the right-hand side is positive. On  $N_A$ , the forms  $\eta_E$  and  $\eta_F$  are either  $dt_j^k$  for  $k = e$  or  $v$ ,  $dt_i$  or those given in Lemmas 5.7 and 5.8. Since  $\eta$  is given by the linear sum of  $\eta_E$  and  $\eta_F$  as in (5.4), Lemma 6.2 and the condition (a) imply the inequalities  $d\hat{\beta}_E \wedge \eta > 0$  and  $d\hat{\beta}_F \wedge \eta > 0$ . This completes the proof.  $\square$

For an immersed oriented circle or arc  $a$  and an edge  $e$  in an oriented graph, set  $I(a, e)$  to be the integer that counts how many times  $a$  passes through  $e$  algebraically.

**Lemma 6.4.** *Suppose that real numbers  $x_1, \dots, x_{n_i}$  are assigned to the oriented edges  $e_1, \dots, e_{n_i}$  on  $\partial R_i$  such that  $\sum_{k=1}^{n_i} I(\partial R_i, e_k) x_k > 0$ . Then there exists an assignment of real numbers  $x'_1, \dots, x'_{n'_i}$  to the oriented edges  $e'_1, \dots, e'_{n'_i}$  of  $G_{R_i}$  such that they satisfy  $\sum_{k=1}^{n'_i} I(\partial R_{ij}, e'_k) x'_k > 0$  for each region  $R_{ij}$ .*

*Proof.* Adding an edge to  $G_{R_i}$  if necessary, we may assume that  $G_{R_i} \cup \partial R_i$  is connected. Then, the graph  $G_{R_i}$  is obtained from  $\partial R_i$  by adding

- (I) a vertex to the interior of an edge,

- (II) an edge to a vertex (in consequence, a new vertex is added to the other end of the edge),
- (III) an edge connecting two vertices, where the two vertices are possibly the same vertex.

We prove the assertion by induction on the total number of steps (I), (II) and (III) to obtain  $G_{R_i} \cup \partial R_i$  from  $\partial R_i$ . The assertion is true for the graph on  $\partial R_i$  by the assumption. Suppose that the assertion holds after applying the steps (I), (II) and (III) finite times and consider to apply one of them once more. In case (I), if the real number assigned to the edge is  $x$  then we assign  $x/2$  to each of the two edges separated by the new vertex, where the orientations of these two edges are the one induced from the original edge. This assignment satisfies the assertion. In case (II), we can assign any real number to the edge since both sides of the added edge belong to the same region. Hence this assignment satisfies the assertion by the assumption of the induction.

In case (III), the two regions adjacent to the added edge are different. Denote these two regions by  $R'_1$  and  $R'_2$ . For  $k = 1, 2$ , let  $x'_k$  be the sum of assigned real numbers along the boundary of  $R'_k$  except the added edge. By the assumption of the induction, we have  $x'_1 + x'_2 > 0$ . Set  $\delta = (x'_1 + x'_2)/2$  and assign the real number  $\delta - x'_1$  to the added edge with orientation induced by  $R'_1$ . Then the sum of real numbers along the boundary of  $R'_1$  is  $\delta > 0$  and that along the boundary of  $R'_2$  is  $x'_2 - (\delta - x'_1) = \delta > 0$ . Thus the assertion holds, and this completes the proof by induction.  $\square$

**6.2. Proof of Theorem 6.1.** Let  $\mathcal{C}$  be a non-degenerate coordinate system of  $P$  and  $\eta$  be the reference 1-form of  $(P, \mathcal{C})$ . Let  $\beta$  be a 1-form on  $P$  constructed in Lemma 6.3. The 1-form  $\hat{\beta}$  on  $N_P$  is defined as explained before Lemma 6.2.

**Lemma 6.5.**  $\hat{\beta} \wedge d\hat{\beta} = 0$ ,  $\hat{\beta} \wedge d\eta = 0$  and  $d\hat{\beta} \wedge \eta > 0$  on  $N_P$ .

*Proof.* Lemma 6.2 implies  $\hat{\beta} \wedge d\hat{\beta} = 0$ , Lemma 5.3 implies  $\hat{\beta} \wedge d\eta = 0$  on  $N_P \setminus \bigcup_{i,j} W_{i,j}$ , and Lemmas 6.2 and 5.3 imply  $\hat{\beta} \wedge d\eta = 0$  on  $W_{i,j}$ . The last assertion follows from the linear sum (5.3) with  $\eta_{\mathcal{R}'_i} = g_{\mathcal{R}'_i}^*(dt_j^k)$  and Lemma 6.3 (a).  $\square$

**Lemma 6.6.** *The 1-form  $\alpha_{P,R} = \hat{\beta} + R\eta$  is a contact form on  $N_P$  whose Reeb vector field is positively transverse to  $P$  for any  $R > 0$ .*

*Proof.* The 1-form  $\alpha_{P,R}$  is a contact form on  $B_j^k \setminus \bigcup_i g_{\mathcal{R}_i}(N_{\mathcal{R}_i})$ , for  $k = e$  or  $v$ , since the form is given as  $\alpha_{P,R} = \hat{\beta} + Rdt_j^k$  and  $d\hat{\beta} \wedge dt_j^k > 0$  holds by Lemma 6.3 (a). It is also a contact form on  $N_{\mathcal{R}_i} \setminus \bigcup_j W_{i,j}$  since the form is given as  $\alpha_{P,R} = \hat{\beta} + Rdt_i$  by Lemma 5.2 and  $d\hat{\beta} \wedge dt_i > 0$  by Lemma 6.3 (a). On  $W_{i,j}$ , the 3-form  $\alpha_{P,R} \wedge d\alpha_{P,R}$  is given as

$$\alpha_{P,R} \wedge d\alpha_{P,R} = \hat{\beta} \wedge d\hat{\beta} + R\eta \wedge d\hat{\beta} + R\hat{\beta} \wedge d\eta + R^2\eta \wedge d\eta,$$

which is positive by Lemma 6.5 and  $\eta \wedge d\eta \geq 0$  in Lemma 5.4.

Next we check that the Reeb vector field  $R_{\alpha_{P,R}}$  of  $\alpha_{P,R}$  is transverse to  $P$ . On  $B_j^k \setminus \bigcup_i g_{\mathcal{R}_i}(N_{\mathcal{R}_i})$ , since  $\beta$  is defined from the 1-form  $x^s dy$  on  $\mathbb{R}^2$ , the Reeb vector field of  $\alpha_{P,R}$  is given as  $\frac{\partial}{\partial t_j^k}$ . Hence the assertion holds.

On  $N_{\mathcal{R}_i} \setminus \bigcup_j W_{i,j}$ ,  $\alpha_{P,R} = \hat{\beta} + Rdt_i$  by Lemma 5.2 and hence  $R_{\alpha_{P,R}} = \frac{1}{R} \frac{\partial}{\partial t_i}$  by Lemma 6.2. Thus the assertion holds.

On  $W_{i,j}$ , by Lemma 5.3,

$$\begin{aligned} \alpha_{P,R} \wedge d\alpha_{P,R} \left( R_{\alpha_{P,R}}, \frac{\partial}{\partial r_i}, \frac{\partial}{\partial \theta_i} \right) &= \left( d\hat{\beta} + R \frac{d\sigma}{dr_i}(r_i) \frac{dh_{i,j}}{d\theta_i}(\theta_i) dr_i \wedge d\theta_i \right) \left( \frac{\partial}{\partial r_i}, \frac{\partial}{\partial \theta_i} \right) \\ &= d\hat{\beta} \left( \frac{\partial}{\partial r_i}, \frac{\partial}{\partial \theta_i} \right) + R \frac{d\sigma}{dr_i}(r_i) \frac{dh_{i,j}}{d\theta_i}(\theta_i). \end{aligned}$$

The right-hand side is positive since  $d\hat{\beta} > 0$  by Lemma 6.3 (a) and  $\sigma$  and  $h_{i,j}$  are monotone increasing. Since  $\alpha_{P,R}$  is a contact form,  $R_{\alpha_{P,R}}$  is positive with respect to  $\left\langle \frac{\partial}{\partial r_i}, \frac{\partial}{\partial \theta_i} \right\rangle$ . This means that  $R_{\alpha_{P,R}}$  is positively transverse to  $P$  on  $W_{i,j}$ .  $\square$

*Proof of Theorem 6.1.* Let  $\hat{\beta}_E$  and  $\hat{\beta}_F$  be the 1-forms on  $N_D$  obtained from the 1-form  $g_D^* \hat{\beta}$  on  $E$  and  $F$ , respectively, by extending it to the whole  $N_D$  as we introduced before Lemma 6.2. Define the 1-form  $\alpha_R$  on  $N_D = D^2 \times [0, 1]$  as

$$(6.2) \quad \alpha_R = (1 - \tau(w))\hat{\beta}_E + \tau(w)\hat{\beta}_F + R\eta,$$

where  $R > 0$ . This coincides with  $\alpha_{P,R}$  on  $g_D^{-1}(N_P)$ . To show that  $\alpha_R$  is a contact form on  $M$ , by Lemma 6.6, it is enough to show that  $\alpha_R$  is a contact form on  $N_D$ . The 3-form  $\alpha_R \wedge d\alpha_R$  is calculated as

$$\begin{aligned} \alpha_R \wedge d\alpha_R &= - \frac{d\tau}{dw}(w) \hat{\beta}_E \wedge \hat{\beta}_F \wedge dw + R \frac{d\tau}{dw}(w) (-\hat{\beta}_E + \hat{\beta}_F) \wedge \eta \wedge dw \\ &\quad + R((1 - \tau(w))\hat{\beta}_E + \tau(w)\hat{\beta}_F) \wedge d\eta \\ &\quad + R((1 - \tau(w))d\hat{\beta}_E + \tau(w)d\hat{\beta}_F) \wedge \eta + R^2 \eta \wedge d\eta, \end{aligned}$$

where we used  $\hat{\beta}_E \wedge d\hat{\beta}_E = \hat{\beta}_F \wedge d\hat{\beta}_F = \hat{\beta}_E \wedge d\hat{\beta}_F = \hat{\beta}_F \wedge d\hat{\beta}_E = 0$  since  $\hat{\beta}_E$  and  $\hat{\beta}_F$  depend only on the coordinates  $(x, y)$  of each local coordinate chart on  $\text{pr}N_A$  and only on  $(r_i, \theta_i)$  on each  $N_{\mathcal{R}_i}$  as in Lemma 6.2.

On  $N_A$ , since  $\beta$  satisfies the condition (b) in Lemma 6.3, the absolute value of the sum of the second and third terms divided by  $R$  is bounded above as

$$\begin{aligned} |B_E + B_F| &\leq |B_E| + |B_F| < \min \left\{ d\hat{\beta}_E \wedge \eta, d\hat{\beta}_F \wedge \eta \right\} \\ &\leq ((1 - \tau(w))d\hat{\beta}_E + \tau(w)d\hat{\beta}_F) \wedge \eta. \end{aligned}$$

This inequality and Lemma 5.9 show that  $\alpha_R \wedge d\alpha_R$  is positive on  $N_A$  for a sufficiently large  $R$ . On  $N_D \setminus N_A$ , we have  $d\eta = 0$  and  $dw \wedge \eta = 0$  by Lemma 5.6 (1). We also have  $d\hat{\beta}_E \wedge \eta > 0$  and  $d\hat{\beta}_F \wedge \eta > 0$  by Lemma 5.6 (1) and Lemma 6.3 (a) and  $\eta \wedge d\eta \geq 0$  by Lemma 5.9. Thus  $\alpha_R \wedge d\alpha_R$  is positive on  $N_D \setminus N_A$  for a sufficiently large  $R > 0$ . Thus  $\alpha_R$  is a contact form on  $N_D$  for a sufficiently large  $R$ .

Next we check that the Reeb flow of  $\alpha_R$  is carried by  $P$ . It had been checked on  $N_P$  in Lemma 6.6. Let  $R_{\alpha_R}$  be the Reeb vector field of  $\alpha_R$ . On  $N_D$ , with coordinates  $(u, v, w)$

of  $N_D$ ,

$$\begin{aligned} \alpha_R \wedge d\alpha_R \left( R_{\alpha_R}, \frac{\partial}{\partial u}, \frac{\partial}{\partial v} \right) &= d((1 - \tau(w))\hat{\beta}_E + \tau(w)\hat{\beta}_F + R\eta) \left( \frac{\partial}{\partial u}, \frac{\partial}{\partial v} \right) \\ &= ((1 - \tau(w))d\hat{\beta}_E + \tau(w)d\hat{\beta}_F \\ &\quad + R((1 - \tau(w))d\eta_E + \tau(w)d\eta_F)) \left( \frac{\partial}{\partial u}, \frac{\partial}{\partial v} \right), \end{aligned}$$

where we used  $dw(\frac{\partial}{\partial u}) = dw(\frac{\partial}{\partial v}) = 0$ . By Lemma 6.3 (a), we have  $((1 - \tau(w))d\hat{\beta}_E + \tau(w)d\hat{\beta}_F) \left( \frac{\partial}{\partial u}, \frac{\partial}{\partial v} \right) > 0$ .

On  $N_D \setminus (\hat{W} \cup \check{W})$ , the term  $((1 - \tau(w))d\eta_E + \tau(w)d\eta_F) \left( \frac{\partial}{\partial u}, \frac{\partial}{\partial v} \right)$  vanishes by Lemma 5.6 (1) and (2) and hence  $\alpha_R \wedge d\alpha_R \left( R_{\alpha_R}, \frac{\partial}{\partial u}, \frac{\partial}{\partial v} \right) > 0$ .

On  $\hat{W}_{i,j}$ , we have  $((1 - \tau(w))d\eta_E + \tau(w)d\eta_F) \left( \frac{\partial}{\partial u}, \frac{\partial}{\partial v} \right) \geq 0$  since

$$d\eta_E \left( \frac{\partial}{\partial u}, \frac{\partial}{\partial v} \right) = g_E^* \left( \frac{d\sigma}{dr_i}(r_i) \frac{dh_{i,j}}{d\theta_i}(\theta_i) dr_i \wedge d\theta_i \right) \left( \frac{\partial}{\partial u}, \frac{\partial}{\partial v} \right) \geq 0$$

on  $E \cap \hat{W}_{i,j}$  by Lemma 5.7 (2) and  $d\eta_F \left( \frac{\partial}{\partial u}, \frac{\partial}{\partial v} \right) = 0$  on  $F \cap \hat{W}_{i,j}$  by Lemma 5.7 (3).

On  $\check{W}_{i,j}$ , we also have  $((1 - \tau(w))d\eta_E + \tau(w)d\eta_F) \left( \frac{\partial}{\partial u}, \frac{\partial}{\partial v} \right) \geq 0$  since  $d\eta_E \left( \frac{\partial}{\partial u}, \frac{\partial}{\partial v} \right) = 0$  on  $E \cap \check{W}_{i,j}$  by Lemma 5.8 (2) and

$$d\eta_F \left( \frac{\partial}{\partial u}, \frac{\partial}{\partial v} \right) = g_F^* \left( \frac{d\sigma}{dr_i}(r_i) \frac{dh_{i,j}}{d\theta_i}(\theta_i) dr_i \wedge d\theta_i \right) \left( \frac{\partial}{\partial u}, \frac{\partial}{\partial v} \right) \geq 0$$

on  $F \cap \check{W}_{i,j}$  by Lemma 5.8 (3).

Thus  $\alpha_R \wedge d\alpha_R \left( R_{\alpha_R}, \frac{\partial}{\partial u}, \frac{\partial}{\partial v} \right) > 0$  holds on the whole  $N_D$ . Since  $\alpha_R$  is a positive contact form,  $R_{\alpha}$  is positively transverse to  $\langle \frac{\partial}{\partial u}, \frac{\partial}{\partial v} \rangle$  on  $N_D$ . This completes the proof.  $\square$

## 7. UNIQUENESS

In this section, we prove the following theorem, which is the uniqueness asserted in Theorem 1.1.

**Theorem 7.1.** *Let  $P$  be a positive flow-spine of  $M$  and  $\alpha_0$  and  $\alpha_1$  be contact forms on  $M$  whose Reeb flows are carried by  $P$ . Then the contact structures  $\ker \alpha_0$  and  $\ker \alpha_1$  are isotopic.*

**Lemma 7.2.** *Let  $\mathcal{C}$  be a non-degenerate coordinate system  $\mathcal{C}$  of  $M$  with respect to a positive flow-spine  $P$ . Let  $\eta$  be the reference 1-form of  $(P, \mathcal{C})$ . For  $i = 0, 1$ , let  $\alpha_i$  be a contact form on  $M$  satisfying  $\alpha_i \wedge d\eta + d\alpha_i \wedge \eta > 0$ . Then there exists a one-parameter family of contact forms connecting  $\alpha_0$  and  $\alpha_1$ .*

*Proof.* For each  $\alpha_i$ , set  $\alpha_{R,i} = \alpha_i + R\eta$  for  $R \geq 0$ . Then

$$\alpha_{R,i} \wedge d\alpha_{R,i} = \alpha_i \wedge d\alpha_i + R(\alpha_i \wedge d\eta + d\alpha_i \wedge \eta) + R^2\eta \wedge d\eta.$$

The assumption  $\alpha_i \wedge d\eta + d\alpha_i \wedge \eta > 0$  and the inequality  $\eta \wedge d\eta \geq 0$  in Lemma 5.9 imply that  $\alpha_{R,i}$  is a contact form for any  $R \geq 0$ .

Set  $\alpha_{R,s} = (1-s)\alpha_0 + s\alpha_1 + R\eta$  for  $s \in [0, 1]$ . Then

$$\begin{aligned} \alpha_{R,s} \wedge d\alpha_{R,s} &= (1-s)^2\alpha_0 \wedge d\alpha_0 + s(1-s)(\alpha_0 \wedge d\alpha_1 + \alpha_1 \wedge d\alpha_0) + s^2\alpha_1 \wedge d\alpha_1 \\ &\quad + R\{((1-s)d\alpha_0 + sd\alpha_1) \wedge \eta + ((1-s)\alpha_0 + s\alpha_1) \wedge d\eta\} \\ &\quad + R^2\eta \wedge d\eta. \end{aligned}$$

Since the fourth term (having the coefficient  $R$ ) is positive by the assumption and the last term is non-negative by Lemma 5.9, this 3-form is positive for any  $s \in [0, 1]$  if  $R$  is sufficiently large. Combining this with the observation in the first paragraph, we have the assertion.  $\square$

**Lemma 7.3.** *Let  $\mathcal{C}$  be a non-degenerate coordinate system of  $M$  with respect to a positive flow-spine  $P$  and let  $\eta$  be the reference 1-form of  $(P, \mathcal{C})$ . Then there exists a contact form  $\alpha$  such that  $\alpha \wedge d\eta + d\alpha \wedge \eta > 0$  and its Reeb flow is carried by  $P$ .*

*Proof.* Let  $\alpha$  be a contact form whose Reeb flow is carried by  $P$  given in Theorem 6.1. On  $N_P$ , it is given, in Lemma 6.6, as  $\alpha = \hat{\beta} + R\eta$ . Thus we have

$$\alpha \wedge d\eta + d\alpha \wedge \eta = \hat{\beta} \wedge d\eta + d\hat{\beta} \wedge \eta + 2R\eta \wedge d\eta > 0$$

by Lemmas 6.5 and 5.9. On  $N_D$ ,  $\alpha$  is given, in (6.2), as  $\alpha_R = (1-\tau(w))\hat{\beta}_E + \tau(w)\hat{\beta}_F + R\eta$ . Thus we have

$$\begin{aligned} \alpha \wedge d\eta + d\alpha \wedge \eta &= \frac{d\tau}{dw}(w)(-\hat{\beta}_E + \hat{\beta}_F) \wedge \eta \wedge dw \\ &\quad + ((1-\tau(w))\hat{\beta}_E + \tau(w)\hat{\beta}_F) \wedge d\eta + ((1-\tau(w))d\hat{\beta}_E + \tau(w)d\hat{\beta}_F) \wedge \eta \\ &\quad + 2R\eta \wedge d\eta. \end{aligned}$$

This is positive on  $N_A$  by the condition (b) in Lemma 6.3 and Lemma 5.9. On  $N_D \setminus N_A$ , we have  $\alpha \wedge d\eta = ((1-\tau(w))d\hat{\beta}_E + \tau(w)d\hat{\beta}_F) \wedge dw$  since  $\eta_D = dw$  by Lemma 5.6 (1), which is positive by the condition (a) in Lemma 6.3. This completes the proof.  $\square$

Next, we explain how to choose a coordinate system for a given contact form on  $M$  and a positive flow-spine  $P$  that carries its Reeb flow. For each vertex  $v_j$  of  $P$ , we choose a neighborhood  $\text{Nbd}(v_j; M)$  of  $v_j$  in  $M$ . Let  $\text{pr}$  be the projection from  $\text{Nbd}(v_j; M)$  to  $\mathbb{R}^2$  that identifies points connected by an orbit of the Reeb flow in  $\text{Nbd}(v_j; M)$ . Choose the coordinates  $x_j^v$  and  $y_j^v$  on  $\text{pr}(S(P))$  as shown in Figure 24.

In  $\text{Nbd}(v_j; M)$ , set the box  $[0, 3]^2 \times [0, 5]$  with coordinates  $(x_j^v, y_j^v, t_j^v)$ , that is used in Section 5.2 to define  $B_j^v$ , so that

- (i) the Reeb vector field  $R_\alpha$  is parallel to  $\frac{\partial}{\partial t_j^v}$  in the same direction, that is, there exists a positive smooth function  $c : [0, 3]^2 \times [0, 5] \rightarrow \mathbb{R}$  such that  $\frac{\partial}{\partial t_j^v} = c(x_j^v, y_j^v, t_j^v)R_\alpha$  in  $[0, 3]^2 \times [0, 5]$ , and
- (ii)  $P \cap B_j^v$  lies in the core of  $B_j^v$ .

The rest pieces  $B_j^e$  and  $N_{\mathcal{R}_i}$  of  $N(P)$  are chosen canonically. We then choose the coordinates  $(u, v, w)$  on  $N_D$  so that  $\frac{\partial}{\partial w} = C(u, v)R_\alpha$  on  $(u, v, w)$ , where  $C(u, v)$  is a positive smooth function on  $(u, v)$ .

We further assume, by choosing  $B_j^v$  and  $B_j^e$  sufficiently small, that

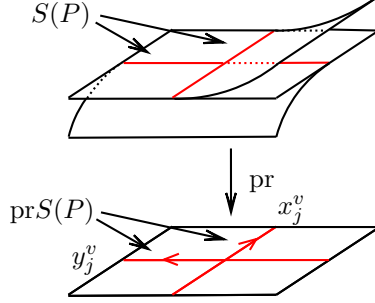


FIGURE 24. The coordinates  $x_j^v$  and  $y_j^v$  on  $\text{pr}(S(P))$ .

- (iii) the coordinate system of  $M$  obtained as above is non-degenerate, and
- (iv) the partial derivatives of  $C(u, v)$  are sufficiently close to 0 on  $\check{W}$ .

The condition (iv) is satisfied since as  $B_j^v$  gets smaller the lengths of Reeb orbits in  $\check{W}_{i,j}$  get close to the same length.

**Lemma 7.4.** *Let  $P$  be a positive flow-spine of  $M$  and  $\alpha$  be a contact form on  $M$  whose Reeb flow is carried by  $P$ . Choose a non-degenerate coordinate system  $\mathcal{C}$  of  $M$  with respect to  $P$  as above. Assume that, for each  $B_j^v$ , the coordinate  $x_j^v$  satisfies  $\alpha\left(\frac{\partial}{\partial x_j^v}\right) < 0$  in the box  $[0, 3]^2 \times [0, 5]$  that contains  $B_j^v$ . Then the reference 1-form  $\eta$  of  $(P, \mathcal{C})$  satisfies  $\alpha \wedge d\eta + d\alpha \wedge \eta > 0$ .*

*Proof.* On  $B_j^k \setminus \bigcup_i g_{\mathcal{R}_i}(N_{\mathcal{R}_i})$  for  $k = e$  or  $v$ , we have  $d\eta = d(dt_j^k) = 0$  and  $d\alpha \wedge \eta > 0$  since, with the coordinates  $(x_j^k, y_j^k, t_j^k)$  of  $B_j^k$ ,

$$d\alpha \wedge \eta \left( \frac{\partial}{\partial x_j^k}, \frac{\partial}{\partial y_j^k}, R_\alpha \right) = dt_j^k(R_\alpha) d\alpha \left( \frac{\partial}{\partial x_j^k}, \frac{\partial}{\partial y_j^k} \right).$$

It satisfies  $dt_j^k(R_\alpha) = dt_j^k\left(\frac{1}{c} \frac{\partial}{\partial t_j^k}\right) = \frac{1}{c} > 0$ , where  $c = c(x_j^k, y_j^k, t_j^k)$ . We also have

$d\alpha\left(\frac{\partial}{\partial x_j^k}, \frac{\partial}{\partial y_j^k}\right) > 0$  otherwise  $\alpha$  cannot be a positive contact form. Thus  $\alpha \wedge d\eta + d\alpha \wedge \eta > 0$  holds on  $B_j^k \setminus \bigcup_i g_{\mathcal{R}_i}(N_{\mathcal{R}_i})$ .

On  $N_{\mathcal{R}_i} \setminus \bigcup_j W_{i,j}$ , we have  $d\eta = 0$  by Lemma 5.3. The inequality  $d\alpha \wedge \eta > 0$  follows from Lemma 5.2 and the same observation used in the last paragraph. Thus  $\alpha \wedge d\eta + d\alpha \wedge \eta > 0$  holds on  $N_{\mathcal{R}_i} \setminus \bigcup_j W_{i,j}$ .

On  $W_{i,j}$ , by Lemmas 5.2 and 5.3,

$$\alpha \wedge d\eta + d\alpha \wedge \eta = \frac{d\sigma}{dr_i}(r_i) \frac{dh_{i,j}}{d\theta_i}(\theta_i) \alpha \wedge dr_i \wedge d\theta_i + d\alpha \wedge \left( dt_i + \sigma(r_i) \frac{dh_{i,j}}{d\theta_i}(\theta_i) d\theta_i \right).$$

The factors  $\frac{d\sigma}{dr_i}(r_i)$  and  $\frac{dh_{i,j}}{d\theta_i}(\theta_i)$  are non-negative and the 3-form  $\alpha \wedge dr_i \wedge d\theta_i$  is positive since  $\frac{\partial}{\partial t_i} = cR_\alpha$  implies  $dr_i \wedge d\theta_i(R_\alpha, \cdot) = 0$ . Thus the first term is non-negative. We have  $dt_i(R_\alpha) > 0$  and  $d\theta_i(R_\alpha) = 0$ , and also have  $d\alpha\left(\frac{\partial}{\partial r_i}, \frac{\partial}{\partial \theta_i}\right) > 0$  otherwise  $\alpha$  cannot

be a positive contact form. Hence the second term is positive. Thus  $\alpha \wedge d\eta + d\alpha \wedge \eta > 0$  holds on  $W_{i,j}$ .

On  $N_D$ ,

$$d\alpha \wedge \eta \left( \frac{\partial}{\partial u}, \frac{\partial}{\partial v}, R_\alpha \right) = \eta(R_\alpha) d\alpha \left( \frac{\partial}{\partial u}, \frac{\partial}{\partial v} \right).$$

Since  $\frac{\partial}{\partial w} = C(u, v)R_\alpha$ , we have  $\eta(R_\alpha) > 0$  on  $N_D \setminus N_A$  by Lemma 5.6 (1). The inequality  $\eta(R_\alpha) > 0$  also holds on  $N_A \setminus (\hat{W} \cup \check{W})$  since  $\eta$  is a linear sum of some of  $dt_j^k$  for  $k = e, v$  and  $dt_i$  and on  $\hat{W} \cup \check{W}$  by Lemmas 5.7 and 5.8. We also have  $d\alpha \left( \frac{\partial}{\partial u}, \frac{\partial}{\partial v} \right) > 0$  otherwise  $\alpha$  cannot be a contact form. Thus  $d\alpha \wedge \eta > 0$ . It remains to show the inequality  $\alpha \wedge d\eta \geq 0$  on  $N_D$ . On  $N_D \setminus (\hat{W} \cup \check{W})$ , we have  $d\eta = 0$  by Lemma 5.6 (1) and (2).

We check  $\alpha \wedge d\eta \geq 0$  on  $\hat{W}_{i,j}$ . From (5.4), the 2-form  $d\eta$  on  $N_D$  is given as

$$d\eta = -\frac{d\tau}{dw}(w)dw \wedge \eta_E + \frac{d\tau}{dw}(w)dw \wedge \eta_F + (1 - \tau(w))d\eta_E + \tau(w)d\eta_F.$$

By Lemma 5.7 (1) and (2),  $dw \wedge \eta_E$  is the extension of  $g_E^* \left( \sigma(r_i) \frac{dh_{i,j}}{d\theta_i}(\theta_i) dt_i \wedge d\theta_i \right)$  and  $d\eta_E$  is the extension of  $g_E^* \left( \frac{d\sigma}{dr_i}(r_i) \frac{dh_{i,j}}{d\theta_i}(\theta_i) dr_i \wedge d\theta_i \right)$  to the whole  $\hat{W}_{i,j}$ . Similarly, by Lemma 5.7 (3),  $dw \wedge \eta_F$  is the extension of  $g_E^* \left( \frac{dh_{i,j}}{d\theta_i}(\theta_i) dt_i \wedge d\theta_i \right)$  to  $\hat{W}_{i,j}$  and  $d\eta_F = 0$  on  $\hat{W}_{i,j}$ . Hence

$$d\eta = g_E^* \left( (1 - \sigma(r_i)) \frac{d\tau}{dw}(w) \frac{dh_{i,j}}{d\theta_i}(\theta_i) dt_i \wedge d\theta_i + (1 - \tau(w)) \frac{d\sigma}{dr_i}(r_i) \frac{dh_{i,j}}{d\theta_i}(\theta_i) dr_i \wedge d\theta_i \right).$$

On  $E \cap \hat{W}_{i,j}$ , we have

$$\begin{aligned} \alpha \wedge d\eta \left( \frac{\partial}{\partial r_i}, \frac{\partial}{\partial \theta_i}, R_\alpha \right) &= - (1 - \sigma(r_i)) \frac{d\tau}{dw}(w) \frac{dh_{i,j}}{d\theta_i}(\theta_i) \alpha \left( \frac{\partial}{\partial r_i} \right) dt_i(R_\alpha) \\ &\quad + (1 - \tau(w)) \frac{d\sigma}{dr_i}(r_i) \frac{dh_{i,j}}{d\theta_i}(\theta_i), \end{aligned}$$

where the coordinates  $(r_i, \theta_i, w)$  are regarded as those on  $\hat{W}_{i,j}$  according to the product structure of  $\hat{W}_{i,j}$  in  $N_D = D^2 \times [-\varepsilon, 1 + \varepsilon]$ . Since  $\hat{W}_{i,j} \subset [0, 3]^2 \times [0, 5]$ , the inequality  $\alpha \left( \frac{\partial}{\partial x_j^v} \right) < 0$  holds on  $\hat{W}_{i,j}$  by the assumption, which implies  $\alpha \left( \frac{\partial}{\partial r_i} \right) < 0$ . Hence we have  $\alpha \wedge d\eta \left( \frac{\partial}{\partial r_i}, \frac{\partial}{\partial \theta_i}, R_\alpha \right) \geq 0$ .

We check  $\alpha \wedge d\eta \geq 0$  on  $\check{W}_{i,j}$ . By Lemma 5.8,

$$d\eta = \frac{d\tau}{dw}(w)g_F^* \left( \sigma(r_i) \frac{dh_{i,j}}{d\theta_i}(\theta_i) dt_i \wedge d\theta_i \right) + \tau(w)g_F^* \left( \frac{d\sigma}{dr_i}(r_i) \frac{dh_{i,j}}{d\theta_i}(\theta_i) dr_i \wedge d\theta_i \right).$$

On  $F \cap \check{W}_{i,j}$ , we have

$$\begin{aligned} \alpha \wedge d\eta \left( \frac{\partial}{\partial r_i}, \frac{\partial}{\partial \theta_i}, R_\alpha \right) &= -\frac{d\tau}{dw}(w)\sigma(r_i) \frac{dh_{i,j}}{d\theta_i}(\theta_i) \alpha \left( \frac{\partial}{\partial r_i} \right) dt_i(R_\alpha) \\ &\quad + \tau(w) \frac{d\sigma}{dr_i}(r_i) \frac{dh_{i,j}}{d\theta_i}(\theta_i), \end{aligned}$$

where  $(r_i, \theta_i, t_i)$  are the coordinates of  $W_{i,j} \subset N'_{\mathcal{R}_i}$  and  $(r_i, \theta_i, w)$  are regarded as the coordinates on  $\check{W}_{i,j}$  according to the canonical product structure of  $\check{W}_{i,j}$  in  $N_D = D^2 \times [-\varepsilon, 1 + \varepsilon]$ , see Figure 25. Since  $g_{\mathcal{R}_i}(W_{i,j}) \subset B_j^v$ ,  $\alpha\left(\frac{\partial}{\partial r_i}\right) < 0$  holds on  $W_{i,j}$  by the assumption. Moreover, the same inequality holds on the whole  $\check{W}_{i,j}$  since  $\frac{\partial}{\partial w} = C(u, v)R_\alpha$  satisfies

$$\mathcal{L}_{\frac{\partial}{\partial w}} \alpha = d(\iota_{\frac{\partial}{\partial w}} \alpha) = dC(u, v),$$

which is sufficiently close to 0 by the assumption (iv), where  $\mathcal{L}_X$  is the Lie derivative and  $\iota_X$  is the interior product for a vector field  $X$ . Hence we have  $\alpha \wedge d\eta\left(\frac{\partial}{\partial r_i}, \frac{\partial}{\partial \theta_i}, R_\alpha\right) \geq 0$ .

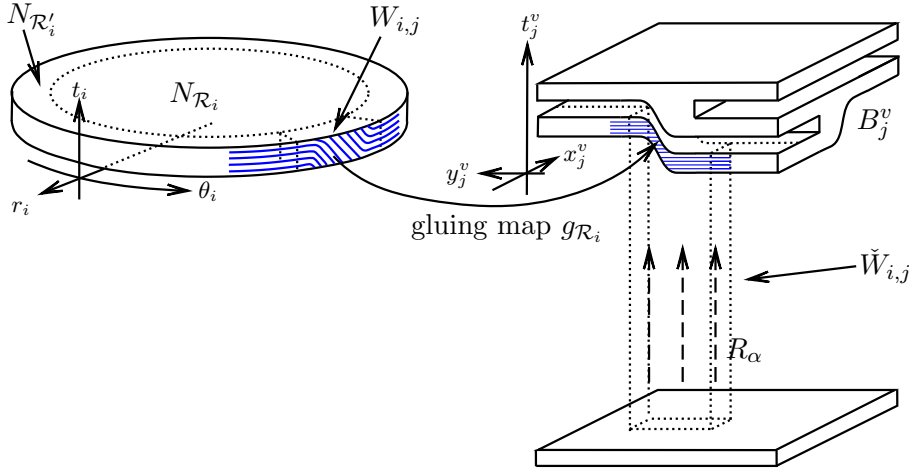


FIGURE 25. The coordinates  $(r_i, \theta_i, w)$  on  $\check{W}_{i,j}$ .

Thus  $\alpha \wedge d\eta + d\alpha \wedge \eta > 0$  is satisfied on the whole  $N_D$ . This completes the proof.  $\square$

**Lemma 7.5.** *For  $i = 0, 1$ , let  $\mathcal{C}_i$  be a non-degenerate coordinate system of  $M$  with respect to a positive flow-spine  $P$  and  $\eta_i$  be the reference 1-form of  $(P, \mathcal{C}_i)$ . Let  $\alpha_i$  be a contact form on  $M$  such that  $\alpha_i \wedge d\eta_i + d\alpha_i \wedge \eta_i > 0$  and its Reeb flow is carried by  $P$ . Then there exists a one-parameter family of contact forms connecting  $\alpha_0$  and  $\alpha_1$ .*

*Proof.* For each  $i = 0, 1$ , let  $G_i$  be the graph obtained as the union of  $\text{pr}_{D^2} S_F$  and  $\text{pr}_{D^2} S_E$  on the unit disk, where the interior points of the unit disk correspond to the Reeb orbits starting and ending at points on  $P$ . Choose a deformation  $G_t$  of graph from  $G_0$  to  $G_1$  in a generic way. Let  $t_1, \dots, t_s$  be the points in  $[0, 1]$  at which  $G_{t_j}$  has a self-tangency or a triple point or an edge passing through a trivalent vertex. We call them degenerate times. For each  $t_j$ , we may obtain a non-degenerate coordinate system  $\mathcal{C}_{t_j}$  from the graph  $G_{t_j}$  canonically. Let  $P_{t_j}$  denote the flow-spine  $P$  in the coordinate system  $\mathcal{C}_{t_j}$  and  $\eta_{t_j}$  be the reference 1-form of  $(P_{t_j}, \mathcal{C}_{t_j})$ . We then make a contact form  $\alpha_{t_j}$  on  $M$  as in Theorem 6.1.

Next we perturb the coordinate system  $\mathcal{C}_{t_j}$  slightly with fixing the contact form  $\alpha_{t_j}$  so that the degenerate time of  $G_{t_j}$  is resolved. Figure 26 shows an example in the case when

an edge passes through a trivalent vertex. The figure in the middle is  $G_{t_j}$ . By small perturbations of  $\mathcal{C}_{t_j}$ , we may obtain the graphs on the left and on the right in the figure. One of the perturbed graphs can be regarded as  $G_{t_j-\varepsilon}$  and the other can be regarded as  $G_{t_j+\varepsilon}$ . For each of them, we choose  $A_{R_i}$  sufficiently narrow so that it satisfies the condition (A) in Section 6.1.

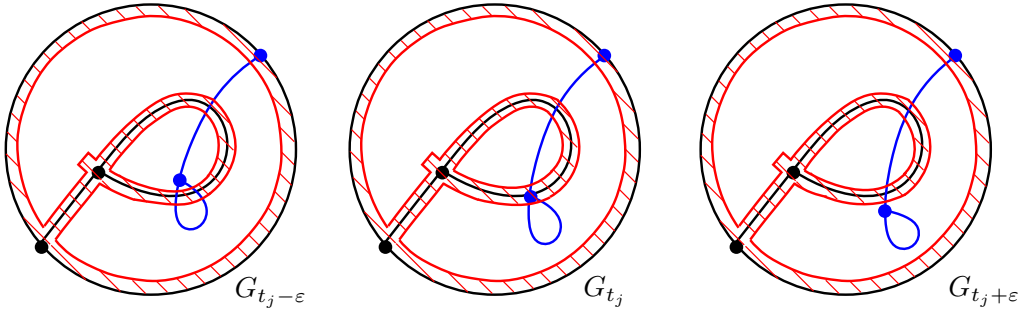


FIGURE 26. Non-degenerate coordinate systems before and after passing through a trivalent vertex.

Let  $P_{t_j-\varepsilon}$  and  $P_{t_j+\varepsilon}$  denote the flow-spine  $P_{t_j}$  in the coordinate systems  $\mathcal{C}_{t_j-\varepsilon}$  and  $\mathcal{C}_{t_j+\varepsilon}$ , respectively. We isotope  $P_{t_j-\varepsilon}$  and  $P_{t_j+\varepsilon}$  in a neighborhood of each vertex so that it satisfies the assumption in Lemma 7.4 if necessary. This is done as shown in Figure 27. The left in the figure is the case where we have  $\alpha(\frac{\partial}{\partial x_j^v}) > 0$ , that is, the assumption is not satisfied. By rotating the flow-spine near the vertex as shown on the right, we may set the coordinates  $(x_j^v, y_j^v, t_j^v)$  so that  $\alpha(\frac{\partial}{\partial x_j^v}) < 0$ .

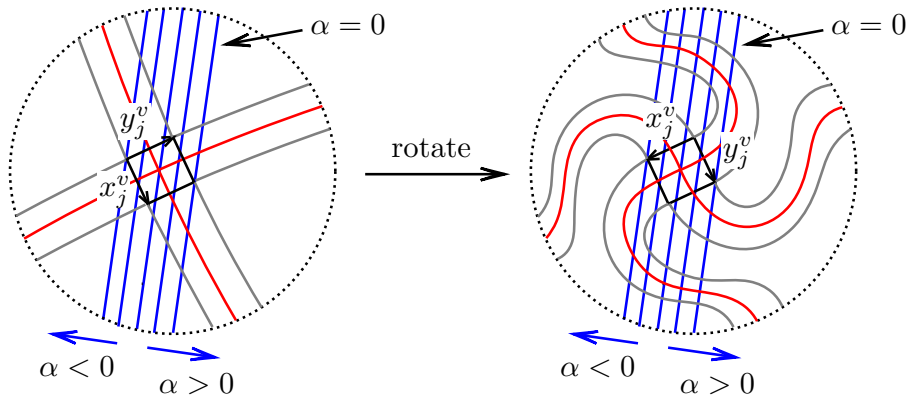


FIGURE 27. Rotate the flow-spine so that the coordinates  $(x_j^v, y_j^v, t_j^v)$  satisfy  $\alpha(\frac{\partial}{\partial x_j^v}) < 0$ .

Applying Lemma 7.4 to these isotoped  $P_{t_j-\varepsilon}$  and  $P_{t_j+\varepsilon}$ , we obtain non-degenerate coordinate systems  $\mathcal{C}_{t_j-\varepsilon}$  and  $\mathcal{C}_{t_j+\varepsilon}$  for  $G_{t_j-\varepsilon}$  and  $G_{t_j+\varepsilon}$  whose reference 1-forms  $\eta_{t_j-\varepsilon}$

and  $\eta_{t_j+\varepsilon}$  satisfy  $\alpha_{t_j} \wedge d\eta_{t_j-\varepsilon} + d\alpha_{t_j} \wedge \eta_{t_j-\varepsilon} > 0$  and  $\alpha_{t_j} \wedge d\eta_{t_j+\varepsilon} + d\alpha_{t_j} \wedge \eta_{t_j+\varepsilon} > 0$ , respectively. We set  $\alpha_t = \alpha_{t_j}$  for  $t \in [t_j - \varepsilon, t_j + \varepsilon]$ . Set  $t_0 = 0$ ,  $t_{s+1} = 1$ ,  $\alpha_t = \alpha_0$  for  $t \in [0, \varepsilon]$  and  $\alpha_t = \alpha_1$  for  $t \in [1 - \varepsilon, 1]$ .

Now, for each  $j = 0, \dots, s$ , we choose a smooth family  $\{\mathcal{C}_t \mid t \in [t_j + \varepsilon, t_{j+1} - \varepsilon]\}$  of non-degenerate coordinate systems connecting  $\mathcal{C}_{t_j+\varepsilon}$  and  $\mathcal{C}_{t_{j+1}-\varepsilon}$ . Then a smooth family of reference 1-form  $\eta_t$  is also obtained for  $t \in [t_j + \varepsilon, t_{j+1} - \varepsilon]$ . For each  $t \in [t_j + \varepsilon, t_{j+1} - \varepsilon]$ , the set of contact forms  $\alpha$  satisfying  $\alpha \wedge d\eta_t + d\alpha \wedge \eta_t > 0$  is open with Whitney  $C^\infty$ -topology, connected by Lemma 7.2 and non-empty by Lemma 7.3. Therefore there exists a one-parameter family of contact forms connecting  $\alpha_{t_j+\varepsilon}$  and  $\alpha_{t_{j+1}-\varepsilon}$  that satisfies  $\alpha_t \wedge d\eta_t + d\alpha_t \wedge \eta_t > 0$  for  $t \in [t_j + \varepsilon, t_{j+1} - \varepsilon]$ . Since  $\alpha_t = \alpha_{t_j}$  for  $t \in [t_j - \varepsilon, t_j + \varepsilon]$ , the family  $\alpha_t$ ,  $t \in [0, 1]$  is a one-parameter family of contact forms connecting  $\alpha_0$  and  $\alpha_1$ .  $\square$

*Proof of Theorem 7.1.* For each  $\alpha_i$ ,  $i = 0, 1$ , we isotope  $P_i$  in a neighborhood of each vertex as shown in Figure 27, if necessary, so that it satisfies the assumption in Lemma 7.4. Applying Lemma 7.4, we obtain a non-degenerate coordinate system  $\mathcal{C}_i$  such that the reference 1-form  $\eta_i$  of  $(P_i, \mathcal{C}_i)$  satisfies  $\alpha_i \wedge d\eta_i + d\alpha_i \wedge \eta_i > 0$ . Thus the contact forms  $\alpha_0$  and  $\alpha_1$  are connected by a one-parameter family of contact forms by Lemma 7.5. By the Gray stability [20],  $\ker \alpha_0$  and  $\ker \alpha_1$  are isotopic.  $\square$

## 8. SURJECTIVITY

In this section, we give the proof of Theorem 1.2. Recall that  $(M, \Sigma, L, \phi)$  is called an open book decomposition of a closed, oriented, smooth 3-manifold  $M$  if  $M$  is homeomorphic to the quotient space obtained from  $\Sigma \times [0, 1]$  by the identification  $(x, 1) \sim (\phi(x), 0)$  for  $x \in \Sigma$  and  $(y, 0) \sim (y, t)$  for each  $y \in \partial\Sigma$  and any  $t \in [0, 1]$  with  $L$  being the quotient of  $\partial\Sigma \times [0, 1]$ .

*Definition.* A vector field  $X$  on  $M$  is called a *monodromy vector field* of the open book  $(M, \Sigma, L, \phi)$  if

- $X$  is tangent to the binding  $L$  and the orientation on  $L$  induced from  $\Sigma$  coincides with the direction of  $X$ , and
- $X$  is positively transverse to  $\text{Int } \Sigma \times \{t\}$  for any  $t \in [0, 1]$ .

In particular, the Reeb vector field used in the definition of the contact structure supported by an open book in Section 2 is a monodromy vector field of the open book.

We first prove the following proposition.

**Proposition 8.1.** *Let  $(M, \Sigma, L, \phi)$  be an open book decomposition of a closed, connected, oriented 3-manifold  $M$  whose page is a surface of genus at least 2 and whose binding is connected. Then there exists a positive flow-spine on  $M$  that carries the flow generated by a monodromy vector field of the open book.*

*Proof.* Let  $g$  be the genus of  $\Sigma$  and  $a_1, \dots, a_g, b_1, \dots, b_{g-1}, c_1, \dots, c_g$  be the simple closed curves on the page as in Figure 28. Let  $\sigma_{a_i}$ ,  $\sigma_{b_i}$  and  $\sigma_{c_i}$  denote the right-handed Dehn twists along  $a_i$ ,  $b_i$  and  $c_i$ , respectively.

We represent the monodromy of the open book by a product of Dehn twists as  $w_1^{m_1} w_2^{m_2} \cdots w_n^{m_n}$ , where  $w_k$  is the Dehn twist along one of the curves  $a_1, \dots, a_g, b_1, \dots, b_{g-1}$ ,

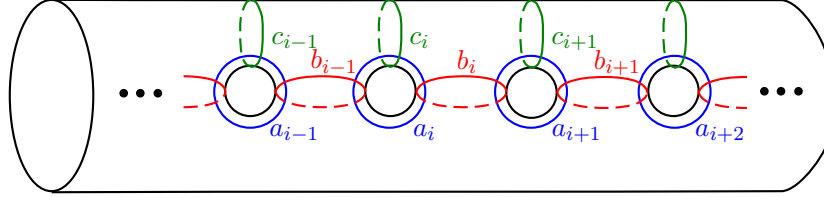


FIGURE 28. Curves for Dehn twists.

$c_1, \dots, c_g$ . Here we read the product from left to right. Let  $f : M \setminus \text{Int Nbd}(L; M) \rightarrow S^1$  be a smooth non-singular map of the open book. Choose  $6n$  points  $q_1, \dots, q_{6n}$  on  $S^1$  in the counter-clockwise order and set  $\Sigma_j = f^{-1}(q_j)$ . We assign to each  $\Sigma_j$  the orientation as a page of the open book.

We first draw a graph, which will become  $S(P)$ , on each  $\Sigma_j$  as shown in Figures 29, 30, 31, 32, 33 and 34, depending on  $j$  modulo 6.

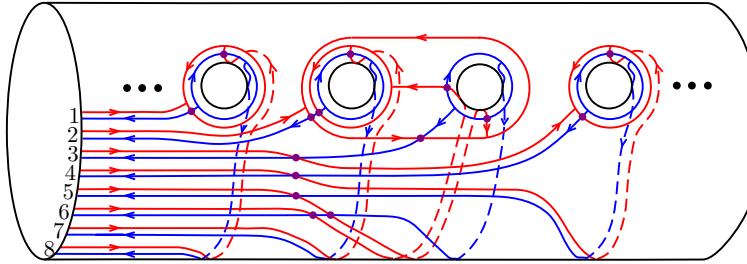


FIGURE 29. The singular set  $S(P)$  on  $\Sigma_{6k}$ .

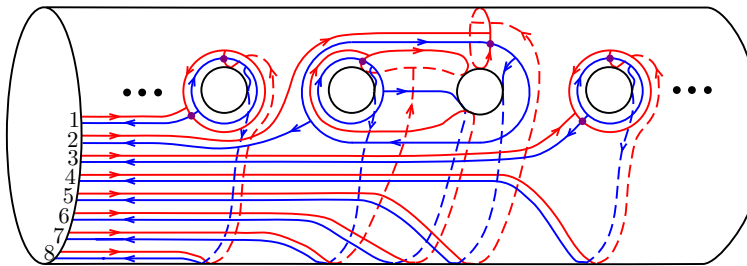
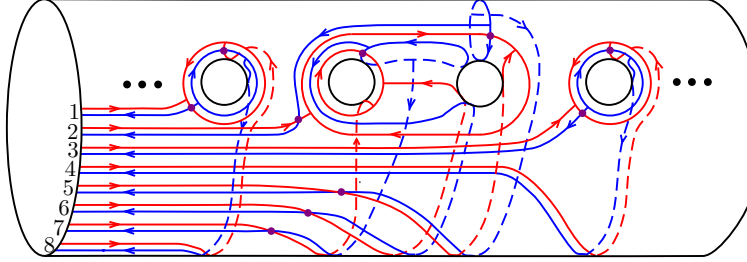
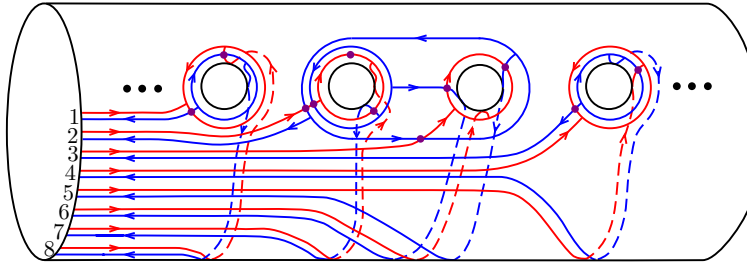
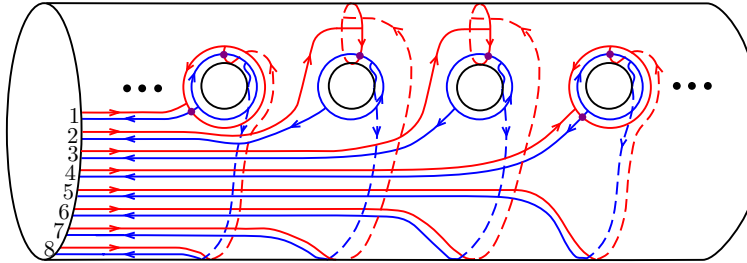
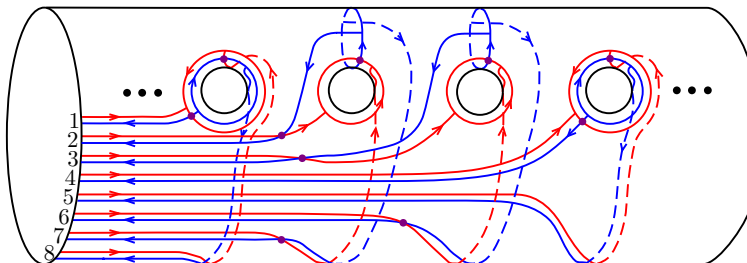


FIGURE 30. The singular set  $S(P)$  on  $\Sigma_{6k+1}$ .

For each  $j = 1, \dots, 6n$ , the red graph  $G_j^{red}$  on  $\Sigma_j$  and the blue graph  $G_j^{blue}$  on  $\Sigma_{j+1}$  coincide as unoriented graphs up to isotopy, which we denote by  $G_j$ , and their orientations are opposite. Here we regard  $\Sigma_{6n+1} = \Sigma_1$ . We attach  $G_j \times [0, 1]$  between  $\Sigma_j$  and  $\Sigma_{j+1}$  such that  $G_j \times \{0\} = G_j^{red}$  and  $G_j \times \{1\} = G_j^{blue}$ . To each region of  $G_j \times [0, 1]$

FIGURE 31. The singular set  $S(P)$  on  $\Sigma_{6k+2}$ .FIGURE 32. The singular set  $S(P)$  on  $\Sigma_{6k+3}$ .FIGURE 33. The singular set  $S(P)$  on  $\Sigma_{6k+4}$ .FIGURE 34. The singular set  $S(P)$  on  $\Sigma_{6k+5}$ .

we assign an orientation so that the induced orientation on the boundary coincides with those of the edges of  $G_j^{red}$  and  $G_j^{blue}$ . See Figure 35 for the orientations on  $G_j \times [0, 1]$ . A vertex of this branched polyhedron can be seen as either an intersection of a red edge and a blue edge on  $\Sigma_j$  or a trivalent vertex on  $\Sigma_j$ . Any vertex in the former case is of  $\ell$ -type since the blue edge intersects the red one from the left to the right with respect to the orientation of the red edge. Other vertices are those appearing in Figure 35 and we can verify that they are of  $\ell$ -type in the figure directly.

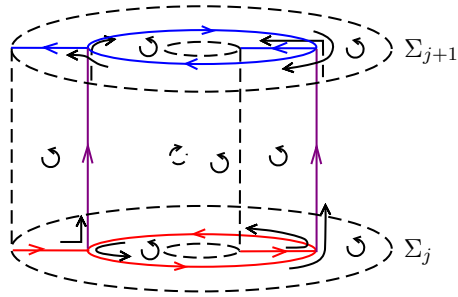


FIGURE 35. Attach  $G_j \times [0, 1]$ . Black arrows in the figure show the smooth directions of the immersion of  $S(P)$  at the vertices.

If  $w_k = \sigma_{a_p}^{m_p}$  then we modify the  $p$ -th blue circle on  $\Sigma_{6k+1}$  as shown on the left in Figure 36 if  $m_p > 0$  and as shown on the right if  $m_p < 0$ . We may verify that all vertices appearing by this modification are of  $\ell$ -type.

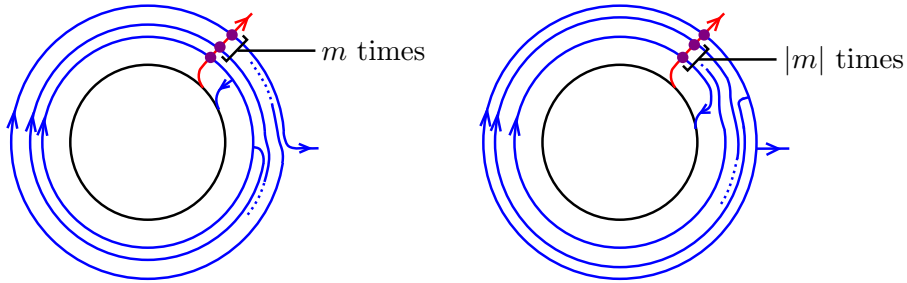


FIGURE 36. Modification of the polyhedron according to the Dehn twists  $\sigma_{a_p}^{m_p}$ .

If  $w_k = \sigma_{b_p}^{m_p}$  then, we apply the same modification to the blue curve on  $\Sigma_{6k+2}$  shown on the left in Figure 37, and if  $w_k = \sigma_{c_p}^{m_p}$  then we do the same modification to the blue curve on  $\Sigma_{6k+5}$  shown on the right. All vertices appearing by these modifications are also of  $\ell$ -type.

We may choose a monodromy vector field of the open book on  $M \setminus \text{Int Nbd}(L; M)$  such that it is positively transverse to the branched polyhedron constructed above. We denote the obtained branched polyhedron embedded in  $M \setminus \text{Int Nbd}(L; M)$  by  $\hat{P}_1$ .

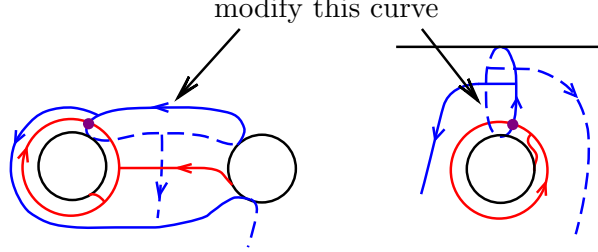


FIGURE 37. Curves for modifications corresponding to the Dehn twists  $\sigma_{b_p}^{m_p}$  and  $\sigma_{c_p}^{m_p}$ .

Next, we construct a branched polyhedron in  $\text{Nbd}(L; M)$ . For each  $(i, j)$ ,  $i = 1, \dots, 2g$ ,  $j = 1, \dots, 6n$ , we set a polyhedron  $P_{i,j}$  shown in Figure 38. Glue the left side of  $P_{i,j}$  and the right side of  $P_{i+1,j}$  canonically, where we regard  $P_{2g+1,j}$  as  $P_{1,j}$ , and denote the obtained polyhedron by  $P_j$  for  $j = 1, \dots, 6n$ . We then glue  $P_j$  and  $P_{j+1}$  so that the top of  $P_{i,j}$  is identified with the bottom of  $P_{i,j+1}$ , where  $P_{6n+1}$  is regarded as  $P_1$ . We denote the obtained polyhedron by  $\hat{P}_2$ . We assign orientations to the regions of  $\hat{P}_2$  as shown in Figure 38, so that  $\hat{P}_2$  is a branched polyhedron. The boundary of  $\hat{P}_2$  consists of  $2g$  circles and a connected graph. Attach a disk  $D_i$  to each of  $2g$  circles and denote the obtained branched polyhedron by  $\hat{P}_3$ . We can embed  $\hat{P}_3$  into the solid torus  $D^2 \times S^1$  properly. We regard this  $D^2 \times S^1$  as  $\text{Nbd}(L; M)$  and glue  $\hat{P}_3$  and  $\hat{P}_1$  so that the simple closed curve on  $\partial\hat{P}_3 \cap P_j$  (green curve) coincides with the boundary of  $\Sigma_j$  in  $\hat{P}_1$ . We denote the obtained branched polyhedron embedded in  $M$  by  $\hat{P}_4$ . We can easily check that all vertices of  $\hat{P}_4$  are of  $\ell$ -type.

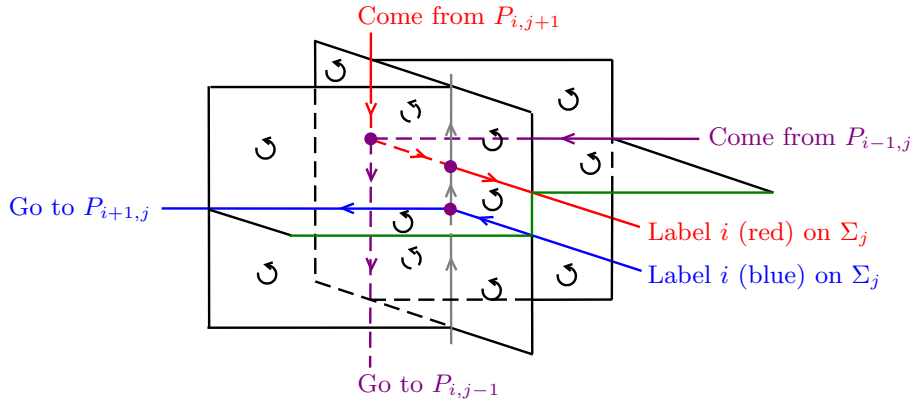


FIGURE 38. The piece  $P_{i,j}$ .

The complement  $M \setminus \hat{P}_4$  consists of  $2g + 6n$  open balls  $B_1, \dots, B_{2g}$  and  $B'_1, \dots, B'_{6n}$ , where the  $2g$  balls  $B_1, \dots, B_{2g}$  are the components bounded by  $\hat{P}_3$  and each  $B'_j$ ,  $j =$

$1, \dots, 6n$ , is the component of  $M \setminus \hat{P}_4$  containing the connected component of  $M \setminus (\hat{P}_4 \cup \text{Nbd}(L; M))$  between  $\Sigma_j$  and  $\Sigma_{j+1}$ .

The singular set  $S(P)$  consists of  $2g + 6n$  immersed circles  $C_1, \dots, C_{2g}$  and  $C'_1, \dots, C'_{6n}$ , where  $C_i$  is a simple closed curve passing through  $P_{i,1}, \dots, P_{i,6n}$ , which is drawn in gray in Figure 38, and  $C'_j$  is a simple closed curve given as follows: Start from Label 1 (red) on  $\Sigma_{6k}$  in Figure 29 and follow the arrow. Let  $P_{i_0,6k}$  be the piece of  $\hat{P}_4$  that contains the starting point. The curve passes through  $P_{i_0,6k+1}$  as depicted with black arrows in Figure 35 and comes back to Label 1 (blue) on  $\Sigma_{6k+1}$ . Then, as shown in Figure 38, it goes to Label 2 on  $\Sigma_{6k+1}$  and then goes down to Label 2 (red) on  $\Sigma_{6k}$ . By the same observation, we see that it passes through Labels 1, 2,  $\dots$ , 8 (red) on  $\Sigma_{6k}$  in this order. This curve goes further and finally comes back to Label 1 (red) on  $\Sigma_{6k}$ . This is the curve  $C'_1$ . By the same way, the curves  $C'_j$ ,  $j = 2, \dots, 6n$ , are defined.

We modify a part of  $C_i$  on  $P_{i,1}$  for each  $i = 1, \dots, 2g$  as shown in Figure 39 and remove the bigon that appears by this move. This modification does not yield a new vertex, connects  $B_i$  to  $B'_1$  and makes  $C_i$  and  $C'_1$  to be one immersed circle. Applying this modification to each of  $C_1, \dots, C_{2g}$ , we obtain a branched polyhedron  $\hat{P}_5$  with only vertices of  $\ell$ -type such that  $M \setminus \hat{P}_5$  consists of  $6n$  open balls  $B''_1, B''_2, \dots, B''_{6n}$  and  $S(P)$  consists of  $6n$  immersed circles  $C''_1, C'_2, \dots, C'_n$ , where  $B''_1$  is the open ball obtained by connecting  $B_1, \dots, B_{2g}$  with  $B'_1$  and  $C''_1$  is the immersed circle obtained by connecting  $C_1, \dots, C_{2g}$  with  $C'_1$ .

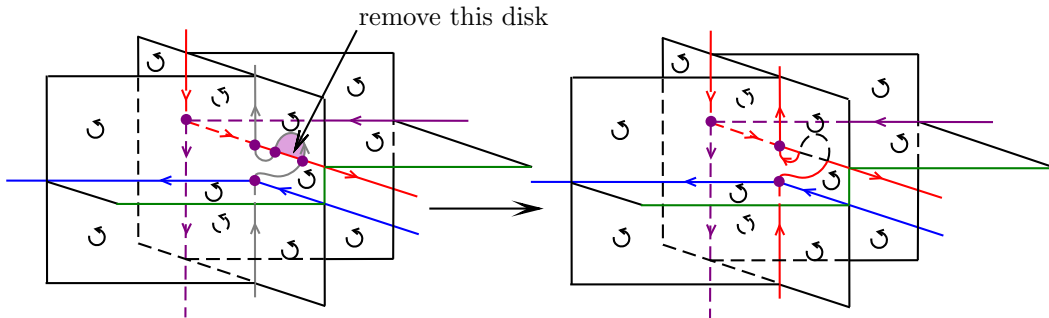


FIGURE 39. Modification of  $C_i$  on  $P_{i,j}$ .

For each  $j = 2, \dots, 6n$ , we apply the same modification to the same part of  $C''_1$  on  $P_{1,j}$ . This does not yield a new vertex, connects  $B'_j$  to  $B''_1$  and makes  $C''_1, C'_2, \dots, C'_n$  to be one immersed circle. The obtained branched polyhedron  $\hat{P}_6$  satisfies that all vertices are of  $\ell$ -type,  $M \setminus \hat{P}_6$  is one open ball and  $S(P)$  is the image of an immersion of one circle.

We can see directly that there exists a monodromy vector field of the open book whose generated flow is carried by  $\hat{P}_6$ . Thus we obtain the assertion.  $\square$

To prove Theorem 1.2, we need to show the following stronger statement.

**Proposition 8.2.** *Let  $(M, \Sigma, L, \phi)$  be an open book decomposition of a closed, connected, oriented 3-manifold  $M$  whose page is a surface of genus at least 2 and whose binding is connected. Then there exists a positive flow-spine  $P$  of  $M$  and a contact form  $\alpha$  on  $M$  such that the Reeb flow is carried by  $P$  and also is a monodromy vector field of the open book.*

*Proof.* By Proposition 8.1, there exists a positive flow-spine  $\hat{P}_6$  whose flow is a monodromy vector field of the open book. In the construction of  $\hat{P}_6$ , the polyhedron  $\hat{P}_3$  is contained in  $\text{Nbd}(L; M)$ . Let  $N_T$  be a small tubular neighborhood of  $\partial\text{Nbd}(L; M)$  in  $M \setminus \text{Int Nbd}(L; M)$ . Let  $(z', r', \theta')$  be local coordinates on  $N_T$  given as shown in Figure 40. Note that the top horizontal faces of  $B_j^c$  are flat by the definition of  $B_j^c$ . We choose coordinates  $(u, v, w)$  on  $N_D$  so that  $\frac{\partial}{\partial w}$  is tangent to  $\partial\text{Nbd}(L; M)$ . Then we take a 1-form  $\beta$  on  $\hat{P}_6$  and make a contact form  $\alpha'$  on  $M$  according to the proof of Theorem 6.1 such that  $\ker \alpha'$  is supported by  $\hat{P}_6$ .

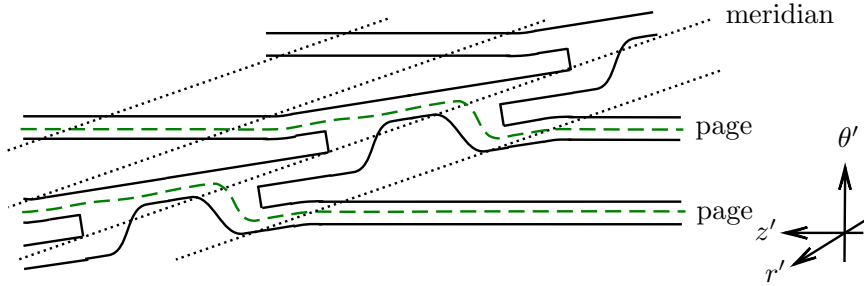


FIGURE 40. Mutual positions of  $N_P$ , pages and the meridians of the open book on  $\partial\text{Nbd}(L; M)$ .

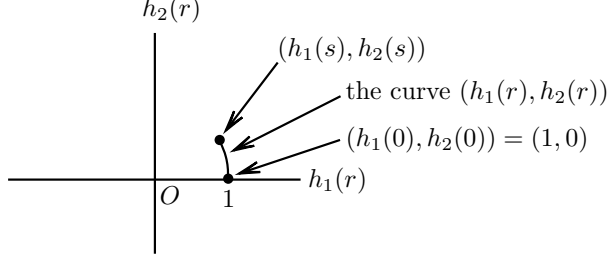
We may set the position of the pages of the open book in  $M \setminus \text{Int Nbd}(L; M)$  in such a way that the pages are transverse to  $R_{\alpha'}$  since the Reeb flow of  $\alpha'$  is carried by  $\hat{P}_6$ . However, it is not always possible to choose positions of pages of the open book in  $\text{Nbd}(L; M)$  so that  $R_{\alpha'}$  is transverse to the pages in  $\text{Nbd}(L; M)$ . For example, if  $R_{\alpha'}$  is winding along  $L$  in the direction opposite to the open book then definitely we cannot choose such positions. For this reason, we need to reconstruct  $\alpha'$  in  $\text{Nbd}(L; M)$  such that  $R_{\alpha'}$  is transverse to the pages of an open book in  $\text{Nbd}(L; M)$ .

Let  $D_s^2 \times S^1$  be the solid torus equipped with the contact form  $\alpha_b = h_1(r)dz + h_2(r)d\theta$ , where  $D_s^2$  is the 2-disk with radius  $s > 0$ ,  $(r, \theta)$  are the polar coordinates of  $D_s^2$ , and  $h_1(r)$  and  $h_2(r)$  are functions such that

- $(h_1(0), h_2(0)) = (1, 0)$ ,
- $\left(\frac{dh_1}{dr}(0), \frac{dh_2}{dr}(0)\right) = (0, 1)$ ,
- $h_1$  is monotone decreasing and  $h_2$  is monotone increasing.

The curve  $(h_1(r), h_2(r))$  is given as shown in Figure 41. Note that  $\alpha_b$  is a contact form and its Reeb vector field  $R_{\alpha_b}$  is parallel to  $-\frac{dh_1}{dr}(r)\frac{\partial}{\partial\theta} + \frac{dh_2}{dr}(r)\frac{\partial}{\partial z}$  in the same direction.

Let  $g_T$  be a diffeomorphism from  $N'_T = \{(r, \theta, z) \in D_s^2 \times S^1 \mid s' \leq r \leq s\}$  to  $N_T$  that maps  $\partial D_{s'} \times \{p\}$ ,  $p \in S^1$ , to the meridians of the open book and  $\{q\} \times S^1$ ,  $q \in \partial D_{s'}$ , to


 FIGURE 41. The curve  $(h_1(r), h_2(r))$ .

the pages in  $N_T$ , where  $s'$  is a positive real number with  $s' < s$  that is sufficiently close to  $s$ , and further satisfies that

- (i)  $g_T^*\eta = \nu_1(\theta, z)d\theta + \nu_2(\theta, z)dz$  with  $\nu_1(\theta, z) > 0$  and  $\nu_2(\theta, z) \geq 0$ , and
- (ii)  $R_{\alpha_b}$  is positively transverse to  $\ker(g_T^*\eta)$ .

We may choose such a diffeomorphism as shown in Figure 42.

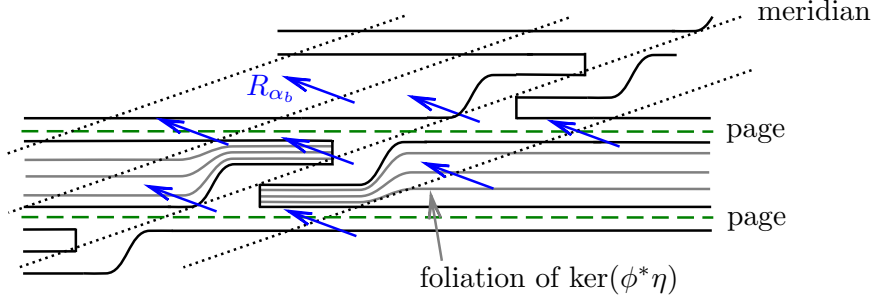


FIGURE 42. Mutual positions of the preimages of  $N_P$ , pages and the meridians of the open book by  $g_T$ , the Reeb vector field  $R_{\alpha_b}$  (blue arrows) and the foliations of  $\ker(\phi^*\eta)$  (drawn in gray) on  $\partial\text{Nbd}(L; M)$ .

Set  $\alpha_c = g_T^*(\alpha')$ . We define a contact form  $\alpha_T$  on  $N_T$  as

$$\alpha_T = (1 - \chi(r))\alpha_b + \chi(r)\alpha_c,$$

where  $\chi$  is a monotone increasing smooth function which is 0 for  $r \leq s'$  and 1 for  $r \geq s$ . Then

$$\begin{aligned} \alpha_T \wedge d\alpha_T &= (1 - \chi(r))^2 \alpha_b \wedge d\alpha_b + \frac{d\chi}{dr}(r) \alpha_b \wedge dr \wedge \alpha_c \\ &\quad + (1 - \chi(r))\chi(r) (\alpha_b \wedge d\alpha_c + \alpha_c \wedge d\alpha_b) + \chi(r)^2 \alpha_c \wedge d\alpha_c. \end{aligned}$$

The second term is  $\frac{d\chi}{dr}(r)\alpha_b \wedge dr \wedge \alpha_c = \frac{d\chi}{dr}(r)(h_1(r)dz + h_2(r)d\theta) \wedge dr \wedge g_T^*(\hat{\beta} + R\eta)$ . Since  $g_T^*\eta = \nu_1(\theta, z)d\theta + \nu_2(\theta, z)dz$  with  $\nu_1(\theta, z) > 0$  and  $\nu_2(\theta, z) \geq 0$  by the condition (i), we have

$$(h_1(r)dz + h_2(r)d\theta) \wedge dr \wedge g_T^*\eta = (h_1(r)\nu_1(\theta, z) - h_2(r)\nu_2(\theta, z))dz \wedge dr \wedge d\theta.$$

We choose  $s > 0$  to be sufficiently small, which implies that  $h_2(r)$  is sufficiently small and hence  $(h_1(r)\nu_1(\theta, z) - h_2(r)\nu_2(\theta, z))dz \wedge dr \wedge d\theta > 0$ . Choosing  $R$  to be sufficiently large, we may conclude that the second term is non-negative.

Now we observe the third term. Substituting  $\alpha_c = g_T^*(\hat{\beta} + R\eta)$ , we have

$$\alpha_b \wedge d\alpha_c + \alpha_c \wedge d\alpha_b = \alpha_b \wedge g_T^*(d\hat{\beta}) + g_T^*(\hat{\beta} + R\eta) \wedge d\alpha_b,$$

where we used  $d\eta = 0$  on  $N_D \setminus (\hat{W} \cup \check{W})$  shown in Lemma 5.6 (1) and (2). Note that  $N_T \cap (\hat{W} \cup \check{W}) = \emptyset$  due to the choice of the coordinates  $(u, v, w)$  in the first paragraph of this proof. Since  $R_{\alpha_b}$  is positively transverse to  $\ker \eta$  due to the condition (ii), we have  $g_T^*\eta \wedge d\alpha_b > 0$ . Hence the third term is positive for a sufficiently large  $R$ . Thus  $\alpha_T$  is a contact form on  $N_T$ . This means that we can glue the contact forms  $\alpha'$  on  $M \setminus \text{Int Nbd}(L; M)$  and  $\alpha_b$  on  $\text{Nbd}(L; M)$  along  $N_T = g_T(N'_T)$  via the gluing map  $g_T$ . We denote the obtained contact form on  $M$  by  $\alpha''$ .

We can extend  $\hat{P}_6$  in  $M \setminus \text{Int Nbd}(L; M)$  into  $\text{Nbd}(L; M)$  such that the vector field  $R_{\alpha''}$  is positively transverse to  $\hat{P}_6$  in  $\text{Nbd}(L; M)$ . Thus the Reeb flow of  $\alpha''$  is carried by  $\hat{P}_6$ . We can also extend the pages of the open book in  $M \setminus \text{Int Nbd}(L; M)$  into  $\text{Nbd}(L; M)$  with the binding  $L = \{0\} \times S^1 \subset D_s \times S^1$  such that  $R_{\alpha''}$  is transverse to the interior of the pages and tangent to  $L$ . Thus  $R_{\alpha''}$  is a monodromy vector field of the open book. This completes the proof.  $\square$

*Proof of Theorem 1.2.* Let  $\xi$  be the given contact structure on  $M$ . By Theorem 2.1, there exist an open book decomposition of  $M$  and a contact form  $\alpha$  on  $M$  such that the Reeb vector field  $R_\alpha$  is a monodromy vector field of the open book. We may assume that the genus of the page of this open book is at least 2 and the binding is connected by using plumbings of positive Hopf bands. Note that this modification of the open book does not change the contact structure [48]. Let  $P$  and  $\alpha''$  be the positive flow-spine of  $M$  and the contact form on  $M$  obtained in the proof of Proposition 8.2, where the Reeb flow of  $\alpha''$  is carried by  $P$  and gives a monodromy vector field of the open book. Since  $\ker \alpha$  and  $\ker \alpha''$  are supported by the same open book, there exists a one-parameter family of contact forms from  $\ker \alpha$  to  $\ker \alpha''$  [19] and hence, by Gray's stability [20], there exists an isotopy from  $\ker \alpha$  to  $\ker \alpha''$ . In particular, there exists a contactomorphism  $\psi$  from  $(M, \ker \alpha)$  to  $(M, \ker \alpha'')$ . Thus, we have proved that, for the given contact structure  $\ker \alpha$ ,  $\psi^*\alpha''$  is a contact form such that  $\ker \alpha = \ker \psi^*\alpha''$  and the flow generated by the Reeb vector field  $R_{\psi^*\alpha''}$  is carried by the positive flow-spine  $\psi^{-1}(\hat{P}_6)$ . That is,  $\ker \alpha$  is supported by  $\psi^{-1}(\hat{P}_6)$ . This completes the proof.  $\square$

The next is a corollary of Theorem 1.2.

**Corollary 8.3.** *Any flow-spine can be deformed to a positive flow-spine by applying first and second regular moves successively.*

*Proof.* For any homotopy class of non-singular flows, there exists a contact structure whose Reeb flow belongs to the same homotopy class [7]. By Theorem 1.2, any contact structure is supported by a positive flow-spine. Therefore, we can find a sequence of regular moves that relates a given flow-spine with the positive one by Theorem 3.3.  $\square$

## 9. DETERMINE CONTACT STRUCTURES OF SOME POSITIVE FLOW-SPINES

In this section, we determine the supported contact structures for several positive flow-spines using Seifert fibrations, coil surgeries, branched covers and regular moves.

**9.1. Abalone and Seifert fibration.** The following lemma will be used to determine the contact structure supported by the positive abalone.

**Lemma 9.1.** *The flow tangent to the fibers of the Seifert fibration in  $S^3$  whose regular fiber is a  $(2,3)$ -torus knot is carried by the positive abalone.*

*Proof.* Consider a DS-diagram of the positive abalone described on the boundary of the unit 3-ball  $B^3 = \{(x, y, z) \in \mathbb{R}^3 \mid x^2 + y^2 + z^2 \leq 1\}$ , see the left in Figure 43. Let  $\Pi : B^3 \rightarrow D^2$  be the projection to the unit disk  $D^2$  given by  $(x, y, z) \mapsto (x, y)$ . Note that  $\Pi^{-1}(\partial D^2)$  is the  $E$ -cycle. We choose the positions of the graphs on the upper and lower hemispheres so that the images of these graphs on  $D^2$  by  $\Pi$  are as shown on the right, where  $R_2^+$  and  $R_2^-$  are identified by the projection. The preimage  $\Pi^{-1}(a)$  of a point  $a \in \text{Int } D^2$  is a vertical interval in  $B^3$  while that of a point on  $\partial D$  is a point on the  $E$ -cycle. Set  $S_1 = \Pi(R_2^+) = \Pi(R_2^-)$ . Let  $S_2$  be the connected component of the complement of the union of the images of the graphs by  $\Pi$  whose closure is adjacent to  $S_1$  along an edge, and  $S_3$  be the other connected component, see the right in Figure 43.

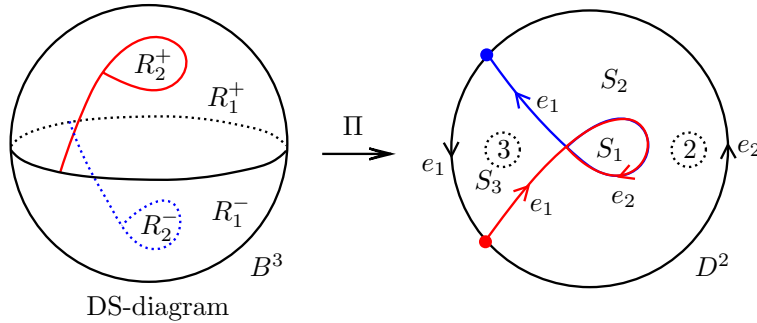


FIGURE 43. The projection  $\Pi : B^3 \rightarrow D^2$ .

We are going to give gluing maps of the regions  $R_1^+$  and  $R_1^-$  and also the regions  $R_2^+$  and  $R_2^-$  on the upper and lower hemispheres so that each vertical interval  $\Pi^{-1}(a)$ ,  $a \in \text{Int } D^2$ , becomes an arc on a fiber of the Seifert fibration in the assertion. We first glue the two regions  $R_2^+$  and  $R_2^-$  so that each vertical interval connecting these two regions becomes a simple closed curve. Let  $\varphi$  denote the quotient map of this gluing. Let  $a$  be a point in  $S_1$ , see Figure 44. The quotient  $\varphi(\Pi^{-1}(a))$  of the interval  $\Pi^{-1}(a)$  is a simple closed curve in  $S^3$  that intersects the region  $R_2$  only once transversely and does not have any other intersection with  $P$ . From the figure of the positive abalone in Figure 5, we see that such a simple closed curve is a  $(2,3)$ -torus knot. This observation works for any point in  $S_1$ . Hence we may regard each fiber of the map  $\varphi(\Pi^{-1}(S_1)) \rightarrow S_1$  as a fiber of the Seifert fibration in  $S^3$  whose regular fiber is a  $(2,3)$ -torus knot.

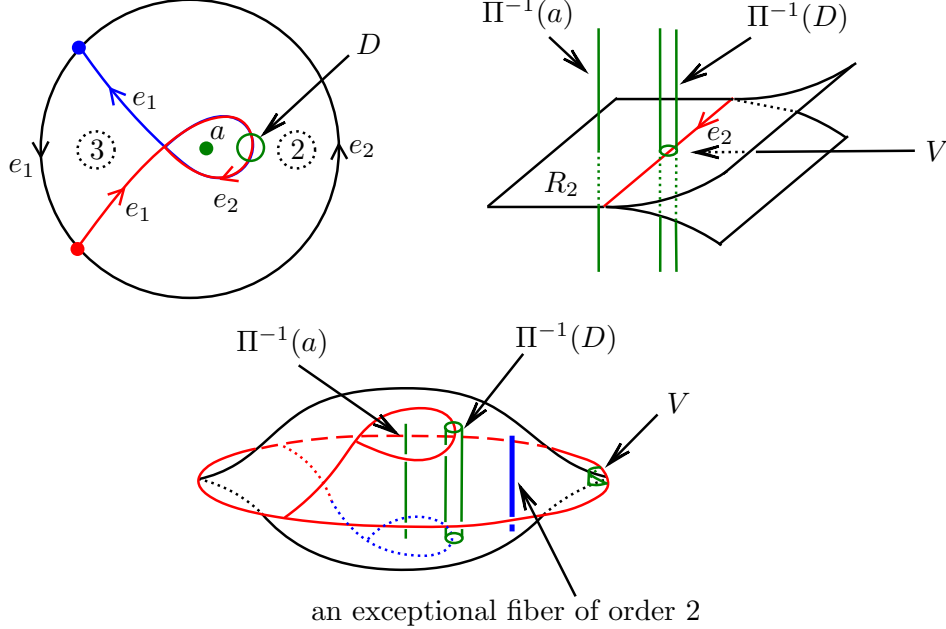


FIGURE 44. The Seifert fibration of the positive abalone.

Next we extend this gluing map to that of  $\text{Nbd}(\partial R_1^+; R_1^+)$  and  $\text{Nbd}(\partial R_1^-; R_1^-)$  as follows. Let  $D$  be a small disk intersecting  $\partial S_1$  as shown in Figure 44. We glue the top and bottom disks  $\Pi^{-1}(D) \cap \partial B^3$  of  $\Pi^{-1}(D)$  as shown on the top-right in the figure, where the union of the preimage  $\Pi^{-1}(D)$  with this gluing and the piece  $V$  depicted in the figure constitutes a solid torus. The Seifert fibration in the previous paragraph extends to this solid torus by choosing the gluing of  $\Pi^{-1}(D)$  and  $V$  suitably. Remark that each fiber of the Seifert fibration passing through  $V$  intersects the region  $R_1$  twice. We extend this gluing map to that of  $\text{Nbd}(\partial R_1^+; R_1^+)$  and  $\text{Nbd}(\partial R_1^-; R_1^-)$  in the same manner. As a result, the fiber corresponding to a point in  $S_1$  intersects  $P$  once, the fiber corresponding to a point in  $\text{Int Nbd}(\partial S_2; S_2)$  intersects it twice and the fiber corresponding to a point in  $\text{Int Nbd}(\partial S_3; S_3)$  intersects it three times. We can extend this fibration to the regions outside the two small open disks labeled with 2 and 3 in the figure. Until this time, every fiber is regular. Finally, for the two solid tori corresponding to these two disks we set the solid tori with exceptional fibers of index 2 and 3, and get the Seifert fibration whose regular fiber is a  $(2, 3)$ -torus knot and whose fibers are transverse to the positive abalone. Thus the assertion holds.  $\square$

Thus we have the following.

**Corollary 9.2.** *The contact structure supported by the positive abalone is the standard contact structure on  $S^3$ .*

*Proof.* The Reeb flow of the contact form  $(2(x_1 dy_1 - y_1 dx_1) + 3(x_2 dy_2 - y_2 dx_2))|_{S^3}$  is tangent to the fibers of the Seifert fibration in Lemma 9.1, where  $(x_1 + \sqrt{-1}y_1, x_2 +$

$\sqrt{-1}y_2$ ) are the standard coordinates of  $\mathbb{C}^2$  and  $S^3$  is the unit sphere in  $\mathbb{C}^2$ . The kernel of this form is contactomorphic to the standard contact structure on  $S^3$ . Thus the assertion follows.  $\square$

**9.2. Coil surgery.** Let  $P$  be a flow-spine in a closed, connected, oriented, smooth 3-manifold  $M$ . Choose a small ball  $B_p^3$  centered at a point  $p$  on an edge of  $S(P)$ . The intersection  $B_p^3 \cap P$  consists of three half-disks meeting along the edge  $B_p^3 \cap S(P)$ , and let  $D_1$  and  $D_2$  be the two of them that induce the same orientation on the edge. Suppose that there exists a simple closed curve  $\gamma'$  on  $P$  such that  $\gamma' \cap S(P) = \{p\}$  and  $\gamma' \cap D_j$  is an arc starting at  $p$  for each  $j = 1, 2$ . The preimage  $\gamma$ , on the DS-diagram, of  $\gamma'$  by the identification map  $j'$  constitutes an arc, which is called a *coil*. For example, the abalone has two coils  $\gamma_1$  and  $\gamma_2$  as shown on the left in Figure 45. The simple closed curve  $\gamma'_1 = j'(\gamma_1)$  is shown on the right.

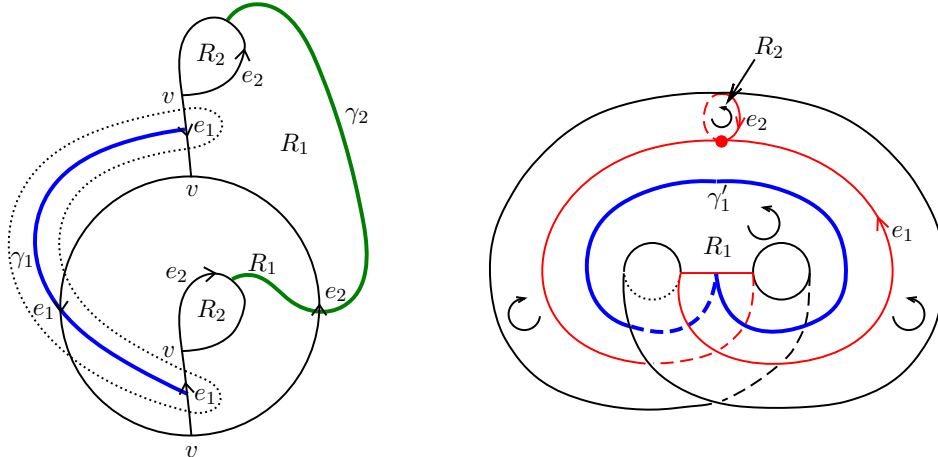


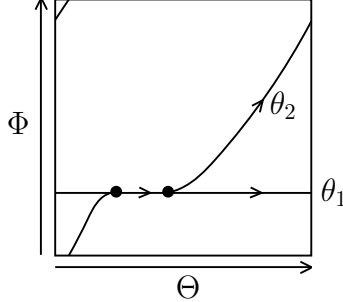
FIGURE 45. Coils on the abalone.

A closed neighborhood  $N_{\gamma'}$  of  $\gamma'$  in  $M$  is a solid torus and the intersection  $\partial N_{\gamma'} \cap P$  is a branched theta-curve on the torus  $\partial N_{\gamma'}$ . The branched theta-curve contains two simple closed smooth curves  $\theta_1$  and  $\theta_2$ , equipped with the orientations induced from that of  $N_{\gamma'} \cap P$ . The labels  $\theta_1$  and  $\theta_2$  are chosen as shown in Figure 46. Let  $\langle \Theta, \Phi \rangle$  be the basis of  $H_1(\partial N_{\gamma'}; \mathbb{Z})$  such that

- the orientation on  $\partial N_{\gamma'}$  induced from that of  $N_{\gamma'}$  coincides with that of  $(\Theta, \Phi)$ ;
- $[\theta_1] = \Theta$  and  $[\theta_2] = \Theta + \Phi$ .

Let  $j$  be the continuous map from  $B^3$  to the 3-manifold of the flow-spine introduced in Section 3.2, where  $B^3$  is the 3-ball bounded by the 2-sphere of the DS-diagram. Note that  $j|_{S^2} = j'$ . The solid torus  $N_{\gamma'}$  is obtained as the image of a 3-ball  $\text{Nbd}(\gamma; B^3)$  by the map  $j$ . Set  $D_\gamma = \text{Nbd}(\gamma; B^3) \cap \partial B^3$ , which is a disk on  $\partial B^3$  containing  $\gamma$ . For example, the region bounded by the dotted curve in Figure 45 is  $D_{\gamma_1}$ . We denote  $j'(D_\gamma) = P \cap N_{\gamma'}$  by  $P_{\gamma'}$ .

Consider the four kinds of annuli with graph shown in Figure 47, that can be found in [46]. They are thought as parts of DS-diagrams. In the figure, dashed lines are parts

FIGURE 46. The branched theta-curve on  $\partial N_{\gamma'}$ 

of the E-cycle. A dotted edge is an arc on a region of the spine, not a part of the singular set of the spine. Let  $A$  be one of these annuli given as a part of a DS-diagram and choose a 3-ball  $B_A$  in  $B^3$  such that  $B_A \cap \partial B^3 = A$ . The boundary of  $B_A$  is the union of  $A$  and two disks  $\Delta_0$  and  $\Delta_1$ . We suppose that  $\partial\Delta_0$  is the boundary given by  $a_3 a_2 a_1 a_3^{-1} a_2^{-1} a_1^{-1}$  and  $\partial\Delta_1$  is the one given by  $a'_3 a'_2 a'_1 (a'_3)^{-1} (a'_2)^{-1} (a'_1)^{-1}$ . The image  $j(B_A)$  is  $T^2 \times [0, 1]$ , where  $T^2 \times \{j\} = j(\Delta_j)$  for  $j = 0, 1$ . The image  $j'(A)$  constitutes a branched polyhedron embedded in  $T^2 \times [0, 1]$ , which we denote by  $P_A$ . The branched polyhedron  $P_A$  has one vertex, which is of  $\ell$ -type if  $A = \mathcal{H}_{\bar{L}}$  or  $\mathcal{H}_R$  and of  $r$ -type if  $A = \mathcal{H}_L$  or  $\mathcal{H}_{\bar{R}}$ .

Let  $\mathcal{H} = \mathcal{H}_1 \mathcal{H}_2 \cdots \mathcal{H}_k$  be a finite sequence of  $\mathcal{H}_L, \mathcal{H}_{\bar{L}}, \mathcal{H}_R$  and  $\mathcal{H}_{\bar{R}}$ . For each  $j = 1, \dots, k-1$ , we identify  $a'_3 a'_2 a'_1 (a'_3)^{-1} (a'_2)^{-1} (a'_1)^{-1}$  of  $\mathcal{H}_j$  with  $a_3 a_2 a_1 a_3^{-1} a_2^{-1} a_1^{-1}$  of  $\mathcal{H}_{j+1}$ . The 3-manifold obtained from  $B_{\mathcal{H}_1} \cup B_{\mathcal{H}_2} \cup \cdots \cup B_{\mathcal{H}_k}$  by the identification map  $j'$  is the union of  $T^2 \times [0, 1]$ 's, which is  $T^2 \times [0, k]$ , containing the branched polyhedron  $P_{\mathcal{H}} = P_{\mathcal{H}_1} \cup P_{\mathcal{H}_2} \cup \cdots \cup P_{\mathcal{H}_k}$ . Then we fill  $a'_3 a'_2 a'_1 (a'_3)^{-1} (a'_2)^{-1} (a'_1)^{-1}$  of  $\mathcal{H}_k$  by the hexagon  $\mathcal{H}_0$  shown on the left in Figure 48 and obtain a disk  $D_{\mathcal{H}}$ . Let  $B_{\mathcal{H}_0}$  be the 3-ball in  $B^3$  such that  $B_{\mathcal{H}_0} \cap \partial B^3 = \mathcal{H}_0$  and set  $N_0 = j(B_{\mathcal{H}_0})$ , which is a solid torus, and  $P_0 = j'(\mathcal{H}_0)$ , which is a branched polyhedron in  $N_0$ . The replacement of  $D_{\gamma}$  by  $D_{\mathcal{H}}$  yields a Dehn surgery of  $M$  along  $\gamma'$  that removes  $(\text{Int } N_{\gamma'}, \text{Int } P_{\gamma'})$  from  $M$  and glues  $((T^2 \times [0, k]) \cup N_0, P_{\mathcal{H}} \cup P_0)$ . This operation is called a *coil surgery* and, in this paper, we denote it by  $(\gamma, \mathcal{H})$ .

*Convention.* The solid torus  $N_0$  is obtained from the cylinder shown on the right in Figure 48 by identifying the top and bottom disks after  $\pi/2$ -rotation. Orient the core of  $N_0$  so that it intersects the branched polyhedron  $P_0$  in  $N_0$  positively. Then we orient the meridian of  $(T^2 \times [0, k]) \cup N_0$  so that its meridian disk is positively transverse to the oriented core of  $N_0$ .

**Lemma 9.3.** *Suppose that  $\mathcal{H} = \mathcal{H}_R^k$ , where  $k \geq 0$ . Then the meridian of  $(T^2 \times [0, k]) \cup N_0$  is  $(k+2)\Theta + (k+1)\Phi$ .*

*Proof.* The solid torus  $N_{\gamma'}$  is obtained from the cylinder shown on the left in Figure 49 by identifying the top and bottom disks after  $\pi/2$ -rotation. Therefore, the meridian is a simple closed curve on  $\partial N_{\gamma'}$  that intersects the polyhedron only along the boundary of the top half-disk, which can be seen as shown on the right. That is  $2\Theta + \Phi$ .

Next we attach  $T^2 \times [0, 1]$  corresponding to  $\mathcal{H}_R$  to  $M \setminus \text{Int } N_{\gamma'}$ , where  $T^2 \times \{0\}$  is the attaching face. The figure in the middle in Figure 50 is a neighborhood of the  $\ell$ -type

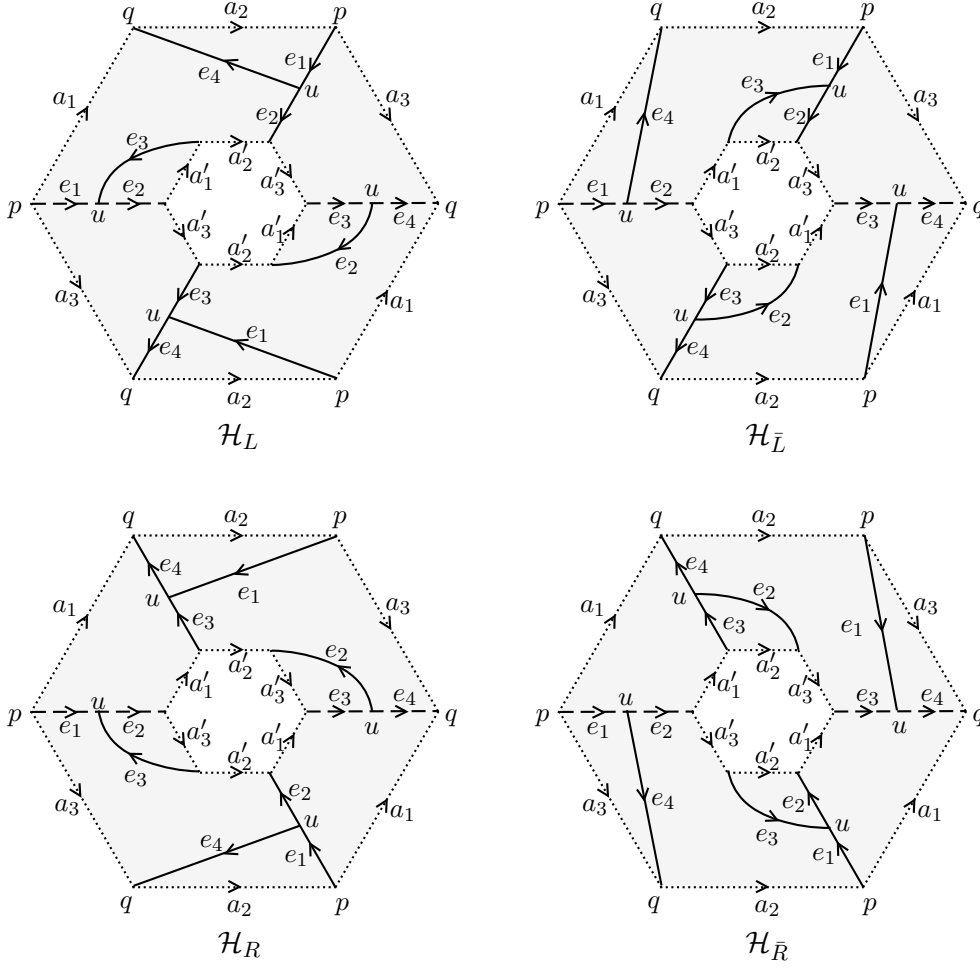


FIGURE 47. The annuli  $\mathcal{H}_L$ ,  $\mathcal{H}_{\bar{L}}$ ,  $\mathcal{H}_R$  and  $\mathcal{H}_{\bar{R}}$ .

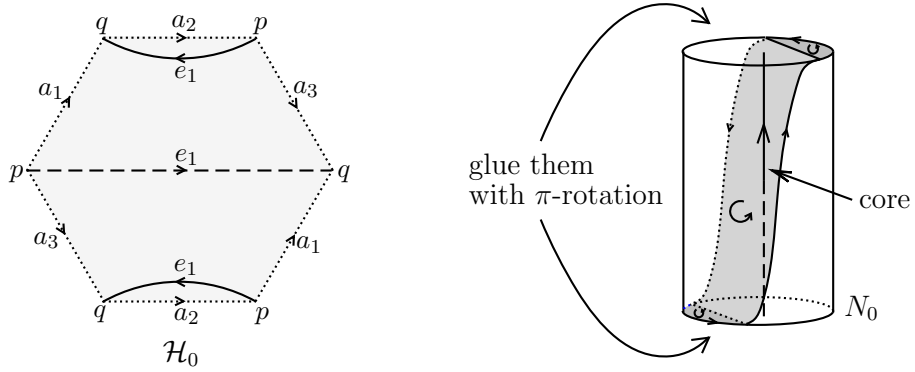


FIGURE 48. A DS-diagram of the solid torus  $N_0$ .

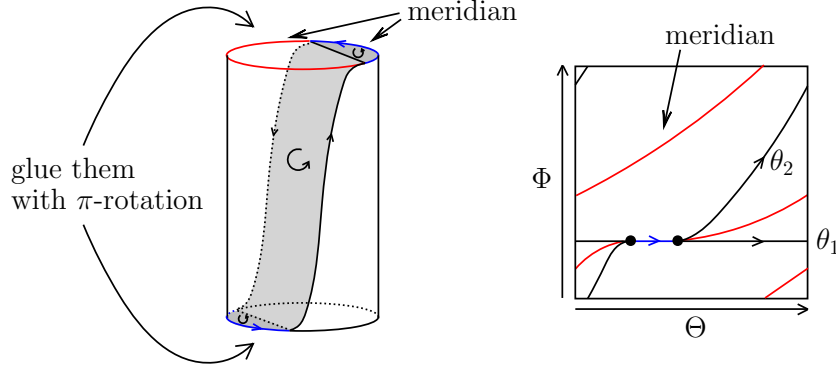


FIGURE 49. The union of blue and red arcs are the meridian of  $N_{\gamma'}$ .

vertex in  $T^2 \times [0, 1]$ , where  $T^2 \times \{0\}$  is the back side and  $T^2 \times \{1\}$  is the front side. We may see how the branched theta-curve changes when we pass the vertex, and conclude that the branched theta-curve on  $T^2 \times \{1\}$  is given as shown on the right in Figure 50. Thus the meridian of the solid torus obtained from  $T^2 \times [0, 1]$  by attaching  $N_0$  along  $T^2 \times \{1\}$  is  $3\Theta + 2\Phi$ . Applying the same observation inductively, we obtain the assertion.  $\square$

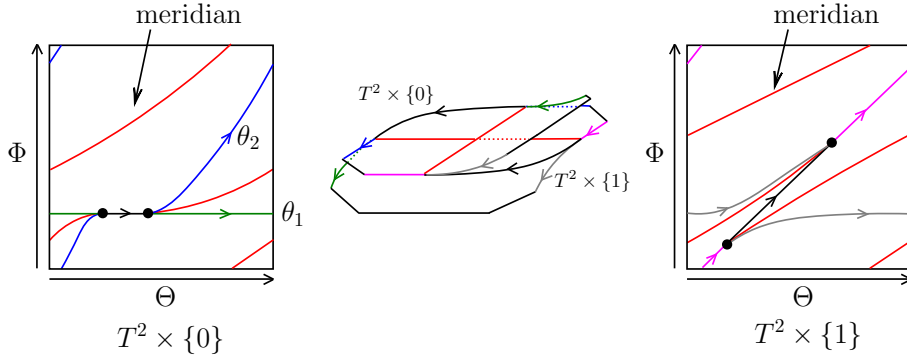


FIGURE 50. The branched theta-curves and meridians on  $T^2 \times \{0\}$  and  $T^2 \times \{1\}$  for  $\mathcal{H}_R$ .

**9.3. Seifert-coil surgery.** We suppose that  $\text{Nbd}(\partial N_{\gamma'}; M \setminus \text{Int } N_{\gamma'})$  consists of regular fibers of a Seifert fibration that is positively transverse to  $P$  and the regular fiber is  $p\Theta + q\Phi$ . After a coil surgery, the Seifert fibration in  $\text{Nbd}(\partial N_{\gamma'}; M \setminus \text{Int } N_{\gamma'})$  canonically extends to  $T^2 \times [0, k] \cup N_0$  with a single exceptional fiber along the core of the attached solid torus. We call such a coil surgery a *Seifert-coil surgery*.

**Lemma 9.4.** *Suppose  $\mathcal{H} = \mathcal{H}_R^k$ ,  $q > p$  and  $q > 0$ . Then we may isotope  $P_{\mathcal{H}} \cup P_0$  so that it is positively transverse to the fibers of the Seifert fibration in  $T^2 \times [0, k] \cup N_0$ .*

*Proof.* The two smooth curves in the branched theta-curve on  $T^2 \times \{0\}$  are  $(\theta_1, \theta_2) = (\Theta, \Theta + \Phi)$ . Those on  $T^2 \times \{1\}$  are  $(2\Theta + \Phi, \Theta + \Phi)$  and those on  $T^2 \times \{2\}$  are  $(3\Theta + 2\Phi, \Theta + \Phi)$ . Hence, applying the same observation inductively, we may conclude that those on  $T^2 \times \{k\}$  are  $((k+1)\Theta + k\Phi, \Theta + \Phi)$ . Since

$$\begin{vmatrix} k+1 & p \\ k & q \end{vmatrix} = (k+1)q - pk = k(q-p) + q > 0 \quad \text{and} \quad \begin{vmatrix} 1 & p \\ 1 & q \end{vmatrix} = q - p > 0,$$

the fibers of the Seifert fibration are positively transverse to  $P$  in  $T^2 \times [0, k]$ . In  $N_0$ ,  $P$  lies as shown on the left in Figure 49 and we may see that they are also positively transverse to  $P$  in  $N_0$ .  $\square$

**Lemma 9.5.** *Suppose  $\mathcal{H} = \mathcal{H}_R^k$ ,  $q > p$  and  $q > 0$ . Let  $\alpha$  be a contact form on  $\text{Nbd}(\partial N_{\gamma'}; M \setminus \text{Int } N_{\gamma'})$  given in the form  $\alpha = h_2(r)d\theta - h_1(r)d\phi$  whose Reeb vector field  $R_\alpha$  is tangent to the fibers  $p\Theta + q\Phi$  of the Seifert fibration, where  $((r, \theta), \phi)$  are the coordinates of  $\text{Nbd}(\partial N_{\gamma'}; M \setminus \text{Int } N_{\gamma'}) = [1, 2] \times S^1 \times S^1$  such that  $[\theta] = \Theta$  and  $[\phi] = \Phi$  in  $H_1(\partial N_{\gamma'}; \mathbb{Z})$ . Then there exists a contact form  $\alpha'$  on  $(T^2 \times [0, k]) \cup N_0$  such that*

- (1)  $\alpha'$  on  $(T^2 \times [0, k]) \cup N_0$  is glued to  $\alpha$  on  $\text{Nbd}(\partial N_{\gamma'}; M \setminus \text{Int } N_{\gamma'})$  smoothly along  $\partial N_{\gamma'} = T^2 \times \{0\}$ ,
- (2) the Reeb vector field  $R_{\alpha'}$  of  $\alpha'$  is transverse to the flow-spine  $P_{\mathcal{H}} \cup P_0$  obtained in Lemma 9.4, and
- (3) the contact structure  $\ker \alpha'$  is positively transverse to the fibers of the Seifert fibration.

Before proving the lemma, we recall how to read the contact structure of  $\alpha = h_2(r)d\theta - h_1(r)d\phi$  and its Reeb vector field  $R_\alpha$  from a curve on the  $(h_1, h_2)$ -plane, that is used in [28]. Let  $\Gamma : [0, r_0] \rightarrow \mathbb{R}^2$  be a curve on the  $(h_1, h_2)$ -plane  $\mathbb{R}^2$  that maps  $r$  to  $(h_1(r), h_2(r))$  and  $\alpha$  be the 1-form given by  $\alpha = h_2(r)d\theta - h_1(r)d\phi$ . This  $\alpha$  is a contact form if and only if  $\frac{dh_1}{dr}h_2 - h_1\frac{dh_2}{dr} > 0$ , and its Reeb vector field  $R_\alpha$  is given as

$$R_\alpha = \frac{1}{\frac{dh_1}{dr}h_2 - h_1\frac{dh_2}{dr}} \left( \frac{dh_1}{dr} \frac{\partial}{\partial \theta} + \frac{dh_2}{dr} \frac{\partial}{\partial \phi} \right).$$

Then the curve  $\Gamma$  satisfies that

- $(0, 0) \notin \Gamma([0, r_0])$  and  $\Gamma$  moves in the clockwise orientation,
- the line connecting  $(0, 0)$  and  $(h_1, h_2)$  represents the slope of  $\ker \alpha$  and the vector  $(h_2, -h_1)$  represents the positive side of  $\alpha$ , and
- the speed vector  $\left( \frac{dh_1}{dr}, \frac{dh_2}{dr} \right)$  is parallel to  $R_\alpha$  and points in the same direction,

where we regard the axes  $h_1$  and  $h_2$  as  $\theta$  and  $\phi$  on  $\partial N_{\gamma'}$ , respectively. See Figure 51.

*Proof of Lemma 9.5.* The meridian of  $N_{\gamma'}$  is  $2\Theta + \Phi$  and that of  $(T^2 \times [0, k]) \cup N_0$  is  $(k+2)\Theta + (k+1)\Phi$  by Lemma 9.3. The smooth curves in the branched theta-curves are  $\Theta + \Phi$  and  $(m+1)\Theta + m\Phi$  for  $m = 0, 1, \dots, k$  as confirmed in the proof of Lemma 9.4. The positions of these meridians and the smooth curves in the theta-curves are shown in Figure 52. Since the fibers of Seifert fibration on  $\text{Nbd}(\partial N_{\gamma'}; M \setminus \text{Int } N_{\gamma'})$  are  $p\Theta + q\Phi$ , the Reeb vector field  $R_\alpha$  near  $\partial N_{\gamma'}$  is represented by the vector  ${}^t(p, q)$ , that is, the contact form  $\alpha$  near  $\partial N_{\gamma'}$  is represented by a short segment from  $r = 1$  to  $r = 2$  lying in the

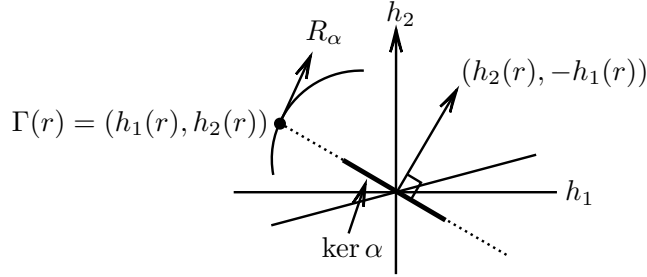


FIGURE 51. How to read  $\ker \alpha$  and  $R_\alpha$  from the curve  $\Gamma(r) = (h_1(r), h_2(r))$ .

direction  ${}^t(p, q)$  as shown in the figure. Note that the vector  ${}^t(p, q)$  is transverse to the two meridians and the smooth curves in the theta-curves by the assumption.

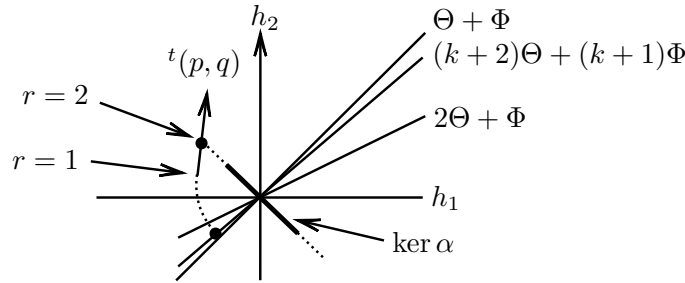


FIGURE 52. The contact form  $\alpha'$  on  $(T^2 \times [0, k]) \cup N_0$ .

Now we extend the coordinates of  $\text{Nbd}(\partial N_{\gamma'}; M \setminus \text{Int } N_{\gamma'})$  to those of  $(T^2 \times [0, k]) \cup N_0$  by extending the coordinate  $r \in [1, 2]$  to  $r \in [0, 2]$ . Then extend the short segment to  $r \in [0, 1]$  in the counter-clockwise orientation so that it ends at a point on the line of  $(k+2)\Theta + (k+1)\Phi$  suitably, see the dotted curve in Figure 52. The curve should end on the line of  $(k+2)\Theta + (k+1)\Phi$  since the line corresponds to the meridian after the coil surgery. This curve gives a contact form on  $(T^2 \times [0, k]) \cup N_0$  that satisfies the required conditions.  $\square$

**9.4. Two sequences of lens spaces.** As we had seen in the proof of Lemma 9.1, the Seifert fibration with index 2 and 3 can be read off from the DS-diagram of the abalone. For each of the coils  $\gamma_1$  and  $\gamma_2$ , the union of fibers of the Seifert fibration obtained as the preimage of the region  $\Delta_{\gamma_i}$  in Figure 53 constitutes a solid torus and it is isotopic to the solid torus of the coil. Therefore, we may apply Seifert-coil surgeries for these coils.

**Lemma 9.6.** (1) *The longitude of the knot  $\gamma'_1$  in  $S^3$  is  $-\Theta$  and the fibers of the Seifert fibration are  $\Theta + 2\Phi$  on  $\partial N_{\gamma'_1}$ .*

(2) *The longitude of the knot  $\gamma'_2$  in  $S^3$  is  $-3\Theta - \Phi$  and the fibers of the Seifert fibration are  $\Phi$  on  $\partial N_{\gamma'_2}$ .*

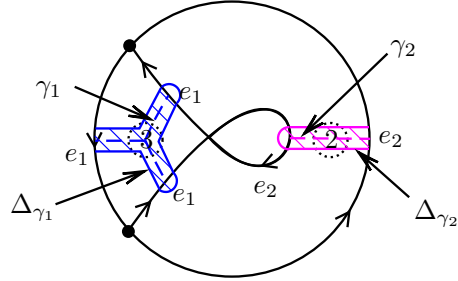


FIGURE 53. The disks  $\Delta_{\gamma_1}$  and  $\Delta_{\gamma_2}$  for Seifert-coil surgeries.

*Proof.* The diagram on the left in Figure 54 represents the complement  $S^3 \setminus \text{Int } N_{\gamma'_1}$ , which is obtained from the 3-ball bounded by the 2-sphere with the diagram shown in the figure by identifying the regions  $R_i^+$  and  $R_i^-$  for each  $i = 1, 2, 3$ . The homology cycles  $[2x_3 + a_2 + a_1]$  and  $[x_3]$  are 0 since these are the boundaries of the disks  $R_1$  and  $R_2$  in the complement, respectively. Hence  $[a_1 + a_2] = 0$ . Since  $a_1 \cup a_2$  is a simple closed curve on  $\partial N_{\gamma'_1}$  that is null-homologous in the complement, it is the preferred longitude. As shown on the right in the figure, we have  $\Theta = -a_1 - a_2$  and hence  $[\Theta] = 0$ . Since the longitude is positively transverse to the meridian, the longitude is given as  $-\Theta$ . Each fiber of the Seifert fibration intersects the meridian three times in the positive direction and the longitude two times in the negative direction. Hence it is  $\Theta + 2\Phi$ .

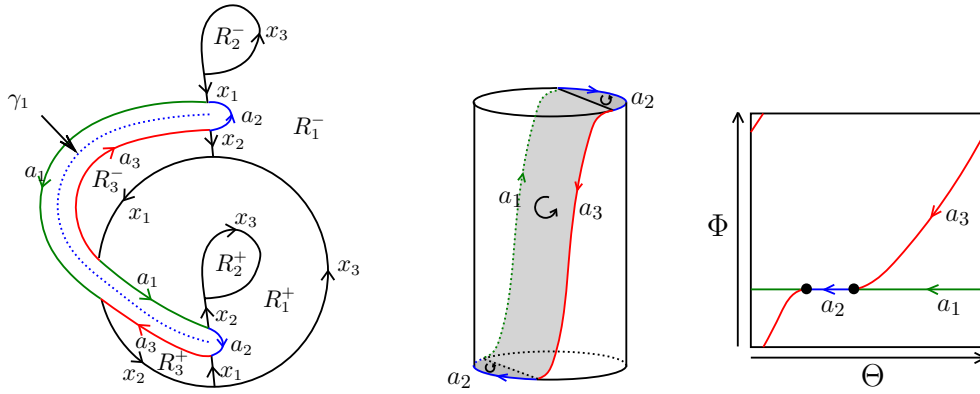
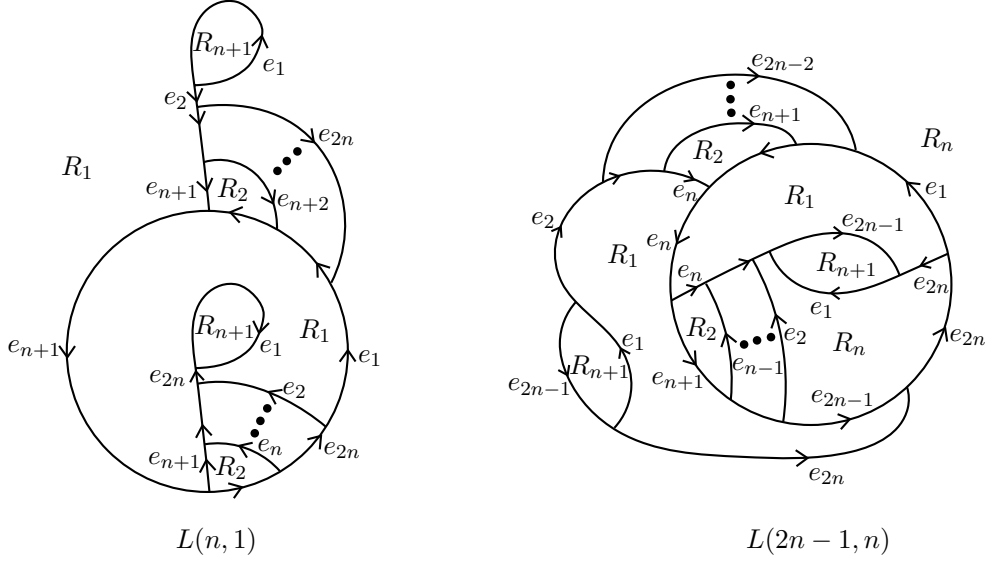


FIGURE 54.  $S^3 \setminus \text{Int } N_{\gamma'_1}$ ,  $N_{\gamma'_1}$  and  $\partial N_{\gamma'_1}$ .

The second assertion can be proved analogously. □

**Theorem 9.7.** *The positive flow-spines given by the DS-diagrams shown in Figure 55 support tight contact structures on  $L(n, 1)$  for  $n \geq 1$  and  $L(2n - 1, n)$  for  $n \geq 2$ .*

*Proof.* The DS-diagram on the left in Figure 55 is obtained from the DS-diagram of the positive abalone in Figure 45 by the Seifert-coil surgery  $(\gamma_1, \mathcal{H}_R^{n-1})$ . The DS-diagram on

FIGURE 55. DS-diagrams of  $L(n, 1)$  and  $L(2n - 1, n)$ .

the right is obtained by the Seifert-coil surgery  $(\gamma_2, \mathcal{H}_R^{n-1})$ . The 3-manifolds represented by the DS-diagrams on the left and right in Figure 55 are homeomorphic to  $L(n, 1)$  and  $L(2n - 1, n)$ , respectively, from Lemmas 9.3 and 9.6. The fibers of the Seifert fibration on  $\partial N_{\gamma'_1}$  are given as  $\Theta + 2\Phi$  and those on  $\partial N_{\gamma'_2}$  are given as  $\Phi$ . Hence, the assumption in Lemma 9.5 is satisfied in both cases. By Lemma 9.4, the positive flow-spines obtained by these surgeries are positively transverse to the fibers of the Seifert fibrations of  $L(n, 1)$  and  $L(2n - 1, n)$ . Let  $\alpha$  be a contact form on  $S^3 \setminus \text{Int}(N_{\gamma'_1} \cup N_{\gamma'_2}) = ([0, 1] \times S^1) \times S^1$  whose Reeb vector field  $R_\alpha$  is tangent to the fibers of the Seifert fibration, which can be given in the form  $h_2(r)d\theta - h_1(r)d\phi$  near the boundary. Note that we can find such a 1-form by the argument in [28]. By Lemma 9.5, we can extend this 1-form to the whole  $S^3$  so that its contact structure is positively transverse to the fibers of the Seifert fibration and its Reeb vector field is transverse to the positive flow-spine  $P_{\mathcal{H}_R^{n-1}} \cup P_0$ . Thus the contact structure is supported by the corresponding positive flow-spine in Figure 55, and it is tight by [41, 36]. This completes the proof.  $\square$

**9.5. Contact structures of positive flow-spines with up to 3 vertices.** There are only one positive flow-spine with one vertex, three positive flow-spines with two vertices, and nine positive flow-spines with three vertices. The DS-diagrams of these flow-spines are listed in the appendix. In this subsection, we show that the contact structures supported by them are all tight.

By the discussion in the previous subsections, we know the following.

- (i) The positive abalone  $1_1$  supports the standard contact structure on  $S^3$  (Corollary 9.2).
- (ii)  $2_2$ ,  $3_5$  and  $3_6$  support tight contact structures on  $\mathbb{RP}^3$ ,  $L(3, 2)$  and  $L(5, 2)$  by Theorem 9.7, respectively.

Furthermore, from the DS-diagrams in the list, we see that

- $2_1$  is obtained from  $1_1$  by taking the double branched cover along the index 2 exceptional fiber of the Seifert fibration in Lemma 9.1.
- $2_3$  is obtained from  $1_1$  by taking the double branched cover along a regular fiber of the Seifert fibration in Lemma 9.1 intersecting the region  $R_2$ .
- $3_1$  is obtained from  $1_1$  by taking the 3-fold branched cover along the index 2 exceptional fiber of the Seifert fibration in Lemma 9.1.
- $3_8$  is obtained from  $1_1$  by taking the 3-fold branched cover along a regular fiber of the Seifert fibration in Lemma 9.1 intersecting the region  $R_2$ .

The Seifert fibration of  $S^3$  in Lemma 9.1 induces Seifert fibrations for these branched covering spaces canonically. The standard contact structure, mentioned in Corollary 9.2, also induces contact structures on these branched covering spaces whose Reeb flows are carried by the flow-spines obtained by the branched covers. These contact structures are tight by [41, 36].

In summary, we have the following conclusion.

- (iii)  $2_1$  and  $3_1$  support the standard contact structure on  $S^3$ .
- (iv)  $2_3$  supports the unique tight contact structure on  $L(3, 2)$ .
- (v)  $3_8$  is a flow-spine of the quaternion space and it supports the contact structure of the link of the singularity  $\{(x, y, z) \in \mathbb{C}^3 \mid x^2 + y^3 + z^3 = 0\} \cap S_\varepsilon^3$  given by the complex tangency, where  $S_\varepsilon^3$  is the 5-sphere centered at the origin and with a sufficiently small radius  $\varepsilon > 0$ . This contact structure is fillable and hence tight.

Note that the uniqueness of the tight contact structure on  $L(3, 2)$  in (iv) follows from Table 1 in Section 2.

**Remark 9.8.** *By considering the  $n$ -th cyclic branched cover along a regular fiber of the Seifert fibration in Lemma 9.1 intersecting the region  $R_2$ , we may obtain a positive flow-spine that supports the contact structure of the link of the singularity  $\{(x, y, z) \in \mathbb{C}^3 \mid x^2 + y^3 + z^n = 0\} \cap S_\varepsilon^3$  given by the complex tangency, see [43]. These contact structures are fillable and hence tight. In particular, when  $n = 5$ , the DS-diagram constitutes a regular dodecahedron and the corresponding 3-manifold is the Poincaré homology 3-sphere.*

The flow-spine  $3_7$  is obtained from  $2_3$  by applying a first regular move in Figure 56. Since this move can be done with keeping the transversality of the flow-spine and the Reeb vector field of  $2_3$ , the contact structures supported by these flow-spines are the same. Thus

- (vi)  $3_7$  supports the unique tight contact structure on  $L(3, 2)$ .

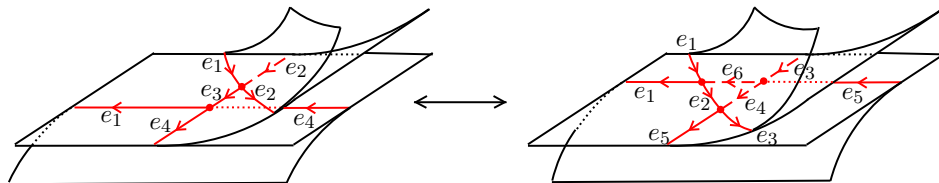


FIGURE 56. A first regular move between  $2_3$  and  $3_7$ .

The remaining positive flow-spines are  $3_2$ ,  $3_3$ ,  $3_4$  and  $3_9$ . The 3-manifolds of  $3_2$ ,  $3_3$ ,  $3_4$  and  $3_9$  are  $\mathbb{RP}^3$ ,  $S^3$ ,  $\mathbb{RP}^3$  and  $L(4, 3)$ , respectively. These can be verified easily since, as we will see in the proofs of the following lemmas, the manifolds corresponding to these flow-spines are obtained from  $S^3$  by Dehn surgery along either a trivial knot or a Hopf link.

**Lemma 9.9.**  $3_3$  supports the standard contact structure on  $S^3$ .

*Proof.*  $3_3$  is obtained from  $1_1$  by the Seifert-coil surgeries  $(\gamma_1, \mathcal{H}_{\bar{L}})$  and  $(\gamma_2, \mathcal{H}_{\bar{L}})$ . Let  $\alpha$  be a contact form on  $S^3$  whose Reeb vector field  $R_\alpha$  is tangent to the fibers of the Seifert fibration in Lemma 9.1. We then apply the two Seifert-coil surgeries for sufficiently narrow neighborhoods  $N_{\gamma'_1}$  and  $N_{\gamma'_2}$  of  $\gamma'_1$  and  $\gamma'_2$ . We extend the 1-form  $\alpha$  on  $S^3 \setminus \text{Int}(N_{\gamma'_1} \cup N_{\gamma'_2})$  to the solid torus attached to  $\partial N_{\gamma'_1}$  as shown in Figure 57 and also extend  $\alpha$  to the solid torus attached to  $\partial N_{\gamma'_2}$  analogously. The longitude in the former case, shown in the figure, is  $-\Theta$  and that in the latter case is  $-3\Theta - \Phi$  by Lemma 9.6. So, in the latter case, the longitude before the surgery in Figure 57 should be replaced by  $-3\Theta - \Phi$ . The fibers of the Seifert fibration on  $\partial N_{\gamma_1}$  and  $\partial N_{\gamma_2}$  are also given in Lemma 9.6. Comparing these information in the figure, we may verify that the obtained contact structure is positively transverse to the fibers of the Seifert fibration and the Reeb vector field is positively transverse to  $3_3$ . This contact structure is tight by [41, 36]. This completes the proof.  $\square$

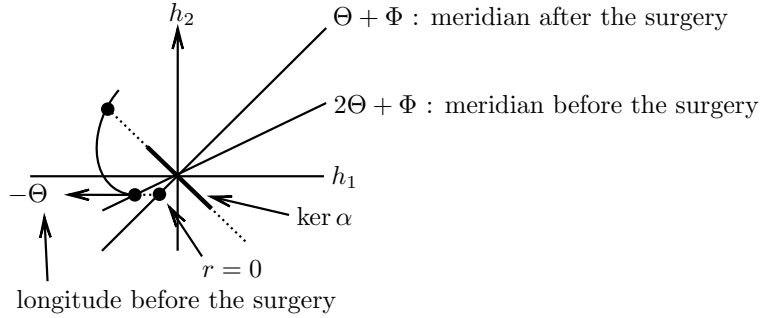


FIGURE 57. Make a contact form for  $3_3$ .

As written in Table 1,  $\mathbb{RP}^3$  admits a unique tight contact structure [9].

**Lemma 9.10.**  $3_4$  supports the tight contact structure on  $\mathbb{RP}^3$ .

*Proof.*  $3_4$  is obtained from  $1_1$  by the Seifert-coil surgeries  $(\gamma_1, \mathcal{H}_{\bar{L}})$  and  $(\gamma_2, \mathcal{H}_R)$ . The fibers of the Seifert fibration on  $N_{\gamma'_1}$  are given as  $\Theta + 2\Phi$ , which satisfies the condition in Lemma 9.5. Let  $\alpha$  be a contact form on  $S^3 \setminus \text{Int}(N_{\gamma'_1} \cup N_{\gamma'_2}) = ([0, 1] \times S^1) \times S^1$  whose Reeb vector field  $R_\alpha$  is tangent to the fibers of the Seifert fibration. Applying Lemma 9.5 with  $k = 1$  for  $N_{\gamma'_1}$  and the argument in the proof of Lemma 9.9, we can extend  $\alpha$  to the whole  $\mathbb{RP}^3$  such that the obtained contact structure is positively transverse to the fibers of the Seifert fibration and the Reeb vector field is positively transverse to  $3_4$ . The contact structure is tight by [41, 36]. This completes the proof.  $\square$

**Lemma 9.11.**  $3_2$  supports the tight contact structure on  $\mathbb{RP}^3$ .

*Proof.* The Seifert fibration of the flow-spine  $2_1$  can be seen as in Figure 58. We can see that the core of the solid torus of the coil  $\gamma$  is in the position of the exceptional fiber of index 3. Hence the coil surgery of  $\gamma$  can be regarded as a Seifert-coil surgery. It can be checked that  $3_2$  is obtained from  $2_1$  by the Seifert-coil surgery  $(\gamma, \mathcal{H}_R)$ . The longitude of the knot  $\gamma'$  in  $S^3$  is  $-\Theta$  on  $\partial N_{\gamma'}$ , which can be verified by the same method as in Lemma 9.6. Since the Seifert fibration has no other exceptional fiber, each fiber of the Seifert fibration on  $\partial N_{\gamma'}$  intersects the meridian of  $\gamma'$  three times positively and the longitude once negatively, which is  $-\Theta + \Phi$ . This satisfies the conditions in Lemma 9.5. Hence we have the assertion by the lemma and [41, 36].  $\square$

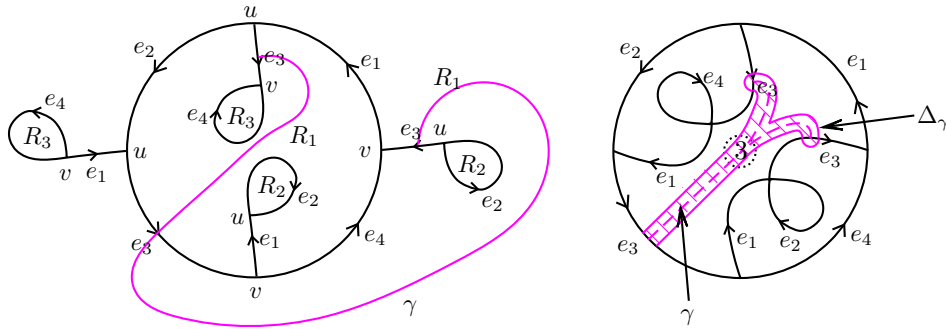


FIGURE 58. The coil  $\gamma$  on  $2_1$  and the disk  $\Delta_\gamma$  for the Seifert-coil surgery.

The tight contact structure on  $L(4, 3)$  is unique as written in Table 1 in Section 2.

**Lemma 9.12.**  $3_9$  supports the tight contact structure on  $L(4, 3)$ .

*Proof.* We first consider the flow-spine  $P$  obtained from  $1_1$  by the Seifert-coil surgeries  $(\gamma_1, \mathcal{H}_L)$  and  $(\gamma_2, \mathcal{H}_R)$ . Remark that the solid torus  $\mathcal{H}_L$  of the first surgery has an  $r$ -type vertex. Hence  $P$  is not a positive flow-spine. The Seifert-coil surgery for  $\gamma_2$  can be done as before. We observe the Seifert-coil surgery for  $\gamma_1$ . The fibers of the Seifert fibration are  $\Theta + 2\Phi$  as in Lemma 9.6. The two smooth curves in the branched theta-curve on  $T^2 \times \{0\}$  are  $(\theta_1, \theta_2) = (\Theta, \Theta + \Phi)$  and those on  $T^2 \times \{1\}$  are  $(\Theta, 2\Theta + \Phi)$ , see Figure 59. Since

$$\begin{vmatrix} 1 & 1 \\ 0 & 2 \end{vmatrix} = 2 > 0 \quad \text{and} \quad \begin{vmatrix} 2 & 1 \\ 1 & 2 \end{vmatrix} = 3 > 0,$$

the fibers of the Seifert fibration are positively transverse to  $P_{\mathcal{H}_L} \cup P_0$ . Since the meridian after the surgery is  $3\Theta + \Phi$  as shown on the right in Figure 59, we may find a contact form whose Reeb vector field is transverse to  $P_{\mathcal{H}_L} \cup P_0$  and whose contact structure is transverse to the fibers of the Seifert fibration as in the proof of Theorem 9.7. This contact structure is tight by [41, 36]. Thus we obtain the flow-spine  $P$  and a contact form  $\alpha$  on  $L(4, 3)$  whose Reeb flow is carried by  $P$ . The DS-diagram of  $P$  is given in Figure 60, where the vertex  $w$  is of  $r$ -type.

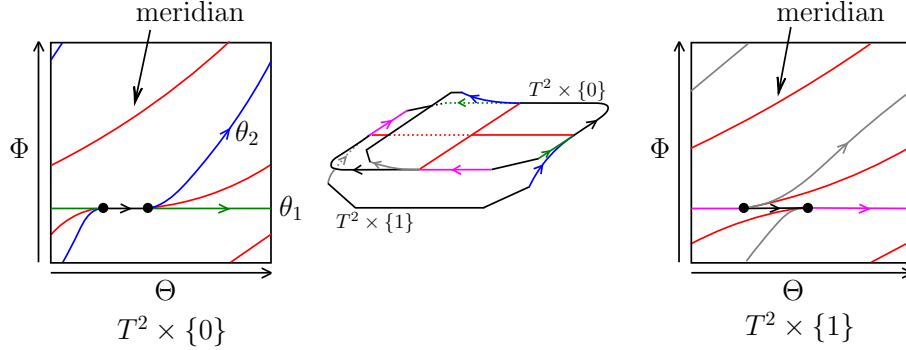


FIGURE 59. The branched theta-curves and meridians on  $T^2 \times \{0\}$  and  $T^2 \times \{1\}$  for  $\mathcal{H}_L$ .

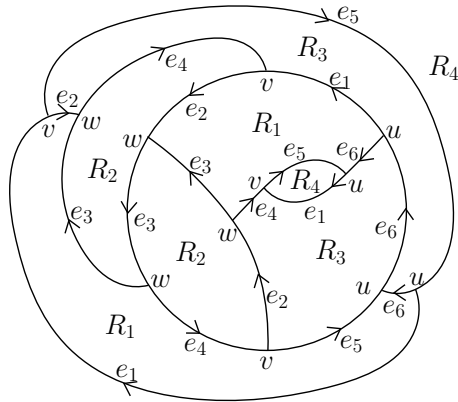


FIGURE 60. The DS-diagram of  $P$ .

We then isotope  $P$  by first and second regular moves as shown in Figure 61, which is done with keeping the transversality of the flow-spine and the Reeb flow of  $\alpha$ . The resulting flow-spine is  $3_9$ . This completes the proof.  $\square$

Summarizing the assertions in this subsection, we obtain the following statement.

**Theorem 9.13.** *The contact structures supported by positive flow-spines with up to 3 vertices are all tight.*

On the other hand, there is a positive flow-spine with 5 vertices that supports an overtwisted contact structure.

**Theorem 9.14.** *The positive flow-spine shown in Figure 62 supports the overtwisted contact structure on  $S^3$  whose homotopy class is the mirror of the standard contact structure.*

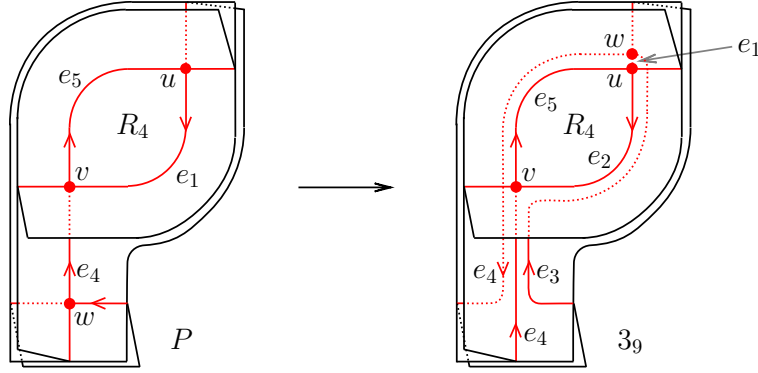


FIGURE 61. Move from  $P$  to  $3_9$ .

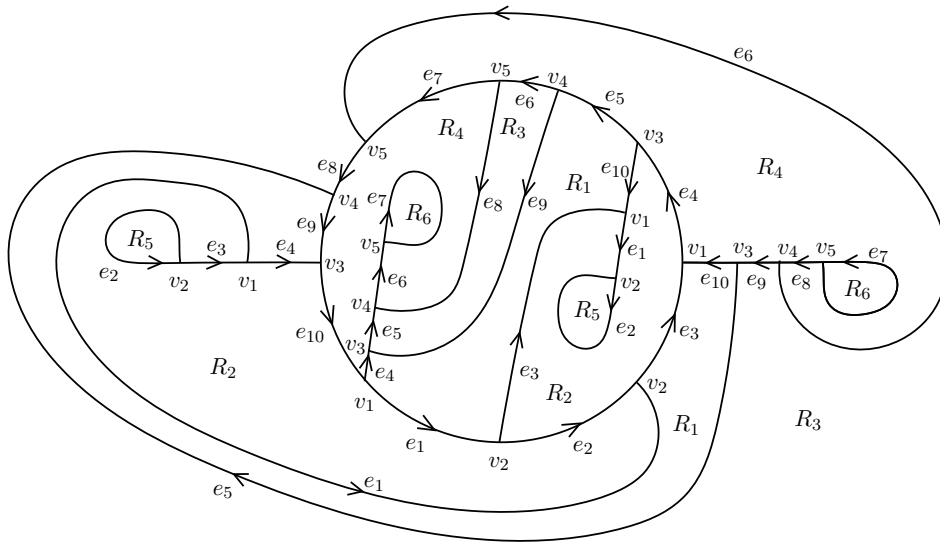


FIGURE 62. A positive flow-spine supporting an overtwisted contact structure.

*Proof.* Let  $P$  be the positive flow-spine given by the DS-diagram in Figure 62. We will show that a Reeb flow carried by  $P$  is homotopic to a flow carried by the negative abalone. In particular, the contact structure is overtwisted by the classification of contact structures on  $S^3$  due to Eliashberg [7, 9].

The neighborhood of the singular set of  $P$  is as shown on the left in Figure 63. Applying first and second regular moves, we obtain the flow-spine  $P'$  on the right. The vertex  $u$  is of  $l$ -type and the vertices  $v$  and  $w$  are of  $r$ -type. Note that we may need to homotope the flow during these moves.

The DS-diagram of  $P'$  is shown on the left in Figure 64. We further homotope the flow so that  $\hat{T}_+(e_1) \cap e_3 = \emptyset$  as shown on the right in Figure 64, where  $\hat{T}_+$  is the map introduced in Section 3.3 and the figure is the one obtained from the DS-diagram of  $P'$

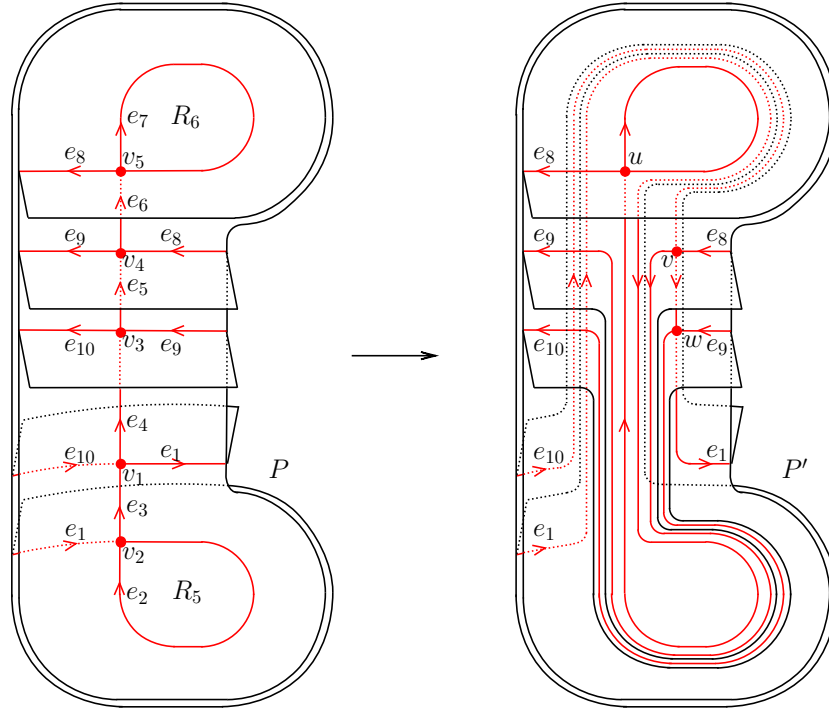


FIGURE 63. Apply regular moves.

by identifying two points connected by an orbit of the non-singular flow in the 3-ball. In particular,  $\hat{T}_+(e_1)$  is contained in the region  $R_1$ .

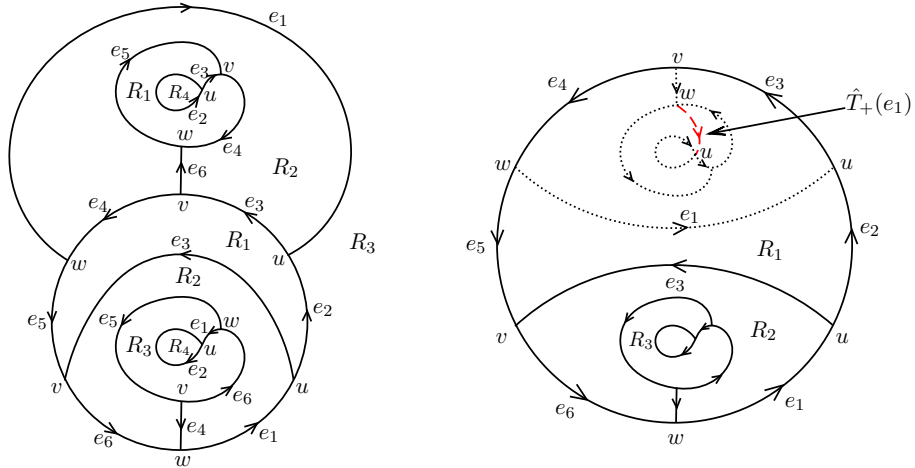


FIGURE 64. Homotope the flow so that  $\hat{T}_+(e_1)$  is contained in  $R_1$ .

Now we cleave the branch of  $P'$  as shown in Figure 6 and obtain the normal pair  $(\mathcal{F}, \Sigma)$ . By this cleaving, each edge  $e_j$  splits into two edges one of which lies on the boundary of the disk and the other lies in the interior of the disk. We denote the one on the boundary by the same character  $e_j$  and denote the other by  $\tilde{e}_j$ . The disk  $\Sigma$  of the normal pair is as shown on the left in Figure 65.

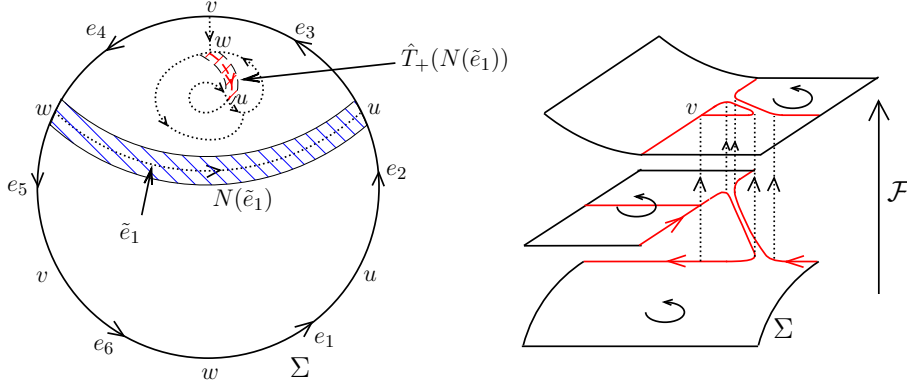


FIGURE 65. Make a new normal pair  $(\mathcal{F}, \Sigma')$ .

To show the assertion, we make a new normal pair  $(\mathcal{F}, \Sigma')$  as follows. Let  $N(\tilde{e}_1)$  be an open neighborhood of the closure of  $\tilde{e}_1$  in  $\Sigma$ . Since the flow is chosen so that  $\hat{T}_+(e_1)$  is contained in  $R_1$ ,  $\hat{T}_+(N(\tilde{e}_1))$  is in the position shown on the left in Figure 65, which is also contained in  $R_1$ . We remove  $N(\tilde{e}_1)$  from  $\Sigma$ , which splits  $\Sigma$  into two disjoint disks, and connect these two disks by a band transverse to the flow  $\mathcal{F}$  near the orbit passing through the vertex  $v$  as shown on the right in Figure 65. Then we can check that the pair of  $\mathcal{F}$  and the obtained disk  $\Sigma'$  is a normal pair. Since  $N(\tilde{e}_1)$  is removed from  $\Sigma$ ,  $(\mathcal{F}, \Sigma')$  does not yield the vertices  $u$  and  $w$ . Moreover, since  $\hat{T}_+(N(\tilde{e}_j))$  is contained in  $R_1$ ,  $\hat{T}_+(\partial\Sigma' \setminus \partial\Sigma)$  does not meet  $\partial\Sigma'$ , where  $\hat{T}_+$  is the map defined from the normal pair  $(\mathcal{F}, \Sigma')$ . This means that the flow-spine obtained from  $(\mathcal{F}, \Sigma')$  has no vertex other than  $v$ . Since  $v$  is of  $r$ -type, the flow-spine is the negative abalone. This completes the proof.  $\square$

**9.6. Complexity of contact 3-manifolds.** The surjection from the set of positive flow-spines to the set of contact 3-manifolds proved in this paper allows us to define a complexity for the set of contact 3-manifolds as an analogy of the Matveev complexity for the set of usual 3-manifolds, see [39, 40].

*Definition.* For a contact 3-manifold  $(M, \xi)$ , we define the *complexity*  $c(M, \xi)$  of  $(M, \xi)$  by the minimum number of vertices of a positive flow-spine that supports  $\xi$ .

The next statement is an immediate consequence of Theorem 1.2.

**Corollary 9.15.**  $c(M, \xi) < \infty$ .

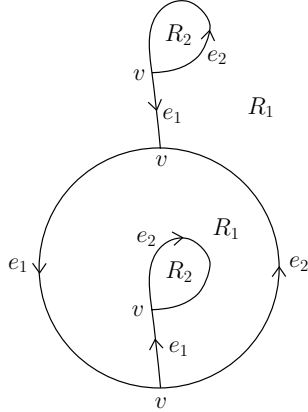
Here  $c(M, \xi) = \infty$  means that there is no positive flow-spine of  $M$  that supports  $\xi$ . By the definition of the complexity, it satisfies the following properties:

- For each  $n \in \mathbb{N}$ , there exists at most finitely many contact 3-manifolds with complexity  $n$ .
- $c(M) \leq c(M, \xi)$ , where  $c(M)$  is the Matveev complexity of  $M$ .

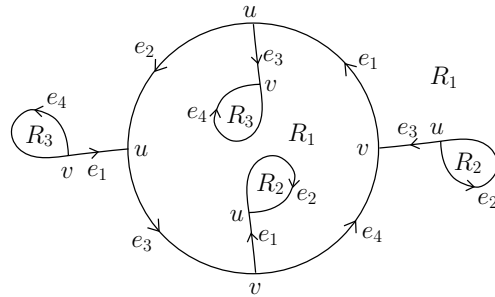
Theorem 1.3 in the introduction is obtained by summarizing the observations in the previous subsection.

APPENDIX A. LIST OF POSITIVE FLOW-SPINES WITH UP TO 3 VERTICES

The labels  $R_1, R_2, R_3$  and  $R_4$  represent the regions of the flow-spine,  $e_1, \dots, e_6$  represent the edges of its singular set, and  $u, v, w$  represent the vertices. The round circle is the  $E$ -cycle of the flow-spine, which is oriented in the counter-clockwise orientation. The edges  $e_1, \dots, e_6$  are also oriented according to this orientation. The notation  $\xi_{\text{std}}$  means the standard contact structure on  $S^3$  and  $\xi_{\text{tight}}$  means a tight contact structure.

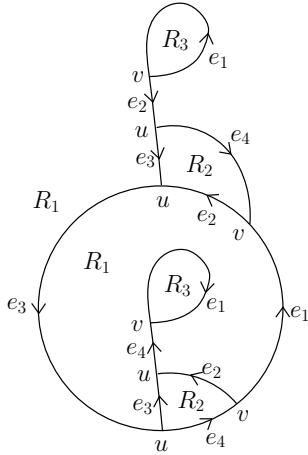


$1_1 (S^3, \xi_{\text{std}})$   
The positive abalone.



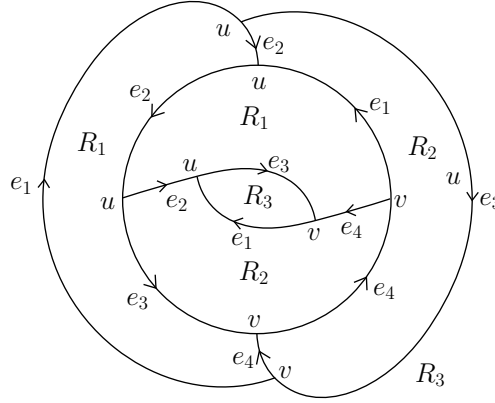
$2_1 (S^3, \xi_{\text{std}})$

The double branched cover of  $1_1$  along a trivial knot.



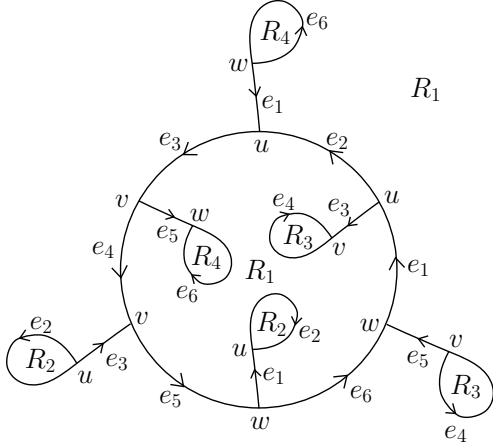
$2_2 (\mathbb{RP}^3, \xi_{\text{tight}})$

This is obtained from  $1_1$  by the coil surgery  $(\gamma_1, \mathcal{H}_R)$ .



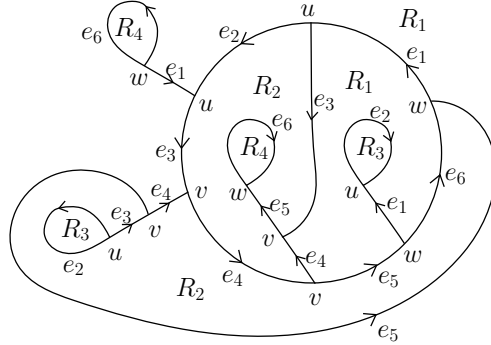
$2_3 (L(3, 2), \xi_{\text{tight}})$

The double branched cover of  $1_1$  along the trefoil.



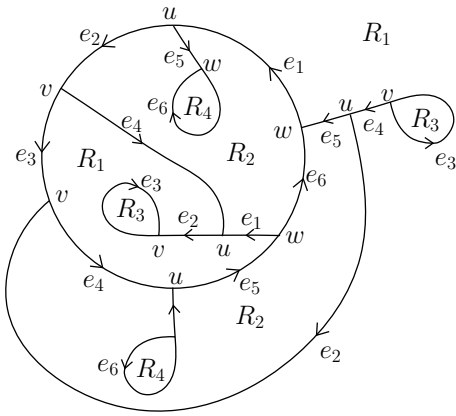
$3_1 (S^3, \xi_{\text{tight}})$

The 3-fold branched cover of  $1_1$  along a trivial knot.



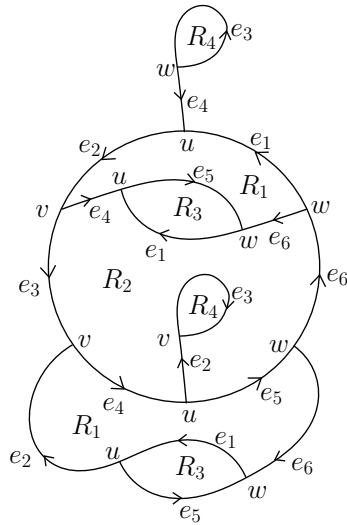
$3_2 (\mathbb{RP}^3, \xi_{\text{tight}})$

This is obtained from  $2_1$  by the coil surgery  $(\gamma, \mathcal{H}_R)$  along  $\gamma$  shown on the left in Figure 58.



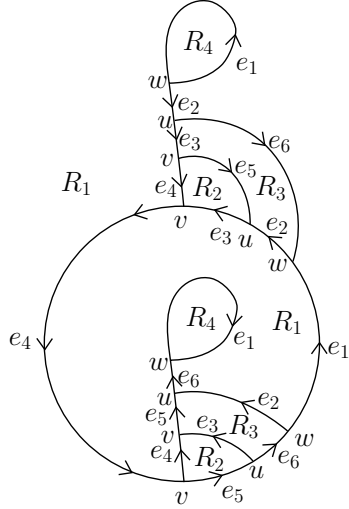
$3_3 (S^3, \xi_{\text{tight}})$

This is obtained from  $1_1$  by the coil surgeries  $(\gamma_1, \mathcal{H}_{\bar{L}})$  and  $(\gamma_2, \mathcal{H}_{\bar{L}})$ .



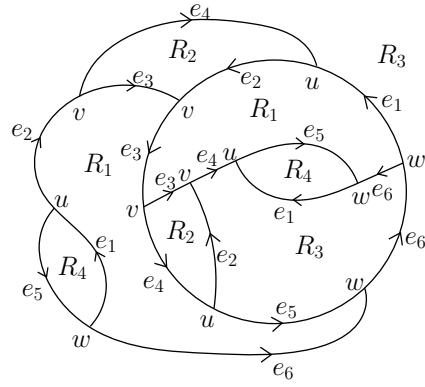
$3_4 (\mathbb{RP}^3, \xi_{\text{tight}})$

This is obtained from  $1_1$  by the coil surgeries  $(\gamma_1, \mathcal{H}_{\bar{L}})$  and  $(\gamma_2, \mathcal{H}_R)$ .



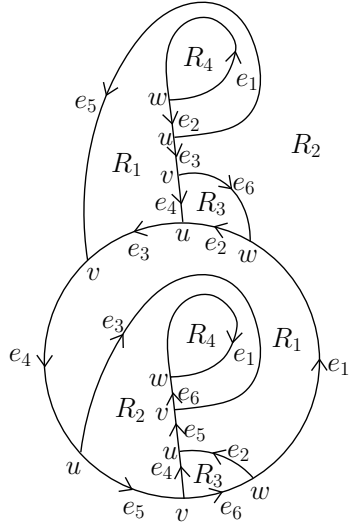
$3_5 (L(3, 1), \xi_{\text{tight}})$

This is obtained from  $1_1$  by the coil surgery  $(\gamma_1, \mathcal{H}_R^2)$ .



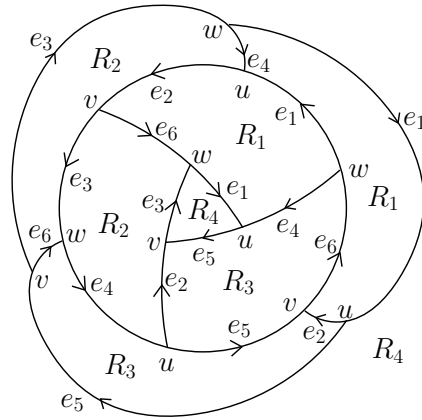
$3_6 (L(5, 2), \xi_{\text{tight}})$

This is obtained from  $1_1$  by the coil surgery  $(\gamma_2, \mathcal{H}_R^2)$ .



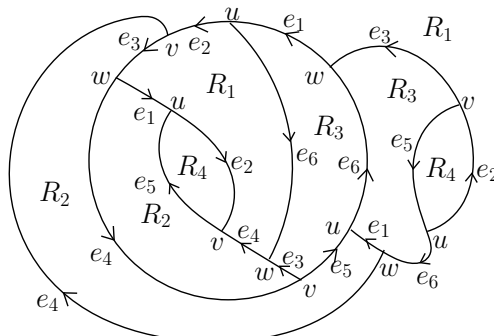
$3_7 (L(3, 2), \xi_{\text{tight}})$

This is obtained from  $2_3$  by a first regular move.



$3_8$  (quaternion space,  $\xi_{\text{canonical}}$ )

The 3-fold branched cover of  $1_1$  along the trefoil.



$\mathfrak{3}_9 (L(4, 3), \xi_{\text{tight}})$

This is obtained from  $1_1$  by applying the coil surgeries  $(\gamma_1, \mathcal{H}_L)$  and  $(\gamma_2, \mathcal{H}_R)$  and then eliminating the  $r$ -type vertex in  $\mathcal{H}_L$ .

#### REFERENCES

- [1] Anisov, S., *Exact values of complexity for an infinite number of 3-manifolds*, Mosc. Math. J. **5** (2005), no. 2, 305–310.
- [2] Benedetti, R., Petronio, C., *Branched standard spines of 3-manifolds*, Lecture Notes in Mathematics 1653, Springer-Verlag, Berlin, 1997.
- [3] Benedetti, R., Petronio, C., *Branched spines and contact structures on 3-manifolds*, Ann. Mat. Pure Appl. (4) **178** (2000), 81–102.
- [4] Bennequin, D., *Entrelacements et équations de Pfaff*, Astérisque, **107–108**, (1983), 87–161.
- [5] Caubel, C., Némethi, A., Popescu-Pampu, P., *Milnor open books and Milnor fillable contact 3-manifolds*, Topology **45** (2006), no. 3, 673–689.
- [6] Colin, V., Giroux, E., Honda, K., *Finitude homotopique et isotopique des structures de contact tendues*, Publ. Math. Inst. Hautes Études Sci. **109** (2009), 245–293.
- [7] Eliashberg, Y., *Classification of overtwisted contact structures on 3-manifolds*, Invent. Math. **98** (1989), no. 3, 623–637.
- [8] Eliashberg, Y., *Filling by holomorphic discs and its applications*, Geometry of low-dimensional manifolds, 2 (Durham, 1989), London Math. Soc. Lecture Note Ser. 151, Cambridge Univ. Press, Cambridge, 45–67, 1990.
- [9] Eliashberg, Y., *Contact 3-manifolds twenty years since J. Martinet’s work*, Ann. Inst. Fourier (Grenoble) **42** (1992), 165–192.
- [10] Eliashberg, Y., Thurston, W., *Confoliations*, University Lecture Series 13, Amer. Math. Soc., Providence, RI, 1998.
- [11] Endoh, M., Ishii, I., *A new complexity for 3-manifolds*, Japan. J. Math. (N.S.) **31** (2005), 131–156.
- [12] Etnyre, J. B., *Tight contact structures on lens spaces*, Commun. Contemp. Math. **2** (2000), no. 4, 559–577.
- [13] Etnyre, J. B., *Lectures on open book decompositions and contact structures*, Floer homology, gauge theory, and low-dimensional topology, 103–141, Clay Math. Proc., 5, Amer. Math. Soc., Providence, RI, 2006.
- [14] Etnyre, J. B., Honda, K., *On the Nonexistence of Tight Contact Structures*, Ann. of Math. **153** (2001), 749–766.
- [15] Fominykh E. A., Wiest, B., *Upper bounds for the complexity of torus knot complements*, J. Knot Theory Ramif., **22** (2013), no. 10, 1350053.
- [16] Geiges, H., *An introduction to contact topology*, Cambridge Studies in Advanced Mathematics 109, Cambridge University Press, Cambridge, 2008.
- [17] Giroux, E., *Convexité en topologie de contact*, Comment. Math. Helvetici **66** (1991), 637–677.

- [18] Giroux, E., *Structures de contact en dimension trois et bifurcations des feuilletages de surfaces*, Invent. Math. **141** (2000) 615–689.
- [19] Giroux, E., *Géométrie de contact: de la dimension trois vers les dimensions supérieures*, Proceedings of the International Congress of Mathematicians, Vol. II (Beijing, 2002), 405–414, Higher Ed. Press, Beijing, 2002.
- [20] Gray, J. W., *Some global properties of contact structures*, Ann. of Math. (2) **69** (1959), 421–450.
- [21] Gromov, M., *Pseudoholomorphic curves in symplectic manifolds*, Invent. Math. **82** (1985), 307–347.
- [22] Honda, K., *On the classification of tight contact structures. I*, Geom. Topol. **4** (2000), 309–368.
- [23] Ikeda, H., *Acyclic fake surfaces*, Topology **10** (1971), 9–36.
- [24] Ikeda, H., *Acyclic fake surfaces which are spines of 3-manifolds*, Osaka Math. J. **9** (1972), 391–408.
- [25] Ikeda, H., Inoue, Y., *Invitation to DS-diagram*, Kobe J. Math. **2** (1985) 169–186.
- [26] Ishii, I., *Flows and spines*, Tokyo J. Math. **9** (1986), 505–525.
- [27] Ishii, I., *Moves for flow-spines and topological invariants of 3-manifolds*, Tokyo J. Math. **15** (1992), 297–312.
- [28] Ishikawa, M., *Compatible contact structures of fibered Seifert links in homology 3-spheres*, Tohoku Math. J. (2) **64** (2012), no. 1, 25–59.
- [29] Ishikawa, M., Nemoto, K., *Construction of spines of two-bridge link complements and upper bounds of their Matveev complexities*, Hiroshima Math. J. **46** (2016), 149–162.
- [30] Jaco, W., Rubinstein, H., Tillmann, S., *Minimal triangulations for an infinite family of lens spaces*, J. Topol. **2** (2009), no. 1, 157–180.
- [31] Jaco, W., Rubinstein, H., Tillmann, S., *Coverings and minimal triangulations of 3-manifolds*, Algebr. Geom. Topol. **11** (2011), no. 3, 1257–1265.
- [32] Jaco, W., Rubinstein, H., Spreer, J., Tillmann, S., *On minimal ideal triangulations of cusped hyperbolic 3-manifolds*, to appear in J. Topol.
- [33] Koda, Y., *Branched spines and Heegaard genus of 3-manifolds*, Manuscripta Mathematica **123** (2007), no. 3, 285–299.
- [34] Koda, Y., *Spines, Heegaard splittings and the Reidemeister-Turaev torsion*, Tokyo J. Math. **30** (2007), no. 2, 417–439.
- [35] Koda, Y., *A Heegaard-type presentation of branched spines and the Reidemeister-Turaev torsion*, Math. Z. **260** (2008), no. 1, 203–228.
- [36] Lisca, P., Matić, G., *Transverse contact structures on Seifert 3-manifolds*, Algebr. Geom. Topol. **4** (2004), 1125–1144.
- [37] Lutz, R., *Structures de contact sur les fibre’s principaux en cercles de dimension 3*, Ann. Inst. Fourier, 27-3 (1977), 1–15.
- [38] Martinet, J., *Formes de contact sur les variétés de dimension 3*, Lecture Notes in Mathematics 209, pp. 142–163, 1971.
- [39] Matveev, S., *Complexity theory of three-dimensional manifolds*, Acta Appl. Math. **19** (1990), no. 2, 101–130.
- [40] Matveev, S., *Algorithmic Topology and Classification of 3-manifolds*, Algorithms and Computation in Mathematics, 9. Springer-Verlag, Berlin, 2003.
- [41] McCarthy, J. D., Wolfson, J. G., *Symplectic gluing along hypersurfaces and resolution of isolated orbifold singularities*, Invent. Math. **119** (1995), 129–154.
- [42] Ozbagci, B., Stipsicz, A.I., *Surgery on Contact 3-manifolds and Stein Surfaces*, Bolyai Society Mathematical Studies 13, Springer, 2004.
- [43] Öztürk, F., Niederkrüger, K., *Brieskorn manifolds as contact branched covers of spheres*, Periodica Mathematica Hungarica **54** (2007), 85–97.
- [44] Petronio, C., *Generic flows on 3-manifolds*, Kyoto J. Math. **55** (2015), no. 1, 143–167.
- [45] Petronio, C., Vesnin, A., *Two-sided bounds for the complexity of cyclic branched coverings of two-bridge links*, Osaka J. Math. **46** (2009), no. 4, 1077–1095.
- [46] Taniguchi, T., Tsuboi, K., Yamashita, M., *Systematic singular triangulations of all orientable Seifert manifolds*, Tokyo J. Math. **28** (2005), 539–561.
- [47] Thurston, W., Winkelnkemper, H., *On the existence of contact forms*, Proc. Amer. Math. Soc. **52** (1975), 345–347.

- [48] Torisu, I., *Convex contact structures and fibered links in 3-manifolds*, Int. Math. Res. Not. **9** (2000), 441–454.
- [49] Vesnin, A. Yu., Fominykh, E. A., *Exact values of complexity for Paoluzzi-Zimmermann manifolds*, Doklady Math. **84** (2011), 542–544.
- [50] Vesnin, A. Yu., Fominykh, E. A., *On complexity of three-dimensional hyperbolic manifolds with geodesic boundary*, Siberian Math. J. **53** (2012), 625–634.

DEPARTMENT OF MATHEMATICS, FACULTY OF SCIENCE AND TECHNOLOGY, KEIO UNIVERSITY, 3-14-1 HIYOSHI, KOHOKU, YOKOHAMA 223-8522, JAPAN

DEPARTMENT OF MATHEMATICS, HIYOSHI CAMPUS, KEIO UNIVERSITY, 4-1-1 HIYOSHI, KOHOKU, YOKOHAMA 223-8521, JAPAN

*E-mail address:* `ishikawa@keio.jp`

DEPARTMENT OF MATHEMATICS, HIROSHIMA UNIVERSITY, 1-3-1 KAGAMIYAMA, HIGASHI-HIROSHIMA, 739-8526, JAPAN

*E-mail address:* `ykoda@hiroshima-u.ac.jp`

DEPARTMENT OF MATHEMATICS, CHUO UNIVERSITY, 1-13-27 KASUGA, BUNKYO-KU, TOKYO, 112-8551, JAPAN

*E-mail address:* `naoe@math.chuo-u.ac.jp`